

ออกซิเดชันเชิงวิวิธพันธุ์ของไซโคลเฮกเซนและเอทิลเบนซีนด้วยตัวเร่งปฏิกิริยาที่ประกอบด้วย
โลหะทรานซิชัน



นางสาว วรางคณา กันจិនะ

ศูนย์วิทยทรัพยากร

จุฬาลงกรณ์มหาวิทยาลัย

วิทยานิพนธ์นี้เป็นส่วนหนึ่งของการศึกษาตามหลักสูตรปริญญาวิทยาศาสตรดุษฎีบัณฑิต

สาขาวิชาปิโตรเคมี

คณะวิทยาศาสตร์ จุฬาลงกรณ์มหาวิทยาลัย

ปีการศึกษา 2552

ลิขสิทธิ์ของจุฬาลงกรณ์มหาวิทยาลัย

HETEROGENEOUS OXIDATION OF CYCLOHEXANE AND ETHYLBENZENE BY
TRANSITION METAL-INCORPORATED CATALYSTS



Miss Warangkana Kanjina

ศูนย์วิทยทรัพยากร

A Dissertation Submitted in Partial Fulfillment of the Requirements
for the Degree of Doctoral of Philosophy Program in Petrochemistry

Faculty of Science

Chulalongkorn University

Academic Year 2009

Copyright of Chulalongkorn University

520477

Thesis Title HETEROGENEOUS OXIDATION OF
CYCLOHEXANE AND ETHYLBENZENE BY
TRANSITION METAL-INCORPORATED
CATALYSTS

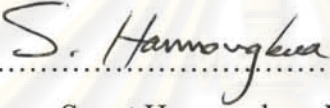
By Miss Warangkana Kanjina

Field of Study Petrochemistry

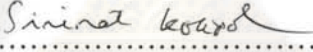
Advisor Associate Professor Wimonrat Trakarnpruk, Ph. D.


Co-advisor Professor Richard D. Ernst, Ph. D.


Accepted by the Faculty of Science, Chulalongkorn University in Partial
Fulfillment of the Requirements for the Doctoral's Degree

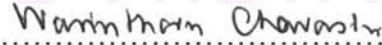

.....Dean of the Faculty of Science
(Professor Supot Hannongbua, Dr.rer.nat.)

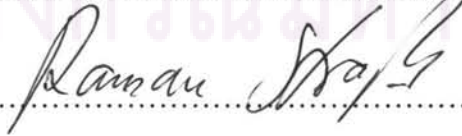
THESIS COMMITTEE


.....Chairman
(Associate Professor Sirirat Kokpol, Ph. D.)


.....Advisor
(Associate Professor Wimonrat Trakarnpruk, Ph. D.)


.....Co-advisor
(Professor Richard D. Ernst, Ph. D.)


.....Examiner
(Assistant Professor Warinthorn Chavasiri, Ph. D.)


.....External Examiner
(Roman Helmuth Adam Strauss, Ph. D.)

วรางคณา กั้นจันะ : ออกซิเดชันเชิงวิวิธพันธุ์ของไซโคลเฮกเซนและเอทิลเบนซีนด้วยตัวเร่งปฏิกิริยาที่ประกอบด้วยโลหะแทรนซิชัน. (HETEROGENEOUS OXIDATION OF CYCLOHEXANE AND ETHYLBENZENE BY TRANSITION METAL-INCORPORATED CATALYSTS) อ.ที่ปรึกษาวิทยานิพนธ์หลัก: รศ. ดร. วิมลรัตน์ ตระการฤกษ์ : อ.ที่ปรึกษาวิทยานิพนธ์ร่วม: Professor Richard D. Ernst, Ph. D., 148 หน้า

งานวิจัยนี้ได้ศึกษาถึงการเตรียมตัวเร่งปฏิกิริยาวิวิธพันธุ์ที่มีประสิทธิภาพสูงสำหรับการออกซิเดชันของไซโคลเฮกเซนและเอทิลเบนซีน วัสดุสามประเภทที่เลือกมาศึกษาคือ เลเยอร์ดับเบิลไฮดรอกไซด์ และโลหะออกไซด์ผสม พอลิออกซิเมทัลเลต และโลหะไนซีโรเจล โดยโลหะแทรนซิชันที่เลือกใช้ในการศึกษาคือ Co, Cu, Ni, Cr และ Mn ตัวเร่งปฏิกิริยาประเภทเลเยอร์ดับเบิลไฮดรอกไซด์ และโลหะออกไซด์ผสมได้นำไปออกซิไดซ์เอทิลเบนซีนด้วยเทอร์เชียรีบิวทิลไฮโดรเปอร์ออกไซด์ รวมทั้งมีการใช้สารออกซิไดซ์อื่น เช่น ไฮโดรเจนเปอร์ออกไซด์ หรืออากาศ ตัวเร่งปฏิกิริยา $Ni_{4.8}Al$ และ $Cu_{1.0}Mg_{2.9}Al$ ออกไซด์ แสดงประสิทธิภาพและความเลือกจำเพาะต่ออะซิโตนที่สูงและสามารถใช้ซ้ำได้ ตัวเร่งปฏิกิริยาพอลิออกซิเมทัลเลตที่มี แคทไอออนเป็นกรด โลหะแอลคาไลน์ และแอลคิลแอมโมเนียมถูกนำมาเปรียบเทียบประสิทธิภาพในการออกซิไดซ์ ไซโคลเฮกเซนและเอทิลเบนซีนด้วยไฮโดรเจนเปอร์ออกไซด์ ตัวเร่งปฏิกิริยาที่มีแอลคิลแอมโมเนียมแสดงประสิทธิภาพสูงสุด ตัวเร่งปฏิกิริยาที่มีโลหะไนซีโรเจลมีความเหมาะสมสำหรับเร่งออกซิเดชันของไซโคลเฮกเซนในเทอร์เชียรีบิวทิลไฮโดรเปอร์ออกไซด์และอากาศโดยปราศจากตัวทำละลายใดๆ ลำดับประสิทธิภาพคือ $Co > Cu > Mn > Cr > Ni$ โดยตัวเร่งปฏิกิริยาทั้งหมดไม่มีการหลุดลงไปในของผสมทำปฏิกิริยา

ศูนย์วิทยทรัพยากร จุฬาลงกรณ์มหาวิทยาลัย

สาขาวิชา ปีใดจะมี ลายมือชื่อนิสิต ๒๕๖๑ กั้นจันะ
ปีการศึกษา 2552 ลายมือชื่อ อ.ที่ปรึกษาวิทยานิพนธ์หลัก W. Traakaporn
ลายมือชื่อ อ.ที่ปรึกษาวิทยานิพนธ์ร่วม R. Ernst

4773868223: MAJOR PETROCHEMISTRY

KEYWORD: HETEROGENEOUS / TRANSITION METAL / OXIDATION

WARANGKANA KANJINA: HETEROGENEOUS OXIDATION OF CYCLOHEXANE AND ETHYLBENZENE BY TRANSITION METAL-INCORPORATED CATALYSTS. THESIS ADVISOR: ASSOC. PROF. WIMONRAT TRAKARNPRUK, Ph. D., THESIS CO-ADVISOR: PROF. RICHARD D. ERNST, Ph. D., 148 pp.

This study is to focus on the preparation of heterogeneous catalysts with high catalytic activities for oxidation of cyclohexane and ethylbenzene. Three classes of materials were studied: layered double hydroxides (LDHs) and their corresponding mixed metal oxides, polyoxometalates and metal incorporated xerogels. Transition metals chosen for the study are Co, Cu, Ni, Cr and Mn. The LDHs and mixed metal oxide catalysts were utilized for the oxidation of ethylbenzene with *tert*-butylhydroperoxide. The use of other oxidants such as hydrogen peroxide or air are also investigated. The Ni_{4.8}Al and Cu_{1.0}Mg_{2.9}Al oxide catalysts showed high activity with high acetophenone selectivity and they can be reused. Polyoxometalate catalysts possessing acid, alkali and alkyl ammonium cations were compared their activity towards oxidation of cyclohexane and ethylbenzene with hydrogen peroxide. The catalyst with alkyl ammonium showed the highest activity. Metal incorporated xerogel catalyst was appropriate to catalyze oxidation of cyclohexane in *tert*-butyl hydroperoxide as well as in air without any solvent. The activity order is Co > Cu > Mn > Cr > Ni. They showed no leaching into the reaction mixture.

ศูนย์วิทยทรัพยากร
จุฬาลงกรณ์มหาวิทยาลัย

Field of Study: Petrochemistry..... Student's signature..... Warangkana Kanjina
Academic year: 2009..... Advisor's signature..... W. Trakarnpruk
Co-Advisor's signature..... R. D. Ernst

ACKNOWLEDGEMENTS

This dissertation was accomplished by the assistance and support from many people and organizations. The author would like to express her gratitude to her thesis advisor, Associate Professor Dr. Wimonrat Trakarnpruk and Professor Dr. Richard D. Ernst for providing valuable advice, encouragement and giving the assistance throughout the course of this research. In addition, the author also wishes to express deep appreciation to Associate Professor Dr. Sirirat Kokpol who was the chairman of the committee, Assistant Professor Dr. Warinthorn Chavasiri and Dr. Roman Helmuth Adam Strauss who were members of the committee, for their valuable suggestions and comments.

Appreciation is also extended to Program of Petrochemistry and Department of Chemistry, Faculty of Science, Graduate School, Chulalongkorn University, the 90th anniversary of Chulalongkorn university fund (Ratchadaphiseksomphot Endowment Fund) and National Center of Excellence for Petroleum, Petrochemicals, and Advanced Materials (NCE-PPAM) for granting financial support to fulfill this study and provision of experimental facilities.

Further acknowledgement is extended to her friends for their help and encouragement during her graduate study. Finally, she is most grateful to her parents and her sister for their entire care and unconditional encouragement throughout her entire education. Finally, the author would like to express her deepest gratitude to all of the teachers who have taught her since her childhood.

ศูนย์วิทยาศาสตร์
จุฬาลงกรณ์มหาวิทยาลัย

CONTENTS

	PAGE
ABSTRACT IN THAI.....	iv
ABSTRACT IN ENGLISH.....	v
ACKNOWLEDGEMENTS.....	vi
CONTENTS.....	vii
LIST OF FIGURES.....	xiii
LIST OF TABLES.....	xvi
LIST OF SCHEMES.....	xviii
LIST OF ABBREVIATIONS.....	xix
CHAPTER I INTRODUCTION	1
1.1 Homogeneous catalysts.....	2
1.2 Heterogeneous catalysts.....	3
1.3 Scope of research work.....	4
1.4 Organization of this research.....	5
CHAPTER II EXPERIMENTAL	6
2.1 Chemicals.....	6
2.2 Equipments.....	7
2.3 Catalyst characterization.....	8
2.3.1 Fourier transform infrared spectroscopy (FTIR).....	8
2.3.2 X-ray diffraction (XRD).....	8
2.3.3 Diffuse reflectance ultraviolet-visible spectroscopy (DRUV) and ultraviolet-visible spectroscopy (UV- vis).....	8
2.3.4 Nitrogen adsorption (Brunauer-Emmett-Teller method (BET)).....	8
2.3.5 Thermogravimetric analysis (TGA).....	9
2.3.6 Temperature program desorption (NH ₃ -TPD).....	9
2.3.7 Temperature program reduction (H ₂ -TPR).....	10
2.3.8 Inductively coupled plasma (ICP).....	10
2.3.9 Soluble basicity.....	10
2.3.10 Gas chromatography (GC).....	10

CONTENTS (CONT.)

	PAGE
CHAPTER III CATALYTIC OXIDATION OF ETHYLBENZENE USING LAYERED DOUBLE HYDROXIDES AND MIXED METAL OXIDES	12
3.1 Introduction.....	12
3.1.1 Layered double hydroxide (LDH).....	12
3.1.2 Preparation of layered double hydroxides.....	14
3.1.3 Thermal treatment of layered double hydroxides.....	14
3.1.4 Rehydration of mixed metal oxide	16
3.2 Literature reviews.....	16
3.3 Preparation of the catalysts.....	19
3.3.1 Alkali coprecipitation method.....	19
3.3.1.1 Binary layered double hydroxides.....	19
3.3.1.2 Ternary layered double hydroxides.....	20
3.3.2 Alkali-free coprecipitation method.....	21
3.3.3 Calcination of layered double hydroxides.....	21
3.3.4 Rehydration of mixed metal oxides.....	21
3.4 Catalyst characterization.....	22
3.4.1 Composition of mixed metal oxide catalysts	22
3.4.2 Surface analysis by nitrogen adsorption of LDHs and mixed metal oxides.....	23
3.4.3 Fourier transform infrared spectroscopy (FTIR) of LDHs and mixed metal oxides.....	26
3.4.4 X-ray diffraction (XRD) of LDHs and mixed metal oxides.....	27
3.4.4.1 XRD of binary layered double hydroxides...	27
3.4.4.2 XRD of binary mixed metal oxides.....	30
3.4.4.3 XRD of ternary layered double hydroxides..	31
3.4.4.4 XRD of ternary mixed metal oxides.....	32
3.4.5 Diffuse reflectance ultraviolet-visible spectroscopy (DRUV).....	33
3.4.6 Thermogravimetric analysis (TGA).....	34

CONTENTS (CONT.)

	PAGE
3.4.7 Thermal stabilities of mixed metal oxide catalysts.....	37
3.4.8 Temperature program reduction (TPR).....	38
3.5 Oxidation of ethylbenzene with binary LDH and mixed metal oxide catalysts.....	42
3.5.1 Effect of oxidant.....	43
3.5.2 Effect of preparation methods and catalyst forms.....	44
3.5.3 Oxidation of ethylbenzene with various catalysts.....	45
3.5.4 Effect of oxidant and substrate (O/S) mole ratios.....	47
3.5.5 Effect of catalyst amount.....	48
3.5.6 Effect of solvent.....	49
3.5.7 Effect of radical scavenger.....	50
3.6 Oxidation of ethylbenzene with ternary LDH and mixed metal oxide catalysts.....	51
3.6.1 Oxidation with various catalysts.....	51
3.6.2 Effect of reaction temperature.....	52
3.6.3 Effect of reaction time.....	53
3.6.4 Effect of oxidant/substrate (O/S) mole ratio.....	54
3.6.5 Effect of radical scavenger.....	55
3.7 Mechanism.....	56
3.8 Reusability of catalysts.....	57
3.9 Heterogeneity of catalysts.....	57
3.10 Conclusion.....	57

CHAPTER IV OXIDATION OF ETHYLBENZENE, CYCLOHEXANE AND CYCLOHEXANOL USING POLYOXOMETALATES 58

4.1 Introduction.....	58
4.2 Literature reviews.....	63
4.2.1 Oxidation of hydrocarbon using polyoxometalate catalysts.....	63
4.2.2 Oxidation of other substrates.....	65
4.3 Preparation of catalysts.....	68

CONTENTS (CONT.)

	PAGE
4.3.1 Disodium salt of molybdophosphoric and tungstophosphoric acids: $\text{Na}_2\text{H}[\text{PMo}_{12}\text{O}_{40}]$ and $\text{Na}_2\text{H}[\text{PW}_{12}\text{O}_{40}]$	68
4.3.2 Molybdophosphoric and tungstophosphoric acids: $\text{H}_3[\text{PMo}_{12}\text{O}_{40}]$ and $\text{H}_3[\text{PW}_{12}\text{O}_{40}]$	68
4.3.3 Tetrabutyl ammonium salts of molybdophosphate and tungstophosphate $[(n\text{-C}_4\text{H}_9)_4\text{N}]_3[\text{PMo}_{12}\text{O}_{40}]$ and $[(n\text{-C}_4\text{H}_9)_4\text{N}]_3[\text{PW}_{12}\text{O}_{40}]$	69
4.3.4 11-Tungsto-1-vanadophosphate: $[(n\text{-C}_4\text{H}_9)_4\text{N}]_4[\text{PW}_{11}\text{VO}_{40}]$, 10-Tungsto-2-vanadophosphate: $[(n\text{-C}_4\text{H}_9)_4\text{N}]_5\text{PW}_{10}\text{V}_2\text{O}_{40}$ and 9-Tungsto-3-vanadophosphate: $[(n\text{-C}_4\text{H}_9)_4\text{N}]_6[\text{PW}_9\text{V}_3\text{O}_{40}]$	70
4.3.5 $[(n\text{-C}_4\text{H}_9)_4\text{N}]_4\text{H}[\text{PW}_{11}\text{M}(\text{H}_2\text{O})\text{O}_{39}]$ where M = Mn, Co, Cu, Cr or Ni.....	71
4.4 Catalyst characterization.....	72
4.4.1 Fourier transform infrared spectroscopy (FTIR).....	72
4.4.2 Nitrogen adsorption (Brunauer-Emmett-Teller method (BET)).....	74
4.4.3 Thermogravimetric analysis (TGA).....	75
4.4.4 Temperature program desorption (NH_3 -TPD).....	76
4.4.5 Temperature program reduction (H_2 -TPR).....	77
4.4.6 Solubility of the catalysts.....	77
4.5 Oxidation of ethylbenzene.....	78
4.5.1 Effect of temperature in solvent-free systems.....	79
4.5.2 Effect of types of substituted metal in ethylbenzene oxidation.....	80
4.5.3 Effect of reaction time in oxidation of ethylbenzene...	81
4.5.4 Effects of oxidant per substrate mole ratios (O/S) and substrate per catalyst mole ratios (S/C).....	82
4.5.5 Reusability of catalysts	82

CONTENTS (CONT.)

	PAGE
4.5.6 Effects of reaction conditions.....	83
4.6 Oxidation of cyclohexane.....	84
4.6.1 Effect of types of substituted metal in cyclohexane oxidation.....	84
4.6.2 Effect of O/S and S/C mole ratios.....	85
4.6.3 Effect of amount of catalyst.....	87
4.6.4 Effect of reaction time in cyclohexane oxidation.....	88
4.7 Stability of the catalyst.....	89
4.8 Mechanism of cyclohexane oxidation with POMs.....	89
4.9 Oxidation of cyclohexanol.....	90
4.9.1 Oxidation of primary alcohols to carboxylic acid....	90
4.9.2 Oxidation of secondary alcohols to ketones.....	91
4.9.3 Oxidation of secondary alcohols to carboxylic acids..	91
4.10 Literature reviews.....	91
4.11 Catalytic study.....	93
4.11.1 Effect of reaction temperature.....	93
4.11.2 Effect of types of catalyst.....	94
4.12 Conclusion.....	96

CHAPTER VOXIDATION OF CYCLOHEXANE USING TRANSITION**METAL INCORPORATED XEROGEL CATALYSTS 97**

5.1 Introduction.....	97
5.1.1 Sol-gel process.....	97
5.2 Literature reviews.....	99
5.3 Preparation of metal incorporated xerogel catalysts.....	101
5.4 Characterization of metal-incorporated xerogel catalysts.....	102
5.4.1 Functional group analysis of metal-incorporated xerogel catalysts.....	102
5.4.2 Phase analysis of metal incorporated xerogels.....	103
5.4.3 Diffuse reflectance ultraviolet-visible spectroscopy (DRUV).....	104

CONTENTS (CONT.)

	PAGE
5.4.4 Surface area measurement (Brunauer-Emmett-Teller method (BET)).....	105
5.5 Catalytic activity.....	106
5.5.1 Effect of types of metal.....	107
5.5.2 Effect of types of anion.....	108
5.5.3 Effect of reaction time.....	108
5.5.4 Effect of air pressure.....	110
5.5.5 Effect of amount of TBHP.....	111
5.5.6 Effect of amount of methyl ethyl ketone.....	112
5.5.7 Effect of catalyst amount.....	113
5.6 Leaching test of metal incorporated xerogel catalysts.....	114
5.7 Conclusion.....	114
REFERENCES.....	115
APPENDIXES.....	128
VITAE.....	148



 ศูนย์วิจัยทรัพยากร
 จุฬาลงกรณ์มหาวิทยาลัย

LIST OF FIGURES

FIGURE	PAGE
3.1 Schematic view of layered double hydroxide structure and general formula.....	13
3.2 The thermal treatment of MgAl-CO ₃ LDH as a function of temperature.....	15
3.3 Structure of hydrotalcite, showing the brucite-type layer with the M ²⁺ and M ³⁺ cations (grey and white octahedra) and the interlayer space with the CO ₃ ²⁻ anions (stripes) and the H ₂ O molecules (black).....	16
3.4 FTIR spectra of NiAl LDH prepared by alkali and alkali-free coprecipitation methods	26
3.5 FTIR spectra of the Ni _{4.8} Al LDH and oxide catalysts prepared by the coprecipitation method.....	27
3.6 XRD patterns of NiAl LDH prepared with alkali and alkali-free coprecipitation methods.....	28
3.7 XRD patterns of Mg _{4.9} Al, Ni _{4.8} Al, Cu _{4.9} Al and Co _{4.5} Al LDHs.....	29
3.8 XRD patterns of binary mixed metal oxide; Mg _{4.9} Al, Ni _{4.8} Al, Co _{4.5} Al and Cu _{4.9} Al oxides	30
3.9 XRD patterns of ternary layered double hydroxides.....	31
3.10 XRD patterns of ternary mixed metal oxides.....	32
3.11 TGA profile of the Co _{4.5} Al LDH.....	35
3.12 TGA profile of the Co _{0.8} Mg _{1.6} Al LDH.....	35
3.13 TGA profile of the Cu _{1.0} Mg _{2.9} Al LDH.....	36
3.14 TGA profile of Ni _{4.8} Al oxide.....	37
3.15 TGA profile of Co _{4.5} Al oxide.....	38
3.16 TPR profiles of Ni _{5.1} Cr, Ni _{4.8} Al, Co _{4.5} Al, and Cu _{4.9} Al oxide catalysts..	39
3.17 TPR profiles of Ni _{0.9} Mg _{2.1} Al, Co _{0.8} Mg _{1.6} Al, Cu _{1.0} Mg _{2.9} Al, Mn _{2.9} Mg _{2.2} Al and Cr _{0.8} Mg _{2.4} Al oxides catalysts.....	40
3.18 Effect of oxidant and substrate mole ratios in the oxidation of ethylbenzene using Ni _{4.8} Al oxide as catalyst and TBHP as oxidant.....	47
3.19 Effect of catalyst amount using Ni _{4.8} Al oxide catalyst.....	48

LIST OF FIGURES (CONT.)

FIGURE	PAGE
3.20 Catalytic oxidation of ethylbenzene using binary mixed metal oxide in the presence of radical scavenger.....	50
3.21 Effect of reaction temperature using the $\text{Cu}_{1.0}\text{Mg}_{2.9}\text{Al}$ oxide catalyst..	52
3.22 Effect of reaction time using $\text{Cu}_{1.0}\text{Mg}_{2.9}\text{Al}$ oxide catalyst.....	53
3.23 Effect of amount of oxidant using $\text{Cu}_{1.0}\text{Mg}_{2.9}\text{Al}$ oxide catalyst.....	54
3.24 Catalytic oxidation of ethylbenzene using ternary mixed metal oxide in the presence of radical scavenger.....	55
4.1 Ball-and-stick representation of the Keggin structure.....	59
4.2 Solubility of polyoxometalates as a function of counter cations.....	60
4.3 Global commercial sources for cyclohexane in 2006.....	61
4.4 Consumption of cyclohexane by region for 2005.....	61
4.5 FTIR spectra of $\text{H}_3[\text{PM}_{12}\text{O}_{40}]$, $\text{Na}_2\text{H}[\text{PM}_{12}\text{O}_{40}]$ and $[(n\text{-C}_4\text{H}_9)_4\text{N}]_3[\text{PW}_{12}\text{O}_{40}]$	73
4.6 Thermogram of $[(n\text{-C}_4\text{H}_9)_4\text{N}]_4\text{H}[\text{PW}_{11}\text{Co}(\text{H}_2\text{O})\text{O}_{39}]$ catalyst.....	75
4.7 Effect of reaction temperature on conversion and selectivity.....	79
4.8 Effect of reaction time on ethylbenzene conversion and product selectivity	81
4.9 Effect of O/S mole ratio to cyclohexane conversion using $[(n\text{-C}_4\text{H}_9)_4\text{N}]_4\text{H}[\text{PW}_{11}\text{CuO}_{39}]$	86
4.10 Effect of catalyst amount to cyclohexane conversion using $[(n\text{-C}_4\text{H}_9)_4\text{N}]_4\text{H}[\text{PW}_{11}\text{CuO}_{39}]$	87
4.11 Effect of reaction time using $[(n\text{-C}_4\text{H}_9)_4\text{N}]_4\text{H}[\text{PW}_{11}\text{CuO}_{39}]$	88
4.12 XRD patterns of $[(n\text{-C}_4\text{H}_9)_4\text{N}]_4\text{H}[\text{PW}_{11}\text{Co}(\text{H}_2\text{O})\text{O}_{39}]$, before and after reaction in catalytic oxidation of cyclohexane.....	89
4.13 Effect of reaction temperature using $[(n\text{-C}_4\text{H}_9)_4\text{N}]_3[\text{PW}_{12}\text{O}_{40}]$	93
4.14 Phase transfer catalysis mechanism.....	95
5.1 Sol-gel process and products	98
5.2 FTIR spectra of cobalt incorporated xerogel catalysts.....	102
5.3 XRD pattern of $\text{Co}(\text{OAc})_2$ -xerogel catalyst.....	103
5.4 Adsorption and desorption isotherm of $\text{Co}(\text{OAc})_2$ -xerogel.....	105

LIST OF FIGURES (CONT.)

FIGURE		PAGE
5.5	Effect of reaction time on cyclohexane oxidation using Co(OAc) ₂ -xerogel... ..	109
5.6	Effect of air pressure on cyclohexane oxidation using Co(OAc) ₂ -xerogel.....	110
5.7	Effect of catalyst amount in cyclohexane oxidation using Co(OAc) ₂ -xerogel.....	113



ศูนย์วิจัยทรัพยากร
 จุฬาลงกรณ์มหาวิทยาลัย

LIST OF TABLES

TABLE	PAGE
1.1 General, selected properties of homogeneous and heterogeneous catalysts.....	3
1.2 Classification of representative heterogeneous catalysts.....	4
2.1 Chemicals and suppliers.....	6
3.1 Ionic radii of metal ions.....	14
3.2 Designation of the binary layered double hydroxides.....	20
3.3 Designation of the ternary layered double hydroxides.....	20
3.4 Composition of binary mixed metal oxide catalysts.....	22
3.5 Composition of ternary mixed metal oxide catalysts.....	22
3.6 Surface area measurement of Ni/Al LDH and oxide prepared with different methods.....	23
3.7 Surface analysis of binary LDH and mixed metal oxide catalysts.....	24
3.8 Surface area measurement of ternary MMgAl LDHs and oxide materials.....	25
3.9 DRUV of binary and ternary mixed metal oxide catalysts.....	33
3.10 Thermogravimetric analysis data of LDHs.....	36
3.11 Oxidation of ethylbenzene using catalysts prepared with alkali and alkali-free coprecipitation.....	44
3.12 Oxidation of ethylbenzene using binary mixed metal oxide catalysts...	45
3.13 Effect of types of solvent using Ni _{4.8} Al oxide.....	49
3.14 Catalytic oxidation of ethylbenzene using ternary metal oxide catalysts.....	51
4.1 FTIR spectra of polyoxometalates.....	72
4.2 Surface area measurements of polyoxometalates.....	74
4.3 Decomposition temperatures and percentage mass loss.....	76
4.4 Acidity of polyoxometalates.....	76
4.5 TPR of various polyoxometalates.....	77
4.6 Effect of types of substituted metal in ethylbenzene oxidation.....	80
4.7 Effect of O/S and S/C mole ratios using [(<i>n</i> -C ₄ H ₉) ₄ N] ₄ H[PW ₁₁ CuO ₃₉] catalyst.....	82
4.8 Oxidation of ethylbenzene at various conditions.....	83

LIST OF TABLE (CONT.)

TABLE		PAGE
4.9	Effect of types of substituted metal in cyclohexane oxidation.....	83
4.10	Oxidation of cyclohexanol with hydrogen peroxide.....	94
4.11	Effect of transition metal substituted polyoxotungstate.....	105
5.1	Absorption band of metal-incorporated xerogel catalysts.....	104
5.2	Surface analysis of metal-incorporated xerogel catalysts.....	105
5.3	Oxidation of cyclohexane using metal-incorporated xerogel catalysts..	107
5.4	Oxidation of cyclohexane using cobalt xerogel catalysts.....	108
5.5	Effect of the amount of TBHP in cyclohexane oxidation using Co(OAc) ₂ -xerogel.....	111
5.6	Effect of amount of MEK in cyclohexane oxidation using Co(OAc) ₂ - xerogel.....	112



ศูนย์วิจัยทรัพยากร
จุฬาลงกรณ์มหาวิทยาลัย

LIST OF SCHEMES

SCHEME	PAGE
1.1 Aerobic oxidation of cyclohexane.....	1
3.1 Autoxidation of ethylbenzene.....	42
3.2 Reaction scheme of the ethylbenzene oxidation	42
3.3 Proposed mechanism oxidation of ethylbenzene with mixed metal oxide catalyst using TBHP as oxidant.....	56
4.1 Oxidation of cyclohexane to adipic acid and caprolactam.....	62
4.2 Reaction scheme of ethylbenzene oxidation.....	78
4.3 Reaction scheme of cyclohexane oxidation and the products found in this study.....	84



ศูนย์วิทยทรัพยากร
จุฬาลงกรณ์มหาวิทยาลัย

LIST OF ABBREVIATIONS

°C	degree Celsius
acac	acetylacetonate
AP	acetophenone
aq	aqueous
atm	atmosphere
BA	benzoic acid
BET	Brunauer-Emmett-Teller
BJH	Barret–Joyner–Halenda
BZ	benzaldehyde
Cl	chloride
cm	centimeter
cm ⁻¹	unit of wavenumber
CO ₃	carbonate
CyH	cyclohexane
CyOH	cyclohexanol
CyONE	cyclohexanone
CyOOH	cyclohexyl hydroperoxide
DRUV	Diffuse reflectance ultraviolet-visible
e.g.	exempli gratia, for example
EB	ethylbenzene
FTIR	Fourier transform infrared spectroscopy
g	gram (s)
GC	gas chromatography
h	hour (s)
ICP	Inductive coupled plasma
JCPDS	Joint Committee on Powder Diffraction Standards
kPa	kilo Pascal
LDH	layered double hydroxide
min	minute (s)
mL	milliliter (s)
mmol	millimole

LIST OF ABBREVIATIONS (CONT.)

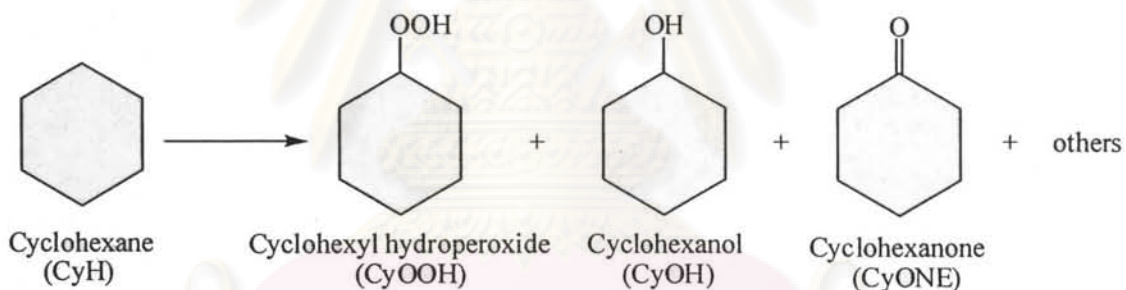
nm	nanometer
NO ₃	nitrate
O/S	oxidant per substrate
OAc	acetate
PE	1-phenyl ethanol
POM	polyoxometalate
ppm	part per million
rpm	round per minute
S/C	substrate per catalyst
st	stretching
TBHP	<i>tertiary</i> -butylhydroperoxide
TCD	thermal conductivity detector
TEOS	tetraethyl orthosilicate
TGA	thermogravimetric analysis
TOF	turnover frequency
TON	turnover number
TPD	temperature program desorption
TPR	temperature program reduction
XRD	X-ray diffraction

ศูนย์วิทยทรัพยากร
จุฬาลงกรณ์มหาวิทยาลัย

CHAPTER I

INTRODUCTION

Heterogeneous catalytic oxidation is extensively used in catalysis for selective and total oxidation processes. Selective oxidation of organic compounds, in particular of hydrocarbons, is the basis of numerous industrial processes yielding organic oxides, aldehydes and organic acids. Alkanes are generally considered chemically inert, a characteristic to which they owe their classification as paraffins. Their selective oxidation consequently poses many challenges. In the particularly case of cyclohexane oxidation, in the actual process it is first oxidized into cyclohexanol and cyclohexanone. The conversion of cyclohexane has to be kept very low in order to avoid over-oxidation to undesired products because the products are more reactive than cyclohexane (Scheme 1.1) [1-2]. Therefore, the industrial process requires rigid control of the conversion to maintain reasonable selectivity values.



Scheme 1.1 Aerobic oxidation of cyclohexane [2].

In this process, the catalyst is a metal complex which can be dissolved in the substrate and thus the reaction is conducted in a homogeneous system. An obvious drawback of this process is the difficulty of separating the catalysts from the reaction mixture and also the environmental problems due to catalyst contamination in the liquid waste. Ideally a catalyst would not be consumed, but it does occur in practice. Even heterogeneous catalysts, which generally have more stability than homogeneous catalysts, undergo chemical changes from thermal decomposition or from the deposition of the substrates and/or products. Thus, activity becomes lower and the catalyst is deactivated. As a result, catalysts must be regenerated or eventually

replaced. Therefore, the development of effectively recyclable heterogeneous catalyst could offer major advantages.

A catalyst is a substance that increases the reaction rate without being consumed in the reaction and thus does not affect the equilibrium. Catalyzed reactions proceed faster than uncatalyzed reactions and can be used in repeated cycles of elementary steps. Catalytic activity is a quantitative measure of how fast a catalyst works, which is usually defined as the rate for conversion of reactants into products. Selectivity of a catalyst is a measure of the catalyst's ability to direct the conversion to the desired products. Therefore, the utilization of catalysis as a means of controlling the rate and direction of a chemical reaction has assumed a dominant role in many ongoing studies by scientists and technologists.

Generally, a catalyst can be classified as heterogeneous or homogeneous. A homogeneous catalyst operates in the same phase as the reagents and no phase boundary exists; this normally means that they are present as solutes in the liquid reaction mixture. A heterogeneous catalyst operates in a different phase from the reactants and it has a phase boundary separating it from the reactants [3-4].

1.1 Homogeneous catalysts [3-6]

Homogeneous catalysis derives its name from its most conspicuous feature: that is, the catalyst is in the same single homogeneous phase (virtually always liquid) as a chemical compound. This characteristic clearly differentiates it from heterogeneous catalysis, which usually implies solid catalysts for vapor or liquid phase reactions. Thus these two catalyst systems are apparently quite different in appearance, in experimental techniques, in theory, and in practical industrial applications.

The major disadvantage of homogeneous transition metal catalysts is the difficulty of separating the catalyst from the product.

Table 1.1 General, selected properties of homogeneous and heterogeneous catalysts

	Homogeneous	Heterogeneous
Active centers	all metal atoms	only surface atoms
Concentration	low	high
Selectivity	high	lower
Diffusion problems	practically absent	present
Reaction condition	mild (50-200 °C)	severe (often > 250 °C)
Application	limited	wide
Activity loss	irreversible reaction with products (cluster formation); poisoning	sintering of the metal crystallites; poisoning
Catalyst properties		
Structure/stoichiometry	defined	undefined
Modification possibilities	high	low
Thermal stability	low	high
Catalyst separation	sometimes laborious (chemical decomposition, distillation, extraction)	fixed-bed: unnecessary suspension: filtration
Catalyst recycling	possible	unnecessary
Cost of catalyst losses	high	low

1.2 Heterogeneous catalysts

Heterogeneous catalysts interact on their surfaces with reactants via chemisorption. The concept of chemisorption is a key to understanding catalyzed reactions. Catalyzed reactions consist of elementary steps on the catalyst surface in which chemical bonds are formed between surface atoms and an adsorbed molecule, followed by formation of new bonds between the fragments.

Heterogeneous catalysts are classified according to their functions as shown in Table 1.2. Transition metals are good catalysts for reactions related to hydrogen and hydrocarbons because these substances readily adsorb on the surfaces of metals. Noble metals that are resistant to oxidation at some relevant temperature may be used

as oxidation catalysts. Many oxides are excellent oxidation catalysts because they interact with oxygen and other molecules.

Table 1.2 Classification of representative heterogeneous catalysts [3]

Class	Example	Function
metals	Fe, Ni, Pd, Pt, Ag	hydrogenation dehydrogenation hydrogenolysis oxidation
metal oxides	NiO, ZnO, MnO ₂ Cr ₂ O ₃ , Bi ₂ O ₃ -MoO ₃	oxidation dehydrogenation

The substrate/catalyst ratio reflects the catalyst's efficiency, which is measured as the turnover number (TON) or turnover frequency (TOF). These definitions, however, vary slightly among the three catalysis fields. In homogeneous catalysis, the TON is the number of cycles that a catalyst can run through before it deactivates, i.e., the number of A molecules that one molecule of catalyst can convert to B molecules. The TOF is simply TON/time, i.e., the number of A molecules that one molecule of catalyst can convert to B molecules in one second, minute, or hour. In heterogeneous catalysis, TON and TOF are often defined per active site, or per gram catalyst.

1.3 Scope of research work

In this research, the catalytic oxidation of cyclohexane and ethylbenzene using heterogeneous catalysts such as layered double hydroxides, mixed metal oxides, polyoxometalates and transition metal incorporated xerogels were investigated. The physical properties of the catalysts, such as crystallinity, elemental content, thermal stability, acidity, basicity and surface area were examined. The effect of reaction parameters such as oxidant, temperature, reaction time, catalyst amount and types of solvent were studied. The stabilities and reusabilities of the catalysts were investigated.

1.4 Organization of this research

Chapter I describes the statement of the problems and scope of this research work. Chapter II lists the chemicals and characterization techniques. Chapter III describes the syntheses of the layered double hydroxide and mixed metal oxide catalysts and the oxidation of ethylbenzene. Chapter IV describes the preparation of polyoxometalates catalysts and their activity on the oxidation of ethylbenzene, cyclohexane and cyclohexanol. Finally, Chapter V describes the preparation of metal-incorporated xerogel catalysts for oxidation of cyclohexane using *tert*-butylhydroperoxide and/or air.



ศูนย์วิจัยทรัพยากร
จุฬาลงกรณ์มหาวิทยาลัย

CHAPTER II EXPERIMENTAL

The chemicals, equipments and characterization techniques for analysis of the catalysts were described.

2.1 Chemicals

All chemicals used are analytical grade.

Table 2.1 Chemical reagents and suppliers

Chemicals	Suppliers
Acetonitrile	Merck, Germany
Acetophenone	Fluka Chemies A.G., Switzerland
Aluminium nitrate nonahydrate	Fluka Chemies A.G., Switzerland
Ammonium carbonate	Aldrich Chemical Company, Inc., USA
Ammonium hydroxide	Fluka Chemies A.G., Switzerland
Barium sulphate	Fluka Chemies A.G., Switzerland
Benzyl alcohol	Fluka Chemies A.G., Switzerland
Benzaldehyde	Fluka Chemies A.G., Switzerland
Benzoic acid	Fluka Chemies A.G., Switzerland
Chromium nitrate	Fluka Chemies A.G., Switzerland
Cobalt acetate	Fluka Chemies A.G., Switzerland
Cobalt chloride	Fluka Chemies A.G., Switzerland
Cobalt nitrate	Fluka Chemies A.G., Switzerland
Copper nitrate	Fluka Chemies A.G., Switzerland
Cyclohexane	Merck, Germany
Cyclohexanol	Merck, Germany
Cyclohexanone	Fluka Chemies A.G., Switzerland
Decane	Fluka Chemies A.G., Switzerland
Diethyl ether	Fluka Chemies A.G., Switzerland
Dichloromethane	Merck, Germany
Disodium hydrogen orthophosphate	APS Chemicals, Ltd., Australia
Dodecanol	Fluka Chemies A.G., Switzerland

Table 2.1 Chemical reagents and suppliers (cont.)

Chemicals	Suppliers
Ethanol	Merck, Germany
Ethylbenzene	Merck, Germany
Heptane	Fluka Chemies A.G., Switzerland
Hexane	Merck, Germany
Hydrochloric acid fuming 37%	Merck, Germany
Hydroquinone	Merck, Germany
Iodine	Merck, Germany
Isooctane	Fluka Chemies A.G., Switzerland
Manganese nitrate	Aldrich Chemical Company, Inc., USA
Magnesium nitrate hexahydrate	Fluka Chemies A.G., Switzerland
Methanol	Merck, Germany
Nickel nitrate	Fluka Chemie A.G., Switzerland
Nitric acid	Merck, Germany
Ortho-phosphoric acid 85%	Merck, Germany
1-Phenyl ethanol	Fluka Chemies A.G., Switzerland
Perchloric acid 70%	Merck, Germany
Sodium carbonate	Aldrich Chemical Company, Inc., USA
Sodium hydroxide	Aldrich Chemical Company, Inc., USA
Sodium (meta) vanadate	Fluka Chemie A.G., Switzerland
Sodium hydrogen carbonate	Aldrich Chemical Company, Inc., USA
Sodium dihydrogen orthophosphate	APS Chemicals, Ltd., Australia
Sodium sulfate anhydrous	Merck, Germany
Tetrabutyl ammonium bromide	Fluka Chemie A.G., Switzerland

2.2 Equipments

- Round bottom flask
- Magnetic stirrer
- Reflux condenser
- Heater and stirrer
- Pressure reactor (stainless steel, size 100 mL)

2.3 Catalyst characterization

The instruments and techniques used for characterization were specified in the following.

2.3.1 Fourier transform infrared spectroscopy (FTIR)

Fourier transform infrared spectra were recorded on a Nicolet FT-IR Impact 410 Spectrophotometer. The solid samples were prepared by pressing the samples with KBr. Infrared spectra were recorded between 400-4000 cm^{-1} in transmittance mode.

2.3.2 X-ray diffraction (XRD)

The XRD patterns of catalysts were obtained on Rigaku, DMAX 2002 Ultima Plus X-ray powder diffractometer equipped with a monochromator and a Cu-target X-ray tube (40 kV, 30 mA) and angles of 2θ ranged from 2-90 degree. X-ray diffraction is used to obtain information about the structure and composition of the catalysts.

2.3.3 Diffuse reflectance ultraviolet-visible spectroscopy (DRUV) and ultraviolet-visible spectroscopy (UV-vis)

Diffuse reflectance UV-visible spectra were recorded on UV-vis 2550 spectrophotometer Shimadzu UV probe. The solid samples were prepared by pressing the sample into a specially designed cell. BaSO_4 was used as the reference material. DRUV-visible was recorded at wavelengths between 200-800 nm in reflectance and transmittance mode. The liquid samples were analyzed with the same equipment but using a quartz cuvette as a sample holder.

2.3.4 Nitrogen adsorption (Brunauer-Emmett-Teller method (BET))

BET specific surface area of the catalysts was carried out using a BELSORP-mini. The principle of this method is by adsorption of a particular molecular species from a gas or liquid onto the surface. Based upon one single adsorbed layer, the quantity of adsorbed material correlates directly the total surface area of the sample. The pore size distributions were obtained according to the Barret–Joyner–Halenda (BJH) method from the adsorption branch data.

2.3.5 Thermogravimetric analysis (TGA)

TGA involves heating a sample in an inert or oxidizing atmosphere and measuring the weight. The weight change over specific temperature ranges provides indications of the composition of the sample and thermal stability. Measurement of the residue mass of substances according to a controlled temperature program was made using Netzsch DMA 242 thermal analyzer with an increment of 20°C/min over the temperature range of 30 to 1000°C under nitrogen atmosphere.

2.3.6 Temperature program desorption (NH₃-TPD)

The acidic properties of samples were measured by temperature programmed desorption (TPD) of NH₃ by a commercial TPD system MODEL BEL-CAT equipped with a quadrupole mass spectrometer.

The chemisorption of pure ammonia gas on the surface of the sample was carried out using Micromeritics Pulse Chemisorb-2705. The sample was kept in a U-shaped quartz tube and the tube was placed in a split furnace. The sample was evacuated at 400°C in helium gas (99.95%) flow for 1 h (heating rate of 10°C/min) after that, samples was pretreated in helium atmosphere for 1 h at predetermined temperature 400°C. prepared by heating at temperature (300°C) was first heated in situ at 300°C in flowing of argon for 2 h to remove the moisture which might have adsorbed during the transfer of sample at various stages. The chemisorption of pure ammonia on the preheated sample was carried out at 120°C by repeatedly injecting the pulse of pure ammonia gas onto the sample till the saturation was observed. The amount of ammonia chemisorbed on the sample in every pulse was shown by thermal conductivity detector (TCD) in the form of integrated area of the ammonia peak. From the peak areas, the acidity in terms of mmol of ammonia chemisorbed per gram of sample was calculated.

2.3.7 Temperature program reduction (H₂-TPR)

Temperature-programmed reduction (TPR) experiments were recorded on a TPR MODEL BEL-CAT equipped with a thermo-conductivity detector (TCD).

The catalyst (0.1 g) was pretreated at 400°C under an O₂ flow and maintained at this temperature for 2 h. The catalyst samples were cooled to 100°C and then maintained at this temperature for 30 min. Subsequently, the sample was switched to 5% hydrogen balance argon mixture and the samples were heated at 10°C/min to a final temperature at 900°C.

2.3.8 Inductively coupled plasma (ICP)

ICP was performed with Perkin Elmer model PLASMA-1000 at the Scientific and Technology Research Equipment Centre (STREC), Chulalongkorn University. The samples were prepared by digestion with concentrated nitric acid and dilute with deionized water.

2.3.9 Basicity measurement

The solid catalysts (0.1 g) were stirred in 6.25 mL of distilled water at room temperature for 1 h and then filtered. The filtrates were titrated with 0.02 M benzoic acid solution (in methanol). The indicator used was bromothymol blue (pH range 6-9). The basicity was calculated from the mmol of benzoic acid used in the titration of ca. 0.1 g of catalyst.

2.3.10 Gas chromatography (GC)

Gas chromatographic analyses were performed on a Varian CP-3800 gas chromatograph equipped with a flame ionization detector and a 30 m (0.25 mm i.d., 0.25 µm film thickness) DB-WAX capillary column with nitrogen gas as the carrier gas, with a pressure of 80 kPa and a flow rate of 1.5 mL/min.

The conditions used for the determination of the substrates and products were set as follows:

Gas chromatography condition for various substrates

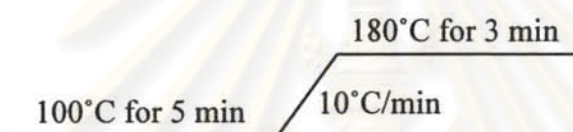
Injector: 220°C

Detector: 250°C

Programmed temperature

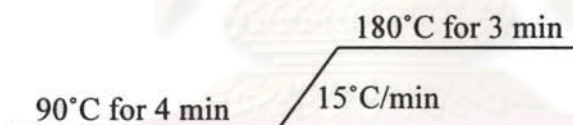
Ethylbenzene

Analytical time = 16.0 min



Cyclohexanol and cyclohexane

Analytical time = 12.3 min



The products were analyzed by gas chromatography using internal standard.

$$\% \text{conversion} = \frac{\text{moles converted}}{\text{moles initial}}$$

$$\% \text{selectivity} = \frac{\text{moles of desired product formed}}{\text{moles of total products formed}} \times 100$$

CHAPTER III

CATALYTIC OXIDATION OF ETHYLBENZENE USING LAYERED DOUBLE HYDROXIDES AND MIXED METAL OXIDES

3.1 Introduction

To increase the value of ethylbenzene, which is a low price chemical, still remains a challenge. Acetophenone is the main product from ethylbenzene oxidation. The use of stoichiometric amounts of oxidizing agent leads to problems with respect to environmental damage, corrosion, recycling and separation. In addition, the use of organic solvents also creates a problem.

Heterogeneous catalysis offers environmentally benign routes for organic synthesis. Reactions which can be carried out without any solvent to give high conversions and selectivities would be especially valuable. The oxidation of ethylbenzene with heterogeneous catalysts has been reported using metal oxide supported on mesoporous materials [8] and metal complexes supported on zeolites [9]. However, low selectivities to acetophenone and high leaching of metal into the reaction products were still a problem.

3.1.1 Layered double hydroxide (LDH)

Layered double hydroxide (LDH) or hydrotalcite-like materials belong to a large class of natural and synthetic anionic clays [10]. These basic solid materials show many potentially attractive applications such as: adsorbents, anion exchangers, and most importantly as basic catalysts [8-15]. Due to the unique properties of these materials, these species are candidates for a number of industrial applications [16]. The general formula of a typical LDH is $[M^{2+}_{1-x} M^{3+}_x (OH)_2][A^{n-}]_{x/n} \cdot mH_2O$ in which M^{2+} represents a divalent metal cation (Mg, Ni, Zn, Co, Fe, etc) and M^{3+} a trivalent metal cation (Al, Fe, Cr, Mn, etc.), while A^{n-} is an n -valent anion. The structure of such a layered double hydroxide is shown in Figure 3.1. The most frequent divalent metals are those whose ionic radii vary from 0.65 Å (Mg) to 0.83 Å (Mn, high spin) whereas the radii of the trivalent metal vary between 0.50 Å (Al) and 0.69 Å (Cr) [17]. The formation of these species generates intercalated hydrotalcite (HT)

structures that are named after the natural mineral $\text{Mg}_6\text{Al}(\text{OH})_{16}\text{CO}_3\cdot 4\text{H}_2\text{O}$. While anions such as SO_4^{2-} , Cl^- , OH^- , NO_3^- or CO_3^{2-} can occupy the intersheet space to balance the positive charges, CO_3^{2-} ion is preferred [18]. The electroneutrality and the stability of layered double hydroxides are assured by the interlamellar anions (A^n) and water molecules. Commonly, x is in the range of 0.20-0.33 ($\text{M}^{2+}/\text{M}^{3+}$ between 2 and 4) [11,19]. The structure and surface properties of hydrotalcites and the resulting mixed metal oxides strongly depend on chemical composition and synthesis procedure [20-21].

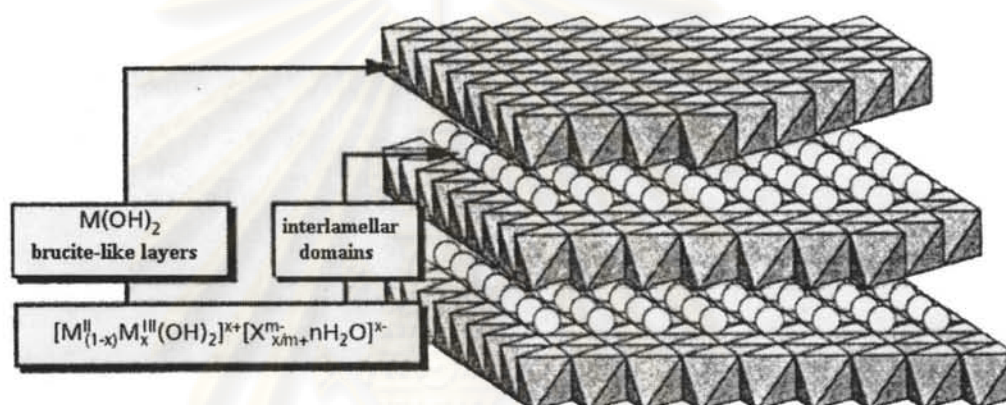


Figure 3.1 Schematic view of layered double hydroxide structure and general formula [22].

As anions in the interlayer space are necessary to counterbalance the positive charge of the brucite-like layers, LDHs are widely used as ion exchangers and for depollution in adsorption [23]. However, the basicity of the LDHs has stimulated their use as catalysts, allowing the substitution of liquid NaOH or KOH solutions to produce less polluting processes, since the formation of salts as byproducts is avoided. LDHs are used as solid base catalysts for many reactions such as biodiesel synthesis [24], aldol condensations [25], Wittig reactions [26], steam reforming of methane [27], oxidations [28] and hydrogenations [29]. Transition metal cations as potential catalytic active centers can be readily incorporated into the hydrotalcite framework via their isomorphic substitution for Mg^{2+} or Al^{3+} cations.

3.1.2 Preparation of layered double hydroxides

LDH compounds have been synthesized by direct methods, which include coprecipitation, sol-gel synthesis, hydrothermal growth and electrochemical synthesis. Indirect methods include all syntheses that use an LDH as a precursor. Examples of these are all anion exchange-based methods such as direct anion exchange, anion exchange by acid attack with elimination of the guest species in the interlayer region and anion exchange by surfactant salt formation [30].

Table 3.1 Ionic radii of metal ions

Cations	Radii (nm)	Electronegativity Pauling
Mg ²⁺	6.6 (7.2)	1.31
Ni ²⁺	6.9	1.91
Co ²⁺	7.2 (HS = 7.4; LS = 6.5)	1.88
Cu ²⁺	7.2 (7.3)	1.90
Mn ²⁺	(HS = 8.3; LS = 6.7)	1.55
Cr ³⁺	6.3	1.66
Al ³⁺	5.1	1.61

LS = low spin; HS = high spin, Values in brackets are from Ref. [31]

3.1.3 Thermal treatment of layered double hydroxides

The important area in layered double hydroxide materials research is phase transformation during compound synthesis as shown in Figure 3.2. Thermal treatments or calcinations of LDHs result progressively in the loss of water molecules at the surface, followed by interlamellar water molecules and lastly, roughly in the 200-350°C range, by the dehydroxylation of the main layers leading to the collapse of the structure. Depending on the interlamellar species, they can also be removed thermally, at either relatively low temperatures (e.g., sulfate or chloride) or at high temperatures (e.g., phosphate). From this process one obtains an LDH having basic mixed metal oxides with a homogeneous interdispersion of the metals and a better resistance to sintering than the corresponding supported material [19-20]. These mixed metal oxides display generally a relatively high specific surface area up to 150 m²/g compared to the prepared LDH (< 100 m²/g).

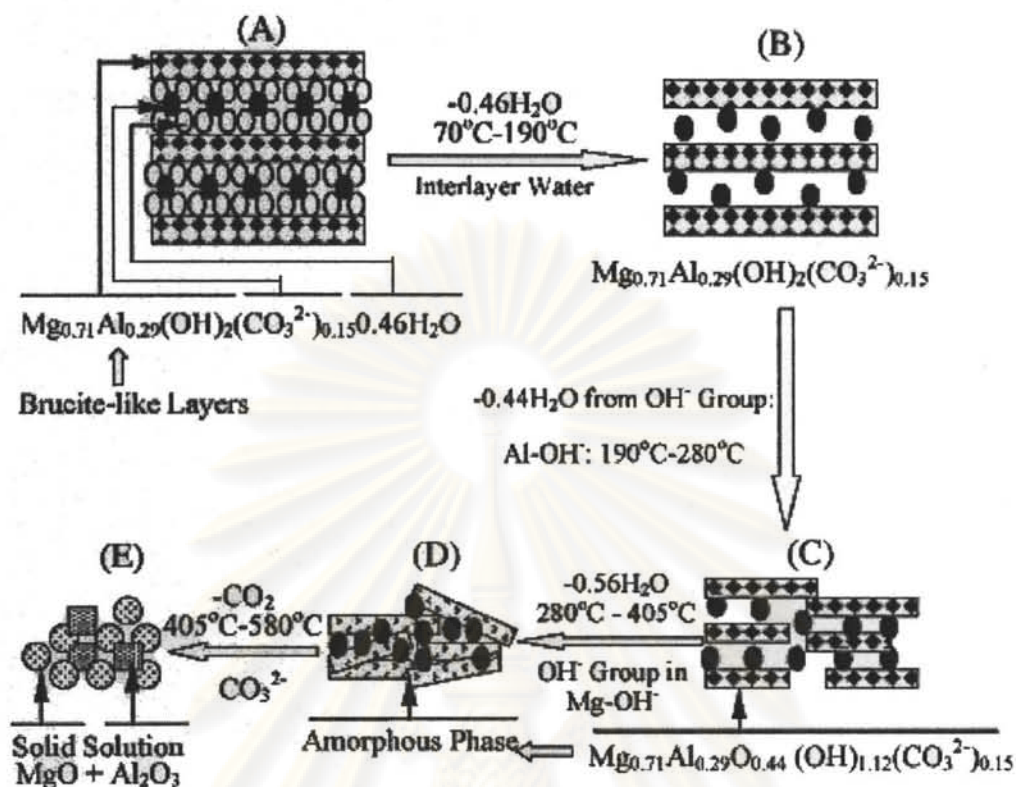


Figure 3.2 The thermal treatment of MgAl- CO_3 LDH as a function of temperature [32].

Five distinct stages have been identified by Yang and co-workers [32] during the thermal decomposition of MgAl- CO_3 LDH.

Stage (A) is the formation of the original MgAl- CO_3 LDH.

Stage (B) develops from Stage (A) by the removal of the loosely held interlayer water molecules in the temperature range of 70-90°C.

Stage (C) evolves from Stage (B) by the removal of OH groups, likely bonded in a bridge Al-(OH)-Mg configuration, which decreases the basal spacing or the thickness of the MgAl- CO_3 LDH layers. It occurs in the temperature range of 190-300°C.

Stage (D) was achieved mostly with the removal of OH groups in Mg-OH (Mg-OH-Mg) in the temperature range of 300-405°C.

Stage (E) is obtained by the decarbonation of Stage (D) in the temperature range of 405-580°C. The weight loss in this temperature range results from the removal of a CO_2 molecule from a CO_3^{2-} anion as described in Equation (3.1) and Figures 3.2-3.3.

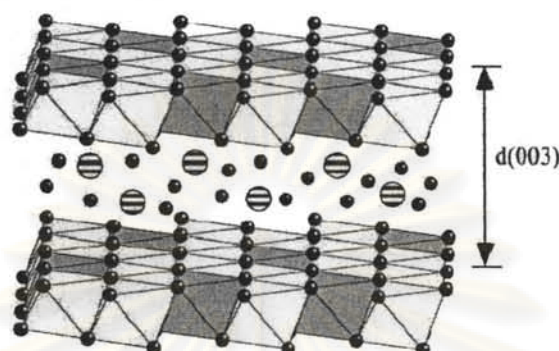
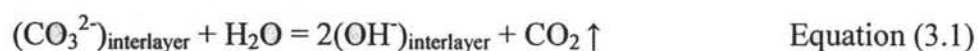


Figure 3.3 Structure of hydrotalcite, showing the brucite-type layer with the M^{2+} and M^{3+} cations (grey and white octahedra) and the interlayer space with the CO_3^{2-} anions (stripes) and the H_2O molecules (black) [32].

3.1.4 Rehydration of mixed metal oxide

The rehydration of mixed metal oxide materials in a solution containing an anion such as carbonate could convert the materials back to their original structures. The rehydration process can also be performed in moist air.

3.2 Literature reviews

Some of the research reports using layered double hydroxide and mixed metal oxide as catalyst are described below.

In 1998, Costantion *et al.* [33] reported the synthesis of ZnAl-CO_3 LDHs by coprecipitation of Zn^{2+} and Al^{3+} hydroxycarbonates. The carbonate was converted into the chloride form $\text{Zn}_{0.65}\text{Al}_{0.35}(\text{OH})_2\text{Cl}_{0.35}\cdot 0.4\text{H}_2\text{O}$, which was then fully exchanged with H_2PO_4^- , HPO_4^{2-} and $\text{C}_6\text{H}_5\text{PO}_3\text{H}^-$ anions. As a consequence of the exchange or of subsequent thermal treatment, hydrogen phosphates and phosphonates reacted with the hydroxyls of the layers and attached themselves to the inorganic layer by a covalent bond.

In 1998, Kaneda *et al.* [34] studied the catalytic activity of $\text{Mg}_{6.0}\text{Al}_{2.0}\text{Ru}_{0.5}(\text{OH})_{16}\text{CO}_3$ LDH for the oxidation of cinnamyl alcohol under an oxygen atmosphere in various solvents. Toluene, chlorobenzene and benzene were good solvents, yielding 95, 93 and 92% cinnamaldehyde. The oxidation of cinnamyl alcohol at 80°C gave the highest yield. However an increase of the reaction temperature to over 100°C resulted in low selectivities. This LDH also catalyzed the oxidation of allylic and benzylic alcohols in toluene at 80°C. The results showed that primary alcohols were oxidized faster than secondary alcohols. This catalyst can be reused, though with an appreciable loss of the activity and selectivity.

In 2001, Bahranowski *et al.* [35] studied the catalytic oxidation of toluene with $[(\text{Zn}_{1-y}\text{Cu}_y)_{1-x}\text{Al}_x(\text{OH})_2](\text{NO}_3)_x \cdot n\text{H}_2\text{O}$ ($x \cong 0.33$, $0.6 \leq y \leq 1.0$, $n \cong 0.5$) layered double hydroxides using H_2O_2 as oxidant. The molar ratio of substrate: H_2O_2 : CH_3CN :water was 1.00:0.97:6.71:4.27. From their results it could be concluded that significant quantities of oxidation products appeared only for the catalyst containing a relatively small amount of Cu, such as in the $\text{Zn}_{0.95}\text{Cu}_{0.05}$ catalyst, which gave toluene conversions of 12.4% and 15.9% at 60 and 90°C, respectively.

In 2002, Carpentier *et al.* [36] reported the preparation of a Mg-Al-Pd LDH by coprecipitation of the corresponding metal chlorides (MgCl_2 , AlCl_3 and H_2PdCl_4). The catalyst, which was calcined at 290°C, showed high activity (80-88% conversion) in the vapor phase oxidation of toluene using molecular oxygen at 290 and 400°C.

In 2004, Choudhary *et al.* [37] published a study involving MnO_4^- exchanged MgAl hydrotalcites ($\text{Mg}/\text{Al} = 2-10$) which were used as catalysts for the solvent-free oxidation of ethylbenzene by molecular oxygen (10 atm) at 130°C. Conversion of ethylbenzene was enhanced when the Mg/Al mole ratio was increased. For Mg/Al mole ratio = 10, the conversion of ethylbenzene was maximized, to 23%. The catalyst showed excellent reusability. However, selectivity to acetophenone remained high (> 95%).

In 2005, Barbosa *et al.* [38] reported the preparation of MgAl hydrotalcites, $\text{Mg}_{(1-x)}\text{Al}_x(\text{OH})_2(\text{CO}_3)_{x/2} \cdot n\text{H}_2\text{O}$, containing an iron-phthalocyanine complex as a catalyst for the oxidation of catechol, using hydrogen peroxide as the oxidant. The

catalysts showed enhanced activities and stabilities, compared to their homogeneous counterparts. The catechol conversions were 63, 73 and 88% for the catalysts with $x = 0.20, 0.25$ and 0.33 , respectively.

In 2005, Kawabota *et al.* [39] reported the preparation of nickel-containing MgAl hydrotalcite catalysts by the coprecipitation method. Catalytic oxidation of benzyl alcohol over $\text{Mg}_{2.5}\text{Ni}_{0.5}\text{Al}$ LDH by oxygen was performed at 60°C . It was found that cyclohexane, hexane and toluene were good solvents, yielding 57.9, 54.0 and 51.8% benzaldehyde as the major product with the maximum selectivity (97.8%) in toluene.

In 2006, Jana *et al.* [40] prepared a NiAl LDH, using a modified coprecipitation method, with Ni/Al mole ratios of 2-5 by using CO_3^{2-} , Cl^- , NO_3^- , or SO_4^{2-} as guest inorganic anions. The catalytic activities were tested in ethylbenzene oxidation with oxygen at 135°C . Activity increased with increasing Ni content, so that a NiAl- CO_3 with Ni/Al mole ratio of 5:1 gave the highest activity (47% conversion and 99% selectivity to acetophenone); however, a NiAl- CO_3 with Ni/Al mole ratio of 3:1 showed 31% conversion. For Cl^- , NO_3^- and SO_4^{2-} anions, one obtained only 28, 24 and 23% conversions and 79, 74 and 64% acetophenone selectivities, respectively. In the presence of hydroquinone no reaction was observed, and thus it can be concluded that this reaction occurred via a free radical mechanism.

In 2006, Hulea *et al.* [41] reported the catalytic oxidation of thiophenes and thioethers with hydrogen peroxide using W-containing layered double hydroxides. The catalysts were prepared by ion exchange of MgAl- NO_3 with tungstate anions at pH 6.5 and 9.5 to produce phosphotungstate-LDH (WO_4^{2-} anion) and W-LDH ($\text{W}_7\text{O}_{24}^{6-}$ anion). The W-LDH catalyst showed higher activity due to higher thermally stability.

In 2007, Llamas *et al.* [42] reported the Baeyer-Villiger oxidation of cyclohexanone to ϵ -caprolactone with hydrotalcite ($\text{Mg}_{0.8}\text{Al}_{0.2}(\text{OH})_2(\text{CO}_3)_{0.1}\cdot 0.7\text{H}_2\text{O}$) catalysts at 70°C , using H_2O_2 as the oxidant in the presence of sodium dodecylbenzenesulfonate as a surfactant at 70°C in 6 h. The effect of solvent on

cyclohexanone conversion was studied. The order of conversion was: benzonitrile (100%) > methanol (73%) > toluene (65%) > 1-butanol (58%) > methanol (73%).

In 2008, George *et al.* [43] synthesized nickel-substituted copper chromite spinel catalysts ($\text{Cu}_{1-x}\text{Ni}_x\text{Cr}_2\text{O}_4$, where $x = 0, 0.25, 0.5, 0.75$ and 1.0) by the coprecipitation method, followed by calcination at 650°C . The catalysts were used for the oxidation of ethylbenzene with TBHP. The results showed that the $\text{Cu}_{0.5}\text{Ni}_{0.5}\text{Cr}_2\text{O}_4$ catalyst gave 56% conversion and 69% selectivity to acetophenone at 70°C for 8 h in acetonitrile. In a solvent-free system the conversion of ethylbenzene was 60%. The CuCr_2O_4 catalyst gave a higher selectivity to 1-phenylethanol. The catalysts were reported to be stable under the reaction condition.

3.3 Preparation of the catalysts

The layered double hydroxide catalyst precursors were prepared by two methods.

3.3.1 Alkali coprecipitation methods [11, 33]

3.3.1.1 Binary layered double hydroxide

Preparation of Ni_xAl LDH with $\text{M}^{2+}/\text{M}^{3+}$ mole ratio of 3 and 5

An aqueous mixture (60 mL) of 54 or 90 mmol of $\text{Ni}(\text{NO}_3)_2 \cdot 6\text{H}_2\text{O}$ and 18 mmol of $\text{Al}(\text{NO}_3)_3 \cdot 9\text{H}_2\text{O}$ (mole ratio of $\text{Ni}/\text{Al} = 3$ and 5) was added slowly to 90 mL of an aqueous solution of Na_2CO_3 (180 mmol). The pH of the mixture was held at 11 by the dropwise addition of 0.1 M NaOH. The resulting gel-like material was heated to 60°C while being stirred vigorously for 18 h, and then filtered and thoroughly washed with distilled water until the filtrate was neutral. Finally, it was dried in an oven at 110°C for 18 h. The material was denoted as Ni_3Al or Ni_5Al LDH.

The same method was used for the preparations of other LDHs by using nitrate salt of Mg, Mn, Co, Cu or Cr. The prepared samples were designated as follows.

Table 3.2 Designation of the binary layered double hydroxide

M^{2+}	M^{3+}	M^{2+}/M^{3+} mole ratio
Ni^{2+}	Al^{3+}	3.0 and 5.0
Co^{2+}	Al^{3+}	5.0
Cu^{2+}	Al^{3+}	5.0
Mg^{2+}	Al^{3+}	5.0
Ni^{2+}	Cr^{3+}	5.0
Co^{2+}	Cr^{3+}	5.0

3.3.1.2 Ternary layered double hydroxides

Ternary LDH materials were synthesized by coprecipitation under low levels of supersaturation as described in the literature [44]. In this method, two aqueous solutions were employed. The first contained nitrates of Ni, Co, Cu, Mg, Mn or Cr and $Al(NO_3)_3 \cdot 9H_2O$ with concentrations of each = 0.06 M, the mole ratios of $Mg^{2+}/M^{2+} = 3$ and $((Mg^{2+}/M^{2+})/Al^{3+}) = 4$, except for the CrMgAl LDH for which the $Cr(NO_3)_3 \cdot 9H_2O : (Mg(NO_3)_2 \cdot 6H_2O) : Al(NO_3)_3 \cdot 9H_2O$ mole ratio was 1:3:1. The second solution, serving as a precipitating agent, contained 0.6 M NaOH and 0.06 M Na_2CO_3 , and was added slowly to the first while maintaining the pH at 10. The samples were aged at 65°C for 18 h, then filtered off, washed thoroughly with distilled water until the filtrate was neutral and dried in air at 110°C for 12 h.

Table 3.3 Designation of the ternary layered double hydroxide

M^{2+} (or Cr^{3+})	M^{3+}
Ni^{2+}, Mg^{2+}	Al^{3+}
Co^{2+}, Mg^{2+}	Al^{3+}
Cu^{2+}, Mg^{2+}	Al^{3+}
Mn^{2+}, Mg^{2+}	Al^{3+}
Cr^{3+}, Mg^{2+}	Al^{3+}

During the preparation of these LDHs, at the aging step of the Cu_5Al LDH the color of the gel-like material changed from blue to gray during the first hour. Then

after 18 h the color was black which indicated copper oxide formation; however, this was not observed in the case of the $\text{Cu}_{1.0}\text{Mg}_{2.9}\text{Al}$ LDH.

3.3.2 Alkali - free coprecipitation method [45]

The procedure was the same as in the coprecipitation method except that Na_2CO_3 was replaced by $(\text{NH}_4)_2\text{CO}_3$. In a typical procedure, an aqueous mixture (60 mL) of 90 mmol of $\text{Ni}(\text{NO}_3)_2 \cdot 6\text{H}_2\text{O}$ and 18 mmol of $\text{Al}(\text{NO}_3)_3 \cdot 9\text{H}_2\text{O}$ (Ni/Al mole ratio = 5) was added slowly to 90 mL of an aqueous solution of $(\text{NH}_4)_2\text{CO}_3$ (180 mmol). The pH of the mixture was held at pH 11 by the dropwise addition of 0.1 M NH_4OH . The resulting gel-like material was heated to 60°C for 18 h and then filtered, and thoroughly washed with distilled water until the filtrate was neutral. Finally, it was dried in an oven at 110°C for 18 h.

3.3.3 Calcination of layered double hydroxides

The calcination of an LDH was carried out in the presence of air at 500°C for 5 h with a heating rate of $5^\circ\text{C}/\text{min}$. The material was then cooled to room temperature, yielding the corresponding mixed oxides. These solids were kept in a desiccator.

3.3.4 Rehydration of mixed metal oxide [46]

0.2 g of sample was stirred in 10 mL of 0.1 M Na_2CO_3 solution at room temperature for 48 h. The mixtures were filtered, washed several times with deionized water, and dried at 110°C for 12 h.

ศูนย์วิทยทรัพยากร
จุฬาลงกรณ์มหาวิทยาลัย

3.4 Catalyst characterization

The compositions of the catalysts were determined by ICP. The structures of the catalysts were characterized by FTIR, DRUV and XRD. Surface characteristics and thermal properties were measured by BET and TGA. The soluble basicity was also determined. The results are described below.

3.4.1 Composition of mixed metal oxide catalysts

After digestion of catalysts with concentrated nitric acid and dilution with water, the metal contents in the catalysts were determined by ICP analysis. The results are given in Tables 3.4-3.5.

Table 3.4 Composition of binary mixed metal oxide catalysts

Catalyst
Ni _{3,1} Al oxide
Ni _{4,8} Al oxide
Co _{4,5} Al oxide
Cu _{4,9} Al oxide
Mg _{4,9} Al oxide
Ni _{5,1} Cr oxide
Co _{4,8} Cr oxide

Table 3.5 Composition of ternary mixed metal oxide catalysts

Catalyst
Ni _{0,9} Mg _{2,1} Al oxide
Co _{0,8} Mg _{1,6} Al oxide
Cu _{1,0} Mg _{2,9} Al oxide
Mn _{0,9} Mg _{2,2} Al oxide
Cr _{0,8} Mg _{2,4} Al oxide

The atomic mole ratios of the catalysts are close to the values expected from the starting solutions. Small variations are due to the solubility differences of the

various types of metal salt. Higher Mg contents were found in these metal oxide materials due to the high solubility of $Mg(NO_3)_2$ at the utilized pH of 10 [29].

3.4.2 Surface analysis by nitrogen adsorption of LDHs and mixed metal oxides

The specific surface areas and the texture of the catalysts were determined by nitrogen physisorption according to the Brunauer-Emmett-Teller (BET) method. The values for the Ni/Al LDH catalysts are shown in Table 3.6. Those for the binary metal and ternary metal catalysts are shown in Tables 3.7-3.8 and the pictures are shown in appendix A.

Table 3.6 Surface area measurement of Ni/Al LDH and oxide prepared with different methods

Method	Catalyst	Surface area (m^2/g)	Pore volume (cm^3/g)	Mean pore diameter (nm)
Alkali	Ni _{3.1} Al LDH	89	0.2	6
	Ni _{3.1} Al oxide	125	0.3	7
	Ni _{4.8} Al LDH	100	0.2	7
	Ni _{4.8} Al oxide	144	0.3	8
Alkali-free	Ni _{4.9} Al LDH	95	0.2	7
	Ni _{4.9} Al oxide	139	0.3	8

The surface areas of all the NiAl LDH catalysts are in the range of 89-100 m^2/g . Calcination removed water on surface, interlamellar water and decarbonation of carbonate species at the interlamellar LDH. Thus, the removal of water and CO_2 molecules during calcination can lead to the formation of channels and pores, which help to increase in specific surface areas. The increases of the specific surface areas are accompanied by increases in the pore volumes. The same result was observed in previous studies [10,47].

Table 3.7 Surface analysis of binary LDH and mixed metal oxide catalysts

Catalyst	Surface area (m ² /g)	Pore volume (cm ³ /g)	Mean pore diameter (nm)
Mg _{4,9} Al LDH	230	0.7	9
Mg _{4,9} Al oxide	306	0.8	12
Co _{4,5} Al LDH	70	0.5	10
Co _{4,5} Al oxide	105	0.6	11
Cu _{4,9} Al LDH	60	0.3	10
Cu _{4,9} Al oxide	77	0.4	12
Ni _{5,1} Cr LDH	60	0.5	15
Ni _{5,1} Cr oxide	71	0.6	17
Co _{4,8} Cr LDH	50	0.5	12
Co _{4,8} Cr oxide	41	0.6	13

The surface area of Mg_{4,9}Al LDH is 230m²/g, which is higher than other LDHs (50-70 m²/g). From a comparison of the Ni_{4,8}Al LDH and Co_{4,5}Al LDH materials, the former is seen to have a higher surface area. After calcination to mixed metal oxides, the Ni-containing catalysts have higher surface areas. This might be due to the stronger interaction between NiO and Al₂O₃ which prevents the sintering of the metal oxide particles [48].

Table 3.8 Surface area measurement of ternary MMgAl LDHs and oxide materials

Catalyst	Surface area (m ² /g)	Pore volume (cm ³ /g)	Mean pore diameter (nm)
Ni _{0.9} Mg _{2.1} Al LDH	114	0.2	7
Ni _{0.9} Mg _{2.1} Al oxide	130	0.3	8
Co _{0.8} Mg _{1.6} Al LDH	100	0.2	9
Co _{0.8} Mg _{1.6} Al oxide	174	0.3	10
Cu _{1.0} Mg _{2.9} Al LDH	118	0.3	10
Cu _{1.0} Mg _{2.9} Al oxide	150	0.4	12
Mn _{0.9} Mg _{2.2} Al LDH	90	0.3	11
Mn _{0.9} Mg _{2.2} Al oxide	110	0.6	21
Cr _{0.8} Mg _{2.4} Al LDH	162	0.5	10
Cr _{0.8} Mg _{2.4} Al oxide	173	0.7	16

From Table 3.8, the ternary LDH samples show surface areas in the range of 90-162 m²/g. After calcination, their corresponding mixed metal oxide samples have increased surface areas (110-174 m²/g). The pore volumes and mean pore diameters of the mixed metal oxide samples were enhanced after being calcined.

ศูนย์วิทยทรัพยากร
จุฬาลงกรณ์มหาวิทยาลัย

3.4.3 Fourier transform infrared spectroscopy (FTIR) of LDHs and mixed metal oxides

The FTIR spectra of the Ni_{4.8}Al LDHs prepared by alkali and alkali-free coprecipitation methods are shown in Figure 3.4.

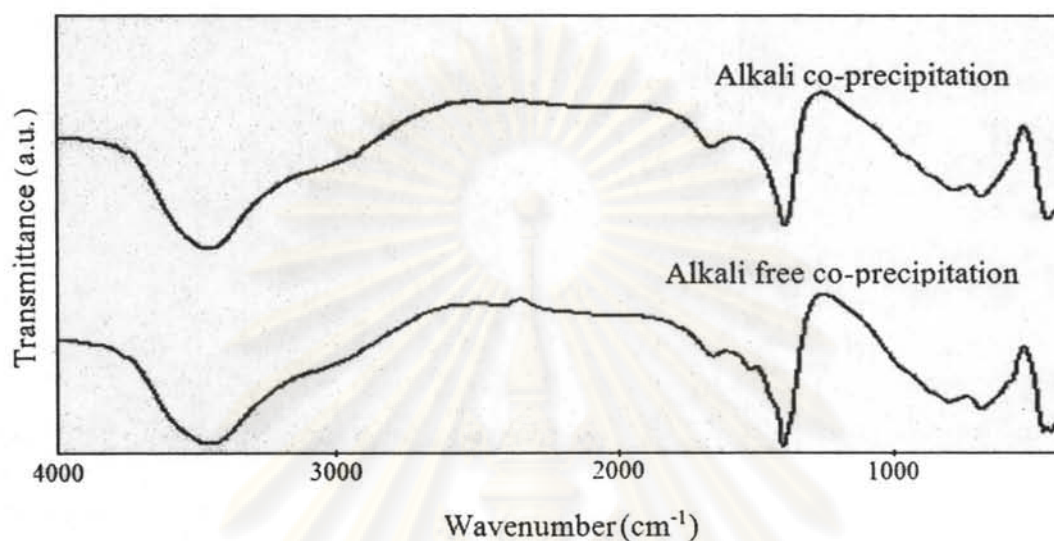


Figure 3.4 FTIR spectra of NiAl LDH prepared by alkali and alkali-free coprecipitation methods.

A band centered around 3400-3500 cm⁻¹ could be associated with an O-H stretch while a water deformation was observed around 1625 cm⁻¹. The sharp absorption appearing around 1380 cm⁻¹ is due to an interlayer vibrational mode of the carbonate ion [46]. The bands observed in the low-frequency region, 850-650 cm⁻¹, correspond to metal-oxygen (M-O) vibrations.

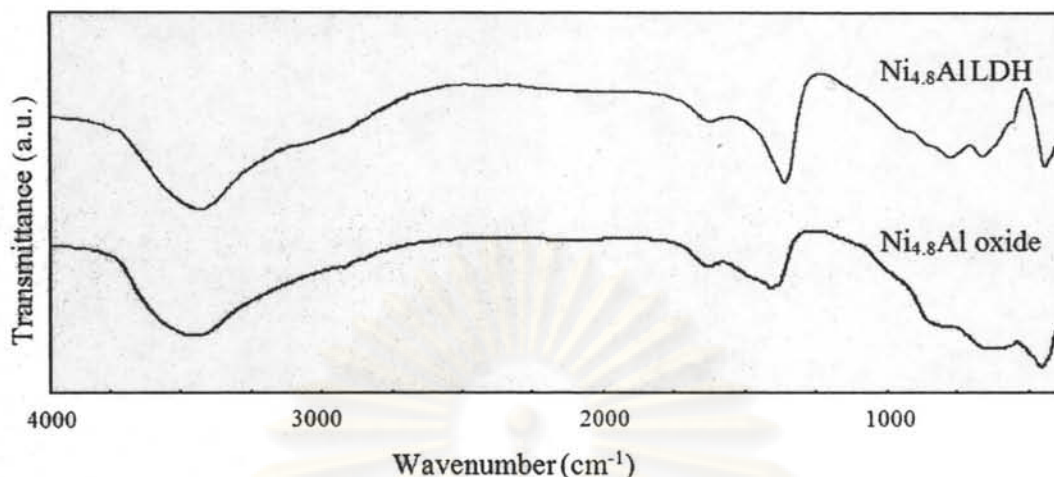


Figure 3.5 FTIR spectra of the $\text{Ni}_{4.8}\text{Al}$ LDH and oxide catalysts prepared by the coprecipitation method.

In Figure 3.5 the FTIR spectrum of *as-synthesized* or LDH shows a peak at 1380 cm^{-1} indicated the carbonate ion in the sample, and the intensity of this peak decreased after calcination. The existence of this peak might arise from the adsorption of carbon dioxide from air onto the surface of metal oxide. The other samples were collected in appendix B.

3.4.4 X-ray diffraction (XRD) of LDHs and mixed metal oxides

Phase of the samples were characterized by powder XRD analyzer, the results are given in appendix C and below.

3.4.4.1 XRD of binary layered double hydroxides

The XRD patterns of the Ni/Al LDH samples prepared by alkali and alkali-free coprecipitation methods are shown in Figure 3.6.

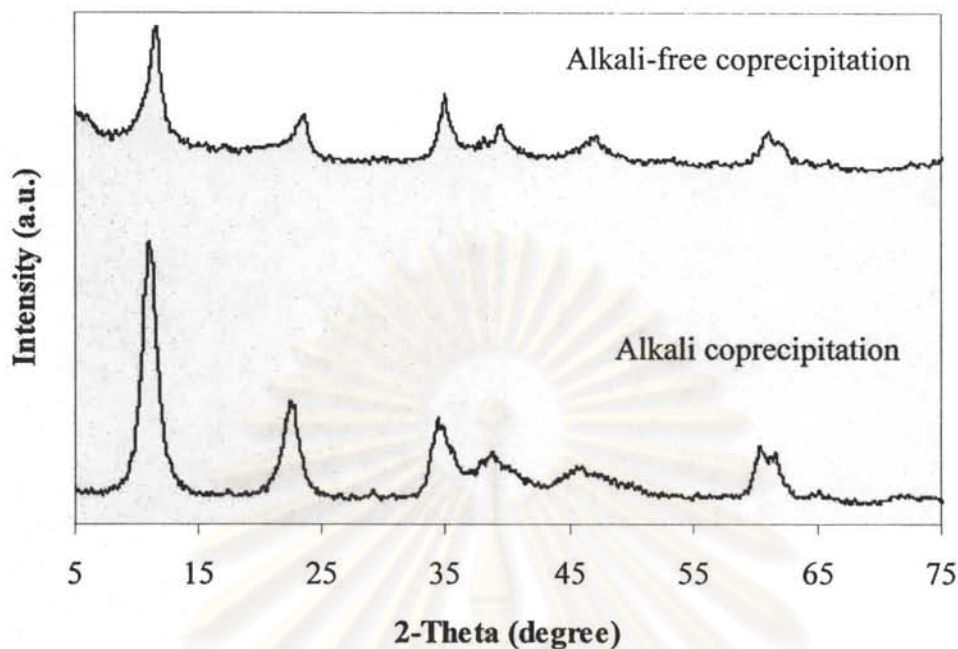


Figure 3.6 XRD patterns of NiAl LDH prepared with alkali and alkali-free coprecipitation methods.

The samples show sharp and intense peaks at low diffraction angles of $2\theta = 11^\circ$, 24° and 35° , ascribed to diffraction by basal planes (003), (006) and (009) of the LDHs, respectively. The broad and less intense peaks at higher angles of $2\theta = 38^\circ$, 46° and 60° can be ascribed to diffraction by the (105), (108) and (110) planes, respectively (JCPDS 41-1428) [10].

ศูนย์วิทยทรัพยากร
จุฬาลงกรณ์มหาวิทยาลัย

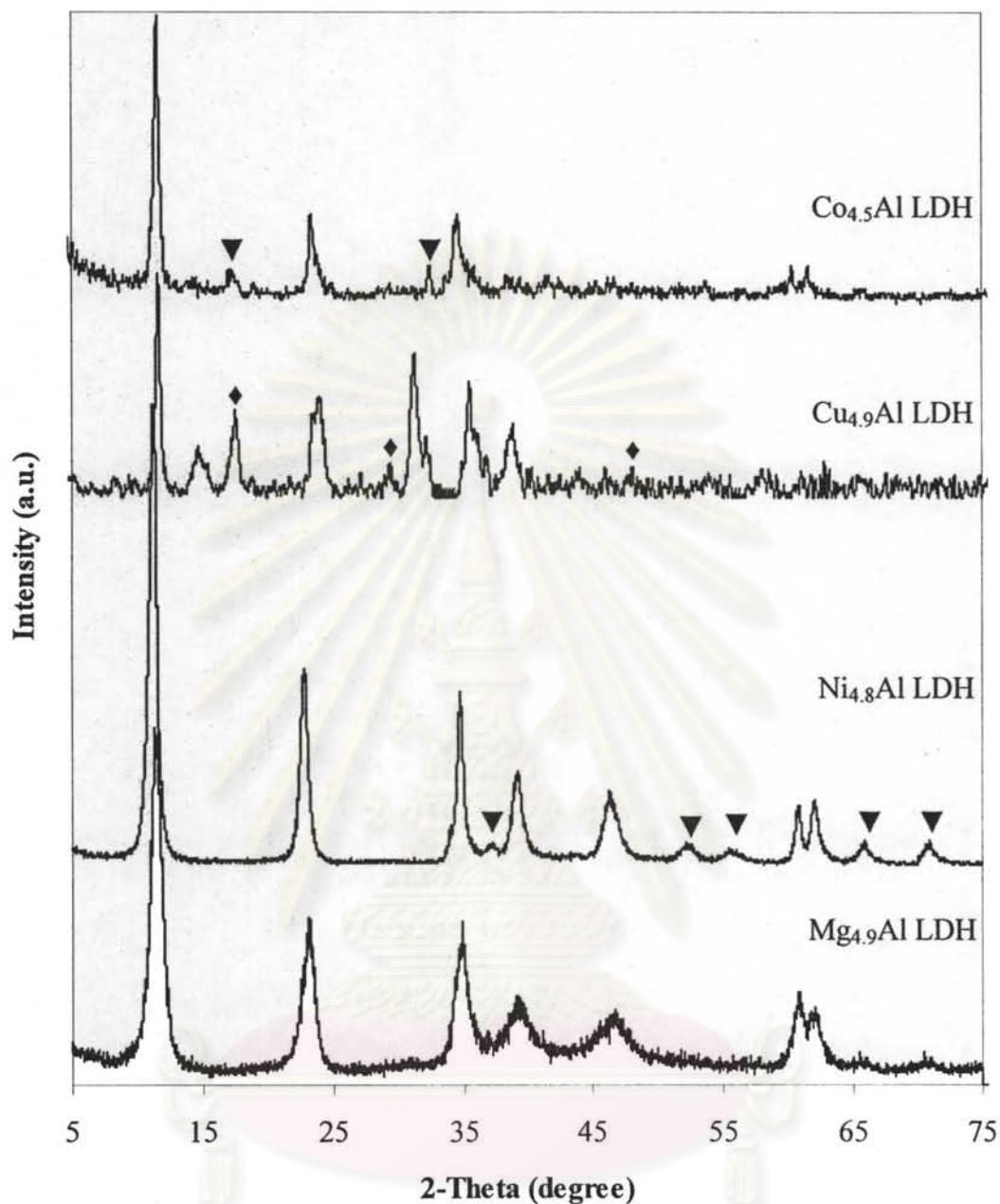


Figure 3.7 XRD patterns of $\text{Mg}_{4.9}\text{Al}$, $\text{Ni}_{4.8}\text{Al}$, $\text{Cu}_{4.9}\text{Al}$ and $\text{Co}_{4.5}\text{Al}$ LDHs. \blacktriangledown unidentified impurity phase, \blacklozenge ($\text{Cu}_2(\text{OH})_2\text{CO}_3$)

From Figure 3.7, one can see that all samples show the layered double hydroxide-like phase. The $\text{Cu}_{4.9}\text{Al}$ and $\text{Co}_{4.5}\text{Al}$ LDHs show a decrease in their degrees of crystallinity. In the case of $\text{Ni}_{4.8}\text{Al}$ LDH, an unidentified impurity phase was present. Such a phase was also observed in the $\text{Cu}_{4.9}\text{Al}$ LDH at $2\theta = 16^\circ, 32^\circ$ and 49° which might be due to copper hydroxide carbonate ($\text{Cu}_2(\text{OH})_2\text{CO}_3$) (JCPDS 76-0660). Indeed, similar results were described in the preparation of Cu/Al LDHs at high Cu/Al ratios [49].

3.4.4.2 XRD of binary mixed metal oxides

The XRD patterns of binary mixed metal oxide samples were shown in Figure 3.8. $Mg_{4.9}Al$ oxide sample showed MgO phase at $2\theta = 37.2^\circ$, 42.9° and 62.1° (JCPDS 45-0946) [50]. $Ni_{4.8}Al$ oxide sample showed NiO phase (JCPDS 44-1159) otherwise $Cu_{4.9}Al$ oxide sample showed CuO phase at $2\theta = 35.6^\circ$, 37.8° , 44.5° and 59.5° (JCPDS 05-0661) [51]. $Co_{4.5}Al$ oxide showed Co_3O_4 (JCPDS 42-1467) or Co_2AlO_4 phase (JCPDS 38-0814) at $2\theta = 37.7^\circ$, 43.1° and 62.4° [52].

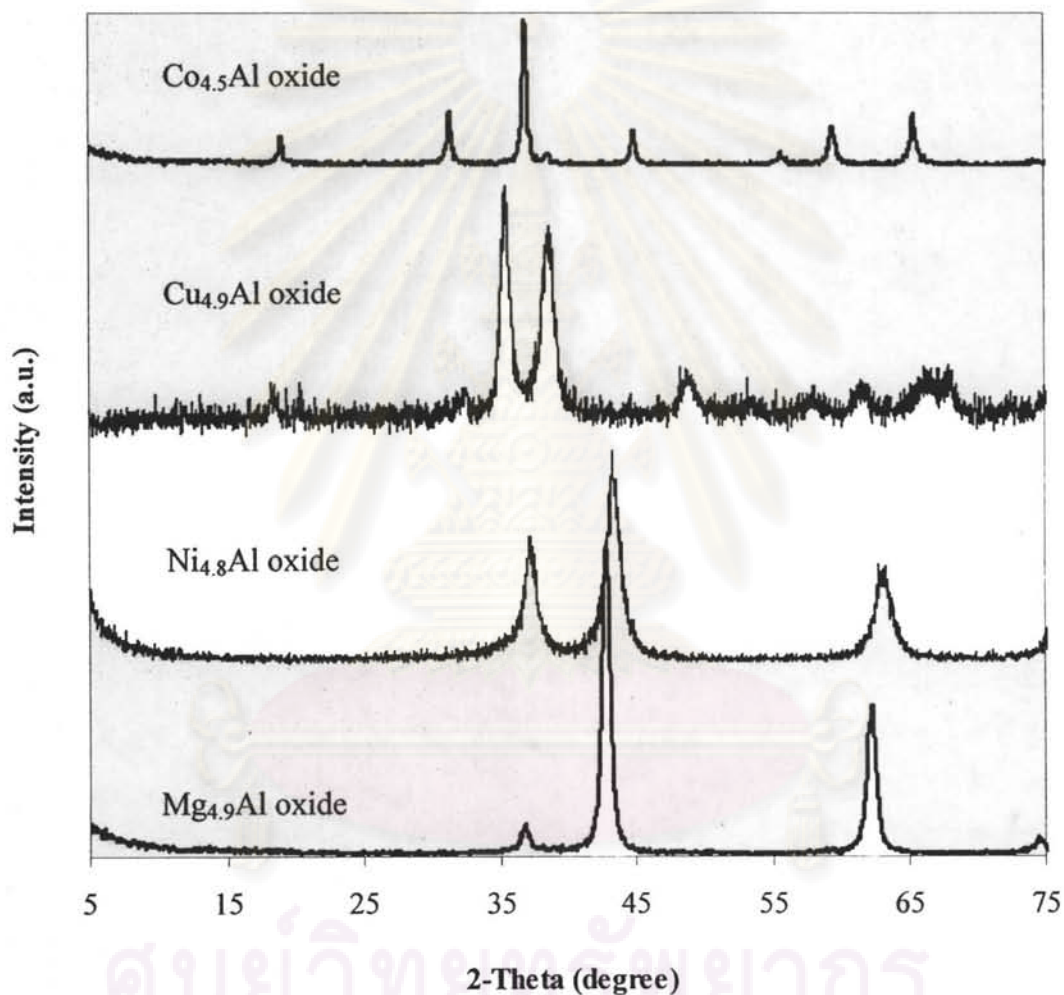


Figure 3.8 XRD patterns of binary metal oxides; $Mg_{4.9}Al$, $Ni_{4.8}Al$, $Co_{4.5}Al$ and $Cu_{4.9}Al$ oxides.

3.4.4.3 XRD of ternary layered double hydroxides

The XRD patterns of the ternary LDHs are shown in Figure 3.9.

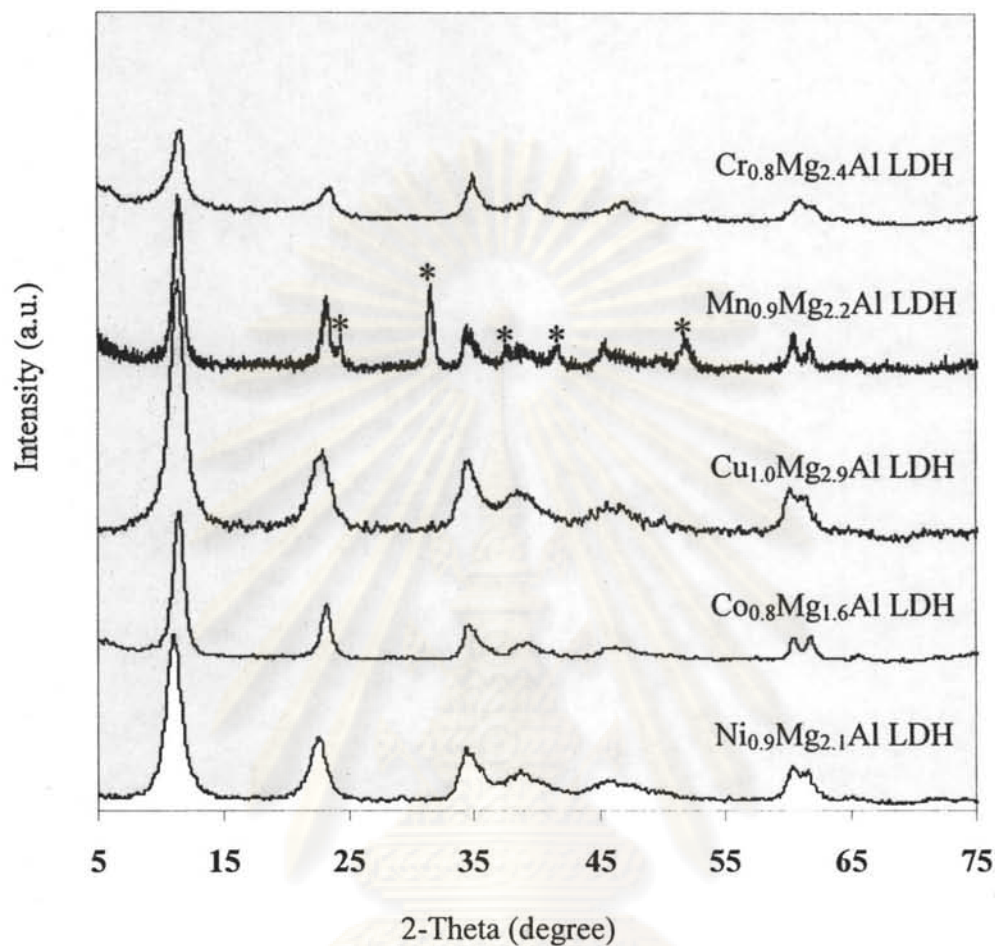


Figure 3.9 XRD patterns of ternary layered double hydroxides.

* MnCO_3 phase

The XRD patterns of the prepared ternary LDHs exhibited sharp and symmetric reflection peaks characteristic of LDHs. It should be noted that the XRD pattern of the Mn-containing LDH showed an impurity phase at $2\theta = 24.3^\circ$, 31.4° , 37.6° , 41.5° , and 51.8° (JCPDS 83-1761) which can be assigned to MnCO_3 [53-55].

จุฬาลงกรณ์มหาวิทยาลัย

3.4.4.4 XRD of ternary mixed metal oxides

Calcination products resulting from treatment of the ternary LDHs at 500°C for 5 h have been obtained and studied, and some pertinent results are shown below.

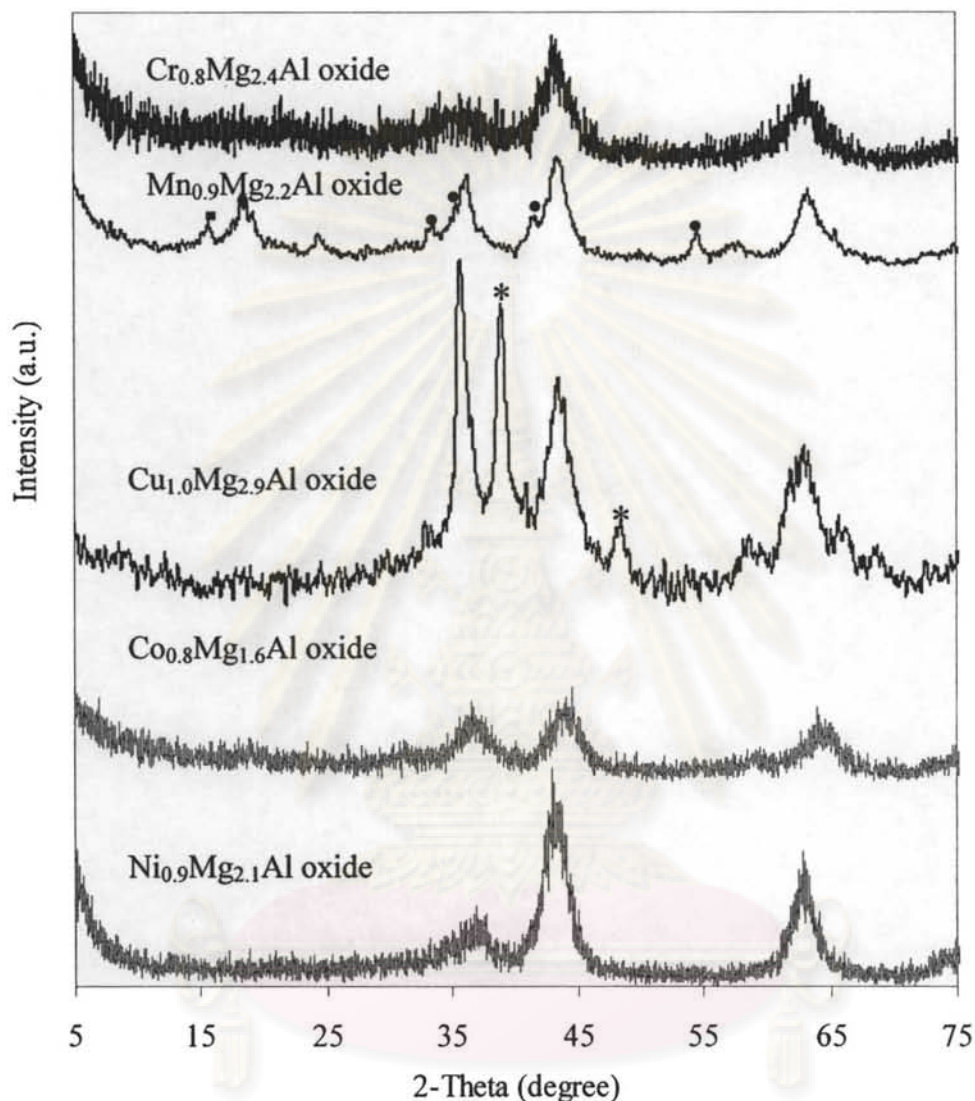


Figure 3.10 XRD patterns of ternary mixed metal oxides.

• Mn_3O_4 , \blacksquare MnO_2 and * CuO

After calcination, MMgAl ($M = \text{Cr}, \text{Mn}, \text{Cu}, \text{Co}$ and Ni) LDHs were collapsed to their corresponding mixed metal oxides. The peaks in the XRD show the presence of the MgO -like phase. The $\text{Cu}_{1.0}\text{Mg}_{2.9}\text{Al}$ oxide sample showed another phase which was ascribed to CuO [51]. In the case of the $\text{Mn}_{0.9}\text{Mg}_{2.2}\text{Al}$ oxide extra phases were observed and attributed to Mn_3O_4 (JCPDS 24-0734) and MnO_2 (JCPDS 4-0779) [53-55].

3.4.5 Diffuse reflectance ultraviolet-visible spectroscopy (DRUV)

The presence and the nature of metal species in the prepared catalysts were investigated with diffuse reflectance ultraviolet visible spectroscopy (Table 3.9). The DRUV pictures are collected in appendix D.

Table 3.9 DRUV of binary and ternary mixed metal oxide catalysts

Catalyst	Wavelength (nm)
Ni _{4.8} Al oxide	220-300, 500-660
Co _{4.5} Al oxide	240-260, 490-530
Cu _{4.9} Al oxide	230-250, 750-800
Ni _{5.1} Cr oxide	220-300, 400-800
Co _{4.8} Cr oxide	250-310, 400-800
Ni _{0.9} Mg _{2.1} Al oxide	250-310, 430-535
Co _{0.8} Mg _{1.6} Al oxide	320-400, 550-800
Cu _{1.0} Mg _{2.9} Al oxide	380-520
Mn _{0.9} Mg _{2.2} Al oxide	200-300, 600-750
Cr _{0.8} Mg _{2.4} Al oxide	280-330, 440-480, 650-800

In the case of the Ni_{4.8}Al, Ni_{5.1}Cr and Ni_{0.9}Mg_{2.1}Al oxide samples, strong and broad reflectance bands at 220-310 and 400-800 nm were observed [39]. For Co_{4.5}Al and Co_{0.8}Mg_{1.6}Al oxide samples, reflectance bands appeared at 240-400 nm, which were due to Co²⁺ in Co₂AlO₄ [40], and the presence of this phase was already pointed out in the XRD pattern (Figures 3.8 and 3.10). The Co_{4.8}Cr oxide catalyst appeared the band 250-310 nm and the weak and very broad band at 400-800 nm.

The Cu_{4.9}Al and Cu_{1.0}Mg_{2.9}Al oxide showed broad band at 230-250 and 380-520 nm which indicated some Cu²⁺ species in both sample [41].

The Mn_{0.9}Mg_{2.2}Al oxide showed two broad reflection bands at 200-300 and 600-750 nm which were attributed to Mn³⁺ and Mn⁴⁺ species. These high oxidation state species were observed because Mn²⁺ is unstable in basic solution and easily oxidized by air [56].

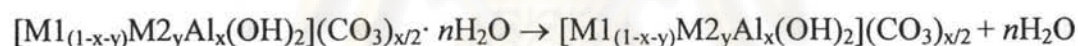
The $\text{Cr}_{0.8}\text{Mg}_{2.4}\text{Al}$ oxide showed peaks at 330-350, 500-530 and 700-800 nm which were assigned to Cr^{6+} and Cr^{3+} in the sample [57-58]. The Cr^{6+} species that were observed in the sample might be due to the oxidation of Cr^{3+} during the preparation steps [18].

3.4.6 Thermogravimetric analysis (TGA)

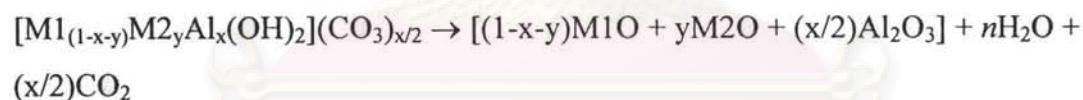
Thermogravimetric analysis of representative binary and ternary LDHs, $\text{Co}_{4.5}\text{Al}$, $\text{Co}_{0.8}\text{Mg}_{1.6}\text{Al}$ and $\text{Cu}_{1.0}\text{Mg}_{2.9}\text{Al}$ are described as follows.

The decompositions take place in two steps: the first one (25-300°C) corresponds to removal of interlayer water molecules and the second one (300-600°C) to removal of interlayer carbonate (as CO_2) and hydroxyl groups [59]. The thermal decomposition of the LDH sample can be written as follows, where M1 and M2 are divalent cation [47].

First weight loss step:



Second weight loss step:



ศูนย์วิทยทรัพยากร
จุฬาลงกรณ์มหาวิทยาลัย

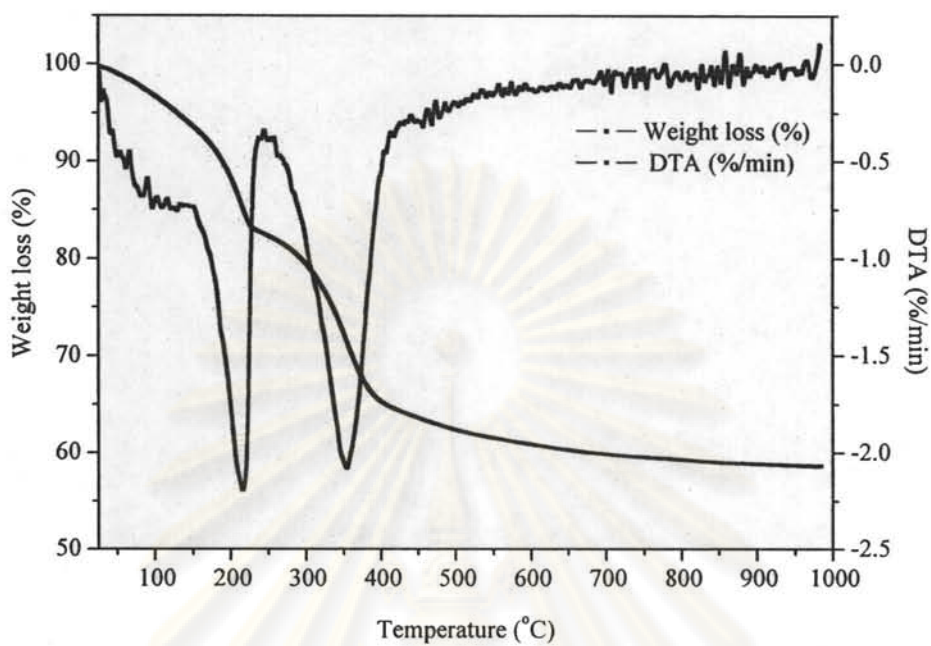


Figure 3.11 TGA profile of the Co_{4.5}Al LDH.

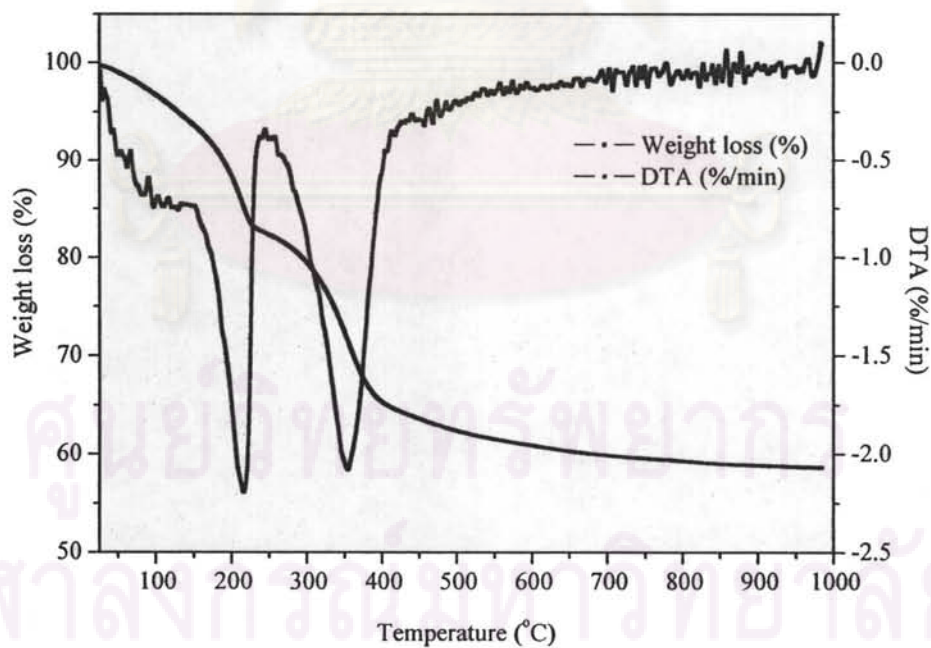


Figure 3.12 TGA profile of the Co_{0.8}Mg_{1.6}Al LDH.

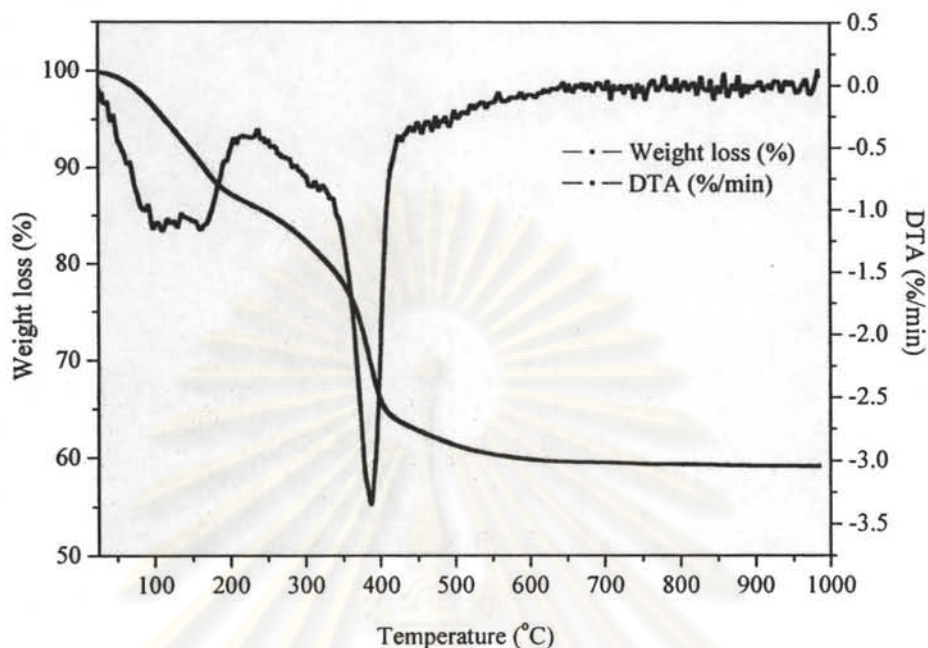


Figure 3.13 TGA profile of the $\text{Cu}_{1.0}\text{Mg}_{2.9}\text{Al}$ LDH.

From the TGA profiles of all of the LDH samples in Figures 3.11-3.13, one can see that the second weight loss in all LDH samples was much greater than the weight loss in the first region, as revealed in Table 3.10. The $\text{Co}_{4.5}\text{Al}$ LDH showed the smallest of the total weight losses, at 25.9%, compared to $\text{Co}_{0.8}\text{Mg}_{1.6}\text{Al}$ (40.6%) and $\text{Cu}_{1.0}\text{Mg}_{2.9}\text{Al}$ LDHs (39.5%). As already observed, greater weight losses occurred in the high Mg content LDHs [44], and the difference can be related to the higher affinity of water for magnesium compared to Co and Cu.

Table 3.10 Thermogravimetric analysis data of LDHs

Catalyst	Temperature range (°C)	Weight loss (%)
$\text{Co}_{4.5}\text{Al}$ LDH	25-280	11.2
	376-342	14.7
$\text{Co}_{0.8}\text{Mg}_{1.6}\text{Al}$ LDH	25-286	18.4
	286-931	22.2
$\text{Cu}_{1.0}\text{Mg}_{2.9}\text{Al}$ LDH	25-301	15.1
	301-850	24.4

3.4.7 Thermal stabilities of mixed metal oxide catalysts

Thermal decompositions of the binary mixed metal oxide samples were observed, the results being presented in Figures 3.14-3.15, and are discussed below.

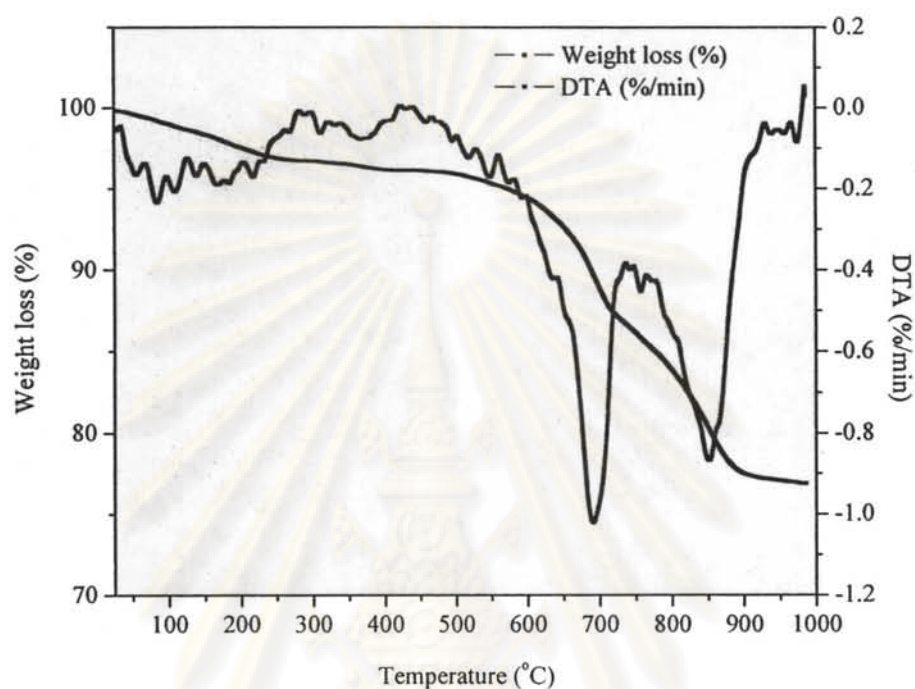


Figure 3.14 TGA profile of $\text{Ni}_{4.8}\text{Al}$ oxide.

ศูนย์วิทยทรัพยากร
จุฬาลงกรณ์มหาวิทยาลัย

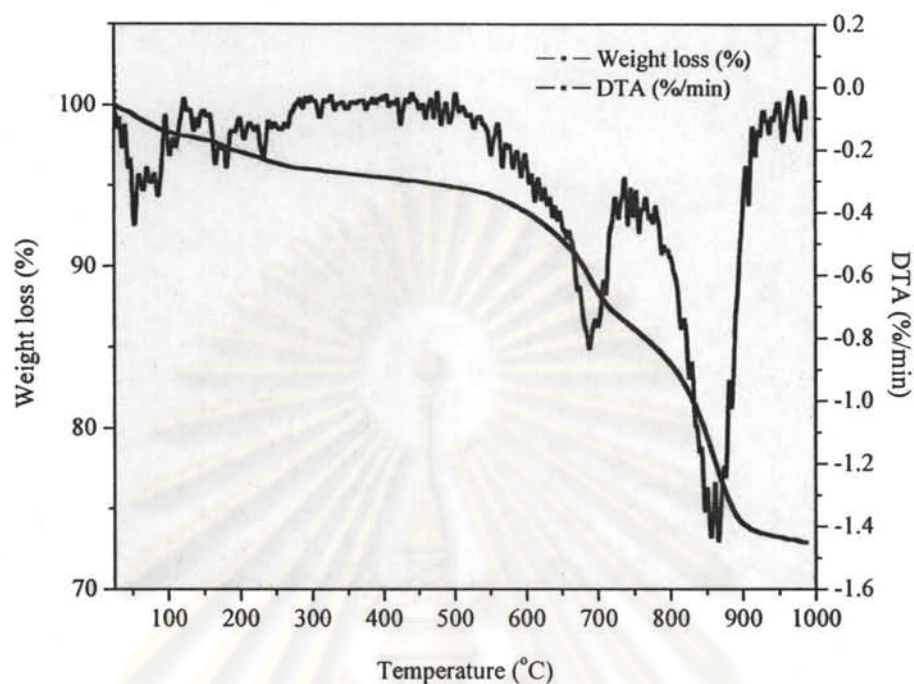


Figure 3.15 TGA profile of $\text{Co}_{4.5}\text{Al}$ oxide.

The $\text{Ni}_{4.8}\text{Al}$ and $\text{Co}_{4.5}\text{Al}$ oxides have similar thermal behaviors; this is in good agreement with observations in an earlier report [60].

All metal oxide samples showed high second weight losses in the temperature range of 250-900°C, related to CO_2 evolution from remaining carbonate [61]. The TGA results suggested that a calcination temperature of 500°C is adequate for the crystallization process leading to conversion of the dried layered double hydroxides to the desired metal oxides [42].

3.4.8 Temperature program reduction (TPR)

For a better understanding of the reducibility of the catalyst, H_2 -TPR studies were carried out. Figure 3.16 performed the H_2 -TPR profiles for the binary and ternary mixed metal oxide catalysts.

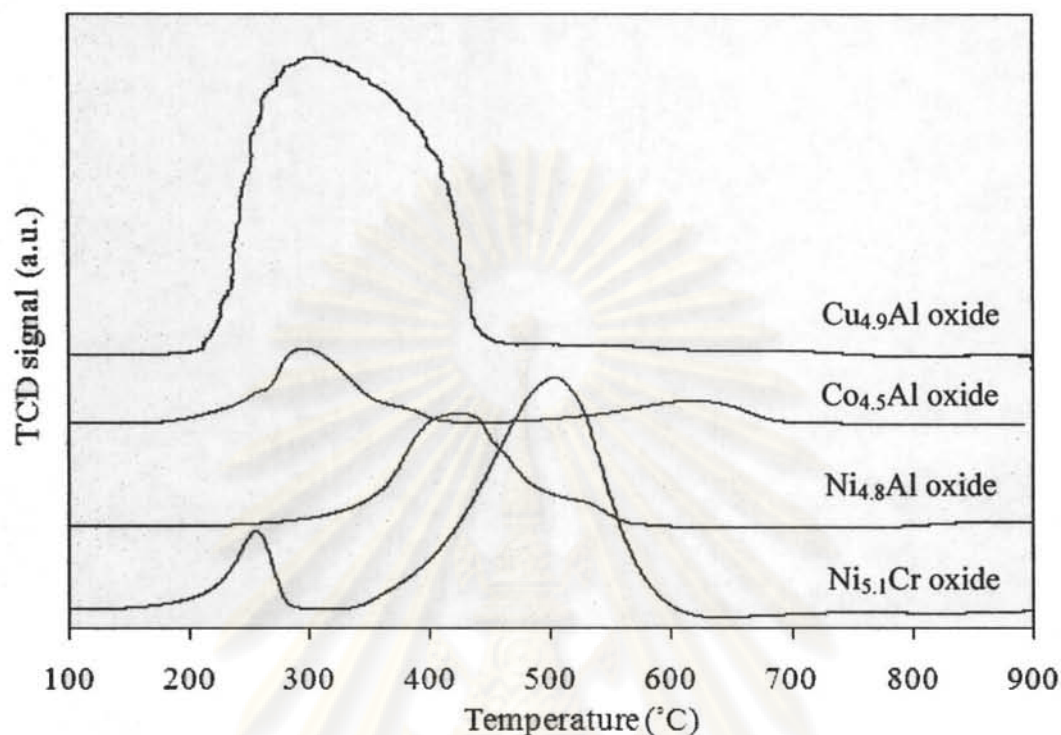


Figure 3.16 TPR profiles of $\text{Ni}_{5.1}\text{Cr}$, $\text{Ni}_{4.8}\text{Al}$, $\text{Co}_{4.5}\text{Al}$, and $\text{Cu}_{4.9}\text{Al}$ oxide catalysts.

TPR profiles of the $\text{Cu}_{4.9}\text{Al}$, $\text{Co}_{4.5}\text{Al}$, $\text{Ni}_{4.8}\text{Al}$ and $\text{Ni}_{5.1}\text{Cr}$ oxide catalysts were investigated in the same conditions.

$\text{Ni}_{5.1}\text{Cr}$ oxide showed two peaks. The first peak, at a relatively low temperature, is attributed to the reduction of Ni^{2+} , whereas the larger peak at a high temperature is attributed to Cr^{3+} reduction [59]. $\text{Ni}_{4.8}\text{Al}$ oxide showed a broad peak at 380–550°C. The result may indicate that Ni is better dispersed in Al than in Cr. For the $\text{Co}_{4.5}\text{Al}$ oxide, the first reduction peak at 380°C is due to Co^{3+} and a peak at 540°C is from Co^{2+} (Weast and co-workers) [62].

The $\text{Cu}_{4.9}\text{Al}$ oxide exhibits a low reduction temperature range of 275–450°C. This peak is clearly due to Cu^{2+} reduction, which occurs at a much lower temperature than observed with other oxides and can be explained by the highly favorable reduction potential of $\text{Cu}^{2+}/\text{Cu}^0$ ($E_0 = 0.337$) [62–63].

TPR profiles of the ternary mixed metal oxide catalysts (MMgAl) were obtained, and are shown in Figure 3.17.

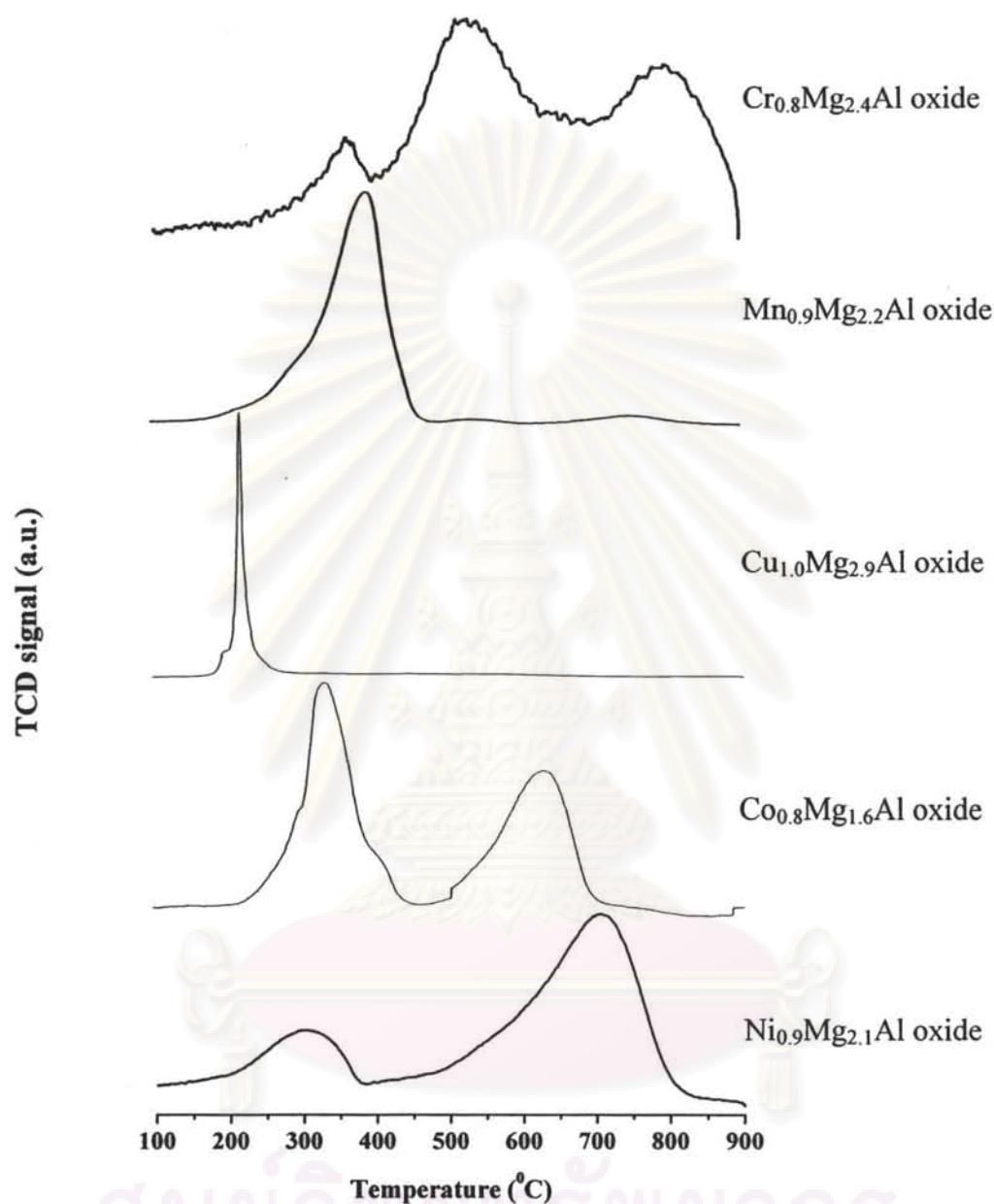


Figure 3.17 TPR profiles of $\text{Ni}_{0.9}\text{Mg}_{2.1}\text{Al}$, $\text{Co}_{0.8}\text{Mg}_{1.6}\text{Al}$, $\text{Cu}_{1.0}\text{Mg}_{2.9}\text{Al}$, $\text{Mn}_{0.9}\text{Mg}_{2.2}\text{Al}$ and $\text{Cr}_{0.8}\text{Mg}_{2.4}\text{Al}$ oxides catalysts.

The $\text{Ni}_{0.9}\text{Mg}_{2.1}\text{Al}$ oxide showed a reduction peak at 200–350°C. This Mg-rich sample might contain embedded Ni species in the Mg matrix, making it more difficult to reduce. This is similar to behavior described for samples with Ni/Mg ratios < 1 for which the reduction of the Ni^{2+} ions is hindered by the Al^{3+} ions inside the oxide phases [50].

In case of the $\text{Co}_{0.8}\text{Mg}_{1.6}\text{Al}$ oxide, two reduction temperatures were observed in the 650-760°C range. This can be explained by the presence of two different Co species in the sample. As described for the XRD data, the presences of the Co_3O_4 oxide and Co_2AlO_4 spinel have already been established (JCPDS 380814).

The $\text{Cu}_{1.0}\text{Mg}_{2.9}\text{Al}$ oxide catalyst displayed a very sharp reduction peak around 180-200°C. A decrease in the reduction temperature compared to that of the binary oxide $\text{Cu}_{4.9}\text{Al}$ may be attributed to the presence of Mg in the sample. This indicates a high dispersion of the CuO phase in the Mg matrix and to easily reducible copper ions.

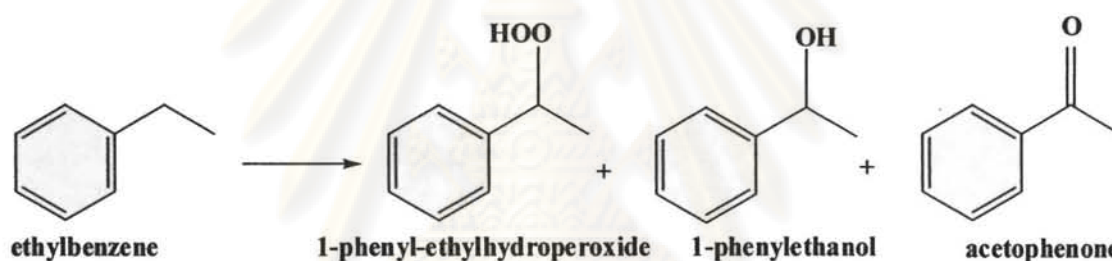
In the case of the $\text{Mn}_{0.9}\text{Mg}_{2.2}\text{Al}$ oxide sample, reduction peaks appeared at 280-350°C and 700°C. These correspond to reduction of two different species, Mn^{3+} to Mn^{2+} [55, 64]. The result was consistent with DRUV analysis which indicated the presence of both Mn^{2+} and Mn^{3+} ions.

In case of the $\text{Cr}_{0.8}\text{Mg}_{2.4}\text{Al}$ oxide, a reduction peak observed at 290-310°C was attributed to the reduction of Cr^{6+} to Cr^{3+} [65]. The peaks at 450-550 and 700-900°C were attributed to the reduction of Cr^{3+} , possibly in the form of Cr_2O_3 or to some other form in the MgO matrix.

3.5 Oxidation of ethylbenzene with binary LDH and mixed metal oxide catalysts

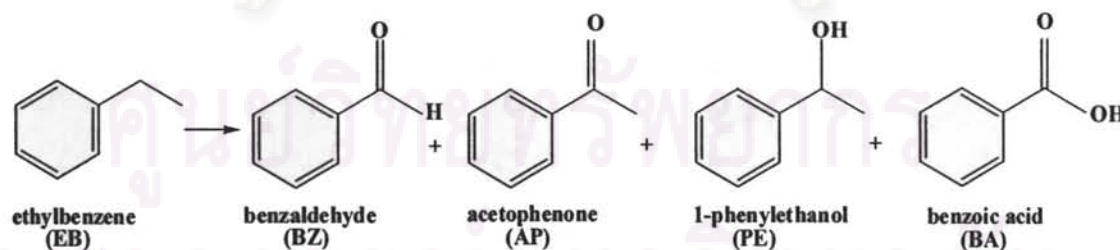
In this study, the catalytic oxidation of ethylbenzene was carried out in a liquid phase, resulting in the formation of the four main important products, benzaldehyde (BZ), acetophenone (AP), 1-phenylethanol (PE) and benzoic acid (BA). The effect of M^{2+}/M^{3+} mole ratio, types of metal, oxidant/substrate mole ratio (O/S), amount of catalyst, types of oxidant and types of solvent were investigated.

Autoxidation or air oxidation of alkylsubstituted aromatics possessing benzylic hydrogen affords benzylic hydroperoxides as the primary products with high selectivity according to a free-radical mechanism was proposed by Hermans and co-workers [66]. The autoxidation of ethylbenzene is given in Scheme 3.1.



Scheme 3.1 Autoxidation of ethylbenzene.

The oxygenated products found in this study from the ethylbenzene oxidation are shown in Scheme 3.2.



Scheme 3.2 Reaction scheme of the ethylbenzene oxidation.

General oxidation procedure of ethylbenzene was carried out in a Parr reactor, the catalyst; substrate and oxidant were placed into the stainless steel reactor located in the electrical heater. The reactor is heated to the desired temperature and reaction

time. After the desired reaction time, the reaction mixture was cooled down and the catalyst was filtered off. The liquid mixture was added 25% H_2SO_4 solution and extract with diethyl ether. The liquid mixture was neutralized with saturated NaHCO_3 solution and dried over Na_2SO_4 anhydrous. The oxygenated products and recovered substrate in a liquid mixture were qualitatively analyzed by gas chromatography using the internal standard method. The mass balance of all samples was in the range 95-105%. The GC diagrams are shown in appendix E.

3.5.1 Effect of oxidant

When the reaction was carried out using hydrogenperoxide (H_2O_2) as an oxidant, ethylbenzene conversion was very low under the reaction condition. This could be due to the fast decomposition of H_2O_2 . However, changing the oxidant from H_2O_2 to *tert*-butylhydroperoxide (TBHP) in aqueous increased the conversion drastically and hence, TBHP was used as an oxidant for further experiments. This result is consistent with an earlier report by George and Sugunan [43].



ศูนย์วิจัยทรัพยากร
จุฬาลงกรณ์มหาวิทยาลัย

3.5.2 Effect of preparation methods and catalyst forms

The LDHs with different $\text{Ni}^{2+}/\text{Al}^{3+}$ mole ratios were prepared by the alkali and alkali-free methods, and studied for the oxidation of ethylbenzene using TBHP as oxidant. The results are shown in Table 3.11.

Table 3.11 Oxidation of ethylbenzene using catalysts prepared with alkali and alkali-free coprecipitation

Preparation method	Catalyst	Conversion (%)	Selectivity (%)	
			AP	Others
alkali coprecipitation	$\text{Ni}_{3.1}\text{Al}$ oxide	51	98	PE 1%, BZ 1%
	$\text{Ni}_{4.8}\text{Al}$ LDH	68	98	PE 1%, BZ 1%
	$\text{Ni}_{4.8}\text{Al}$ oxide	75	98	PE 1%, BZ 1%
alkali-free coprecipitation	$\text{Ni}_{4.9}\text{Al}$ oxide	70	98	PE 1%, BZ 1%

Reaction conditions: ethylbenzene 10 mmol, catalyst 0.2 g, TBHP 20 mmol, 130°C, 12 h.

AP = acetophenone, PE = 1-phenylethanol, BZ = benzaldehyde, BA = benzoic acid

Comparing the results obtained for samples having Ni/Al mole ratios of 3.1 and 4.8, one can see that the catalytic activity increased with the catalyst's Ni/Al ratio due to the increase in the number of active sites (Ni^{2+} species). The difference in activity between $\text{Ni}_{4.8}\text{Al}$ LDH and oxide catalysts may be explained by the different base site types. The active sites in LDH are hydroxide groups which are weak basic site whereas calcined LDH contain surface OH groups as well as O^{2-} centers linked to metal atoms which are strong basic sites. The catalytic activity of catalyst prepared by the alkali coprecipitation method is slightly higher than that found for catalysts prepared via the other method.

The effect of reaction time was investigated for the ethylbenzene oxidation over $\text{Ni}_{4.8}\text{Al}$ oxide. When increasing the reaction time, conversion of ethylbenzene increased without significantly affecting acetophenone selectivity. The highest

conversion of ethylbenzene was 94% in 24 h. No significant improvement in the oxidation of ethylbenzene was observed upon an increase in time to 36 h.

3.5.3 Oxidation of ethylbenzene with various catalysts

Catalytic performances of binary mixed metal oxide in ethylbenzene oxidation are collected in Table 3.12.

Table 3.12 Oxidation of ethylbenzene using binary mixed metal oxide catalysts

Catalyst	Conversion (%)	Selectivity (%)	
		AP	Others
-	15	98	PE 1%, BZ 1%
Mg _{4.9} Al oxide	55	98	PE 1%, BZ 1%
Ni _{4.8} Al oxide	75	98	PE 1%, BZ 1%
Co _{4.5} Al oxide	72	95	PE 4%, BZ 1%
Cu _{4.9} Al oxide	70	95	PE 4%, BZ 1%
Ni _{5.1} Cr oxide	78	76	PE 10%, BZ 11%, BA 3%
Co _{4.8} Cr oxide	65	93	PE 4%, BZ 2%, BA 1%
NiO	38	98	PE 1%, BZ 1%
CoO	36	98	PE 1%, BZ 1%

Reaction conditions: ethylbenzene 10 mmol, catalyst 0.2 g, TBHP 20 mmol, 130°C, 12 h.

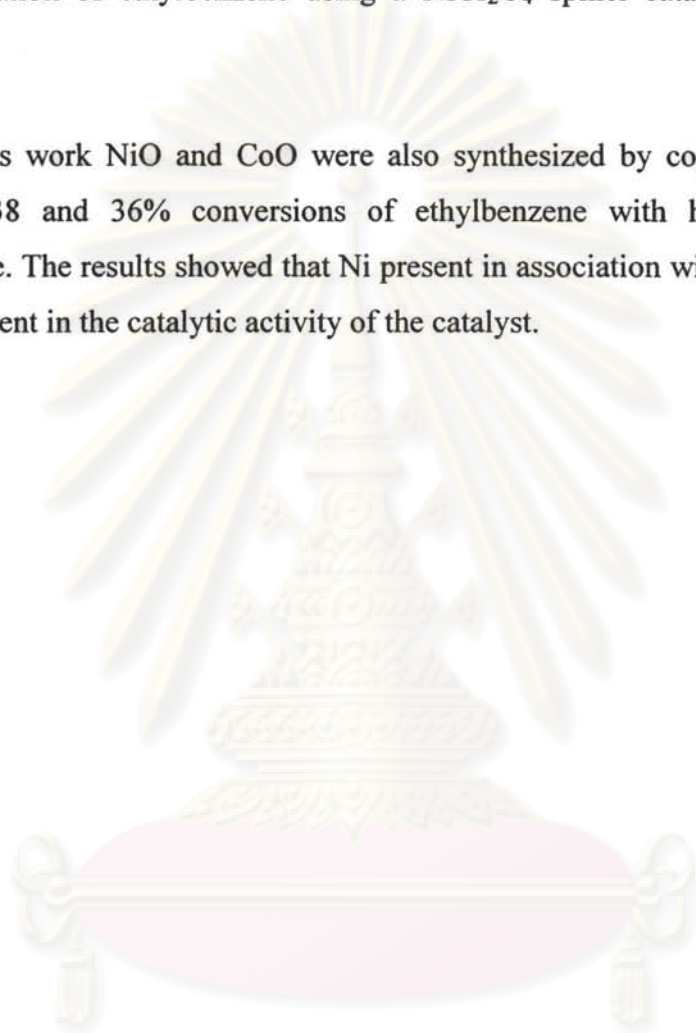
AP = acetophenone, PE = 1-phenylethanol, BZ = benzaldehyde, BA = benzoic acid

When the oxidation reaction was carried out without catalyst, the conversion of ethylbenzene was only 15%; this might be due to autoxidation. In the presence of a catalyst, higher conversions were obtained. The catalyst activity order is: Ni_{4.8}Al oxide > Co_{4.5}Al oxide > Cu_{4.9}Al oxide >> Mg_{4.9}Al oxide.

However, there is no relationship between surface area, soluble basicity (see appendix F) and catalytic activity. The activities of Ni_{4.8}Al, Co_{4.5}Al and Cu_{4.9}Al oxide catalysts were found to correspond with their reducibilities. However, the Cu_{4.9}Al oxide gave a lower activity; this might be due to the lower crystallinity as found in other work [13].

In a series of Ni containing oxide catalyst, $\text{Ni}_{5.1}\text{Cr}$ oxide gave a higher activity than $\text{Ni}_{4.8}\text{Al}$ oxide due to higher Ni content. However, in terms of product selectivity, the $\text{Ni}_{5.1}\text{Cr}$ oxide showed lower selectivities to acetophenone but a much higher selectivity to benzaldehyde. This phenomenon is in agreement with results reported for the oxidation of ethylbenzene using a NiCr_2O_4 spinel catalyst and TBHP as oxidant [43].

In this work NiO and CoO were also synthesized by coprecipitation. They gave only 38 and 36% conversions of ethylbenzene with high selectivity of acetophenone. The results showed that Ni present in association with Al might lead to an improvement in the catalytic activity of the catalyst.



ศูนย์วิทยทรัพยากร
จุฬาลงกรณ์มหาวิทยาลัย

3.5.4 Effect of oxidant and substrate mole ratios

Comparisons between the effect of TBHP concentration on conversion and acetophenone selectivity using the $\text{Ni}_{4.8}\text{Al}$ oxide catalysts can be made from the data as shown in Figure 3.18.

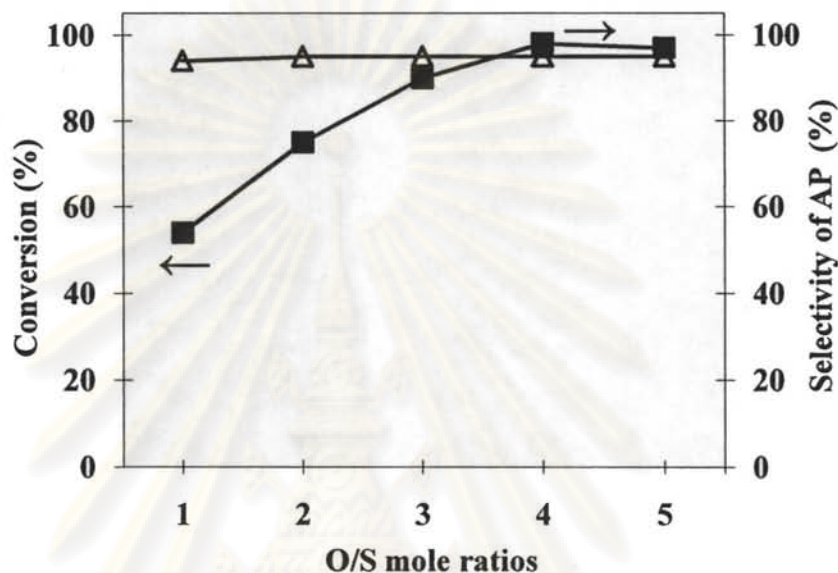


Figure 3.18 Effect of oxidant and substrate mole ratios in the oxidation of ethylbenzene using $\text{Ni}_{4.8}\text{Al}$ oxide as catalyst and TBHP as oxidant. Reaction conditions: ethylbenzene 10 mmol, catalyst 0.2 g, 130°C, 12 h.

From Figure 3.18, when the TBHP concentration was changed from an oxidant/substrate mole ratio of 1 to 5, the increase in conversion with TBHP was clearly observed for the $\text{Ni}_{4.8}\text{Al}$ oxide catalyst as described earlier by George and Sugunan [43]. At the relatively high oxidant/substrate mole ratios of 4 and 5, the ethylbenzene conversion leveled off. There was no significant difference in acetophenone selectivity, which indicated that TBHP concentration did not affect the reaction pathway.

3.5.5 Effect of catalyst amount

With the other reaction conditions being maintained constant, the influence of catalyst amount on the activity of oxidation of ethylbenzene has been studied, varying in the range of 0.1-0.5 g of catalyst in the reaction mixture, the results shown in Figure 3.19.

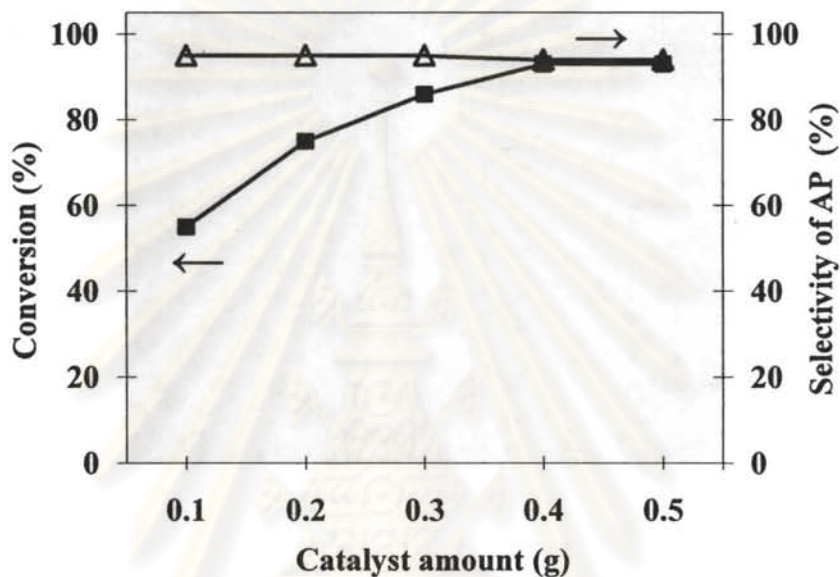


Figure 3.19 Effect of catalyst amount using $\text{Ni}_{4.8}\text{Al}$ oxide catalyst.
Reaction conditions: ethylbenzene 10 mmol, TBHP 20 mmol, 130°C , 12 h.

The activity of the $\text{Ni}_{4.8}\text{Al}$ oxide increased almost linearly with the catalyst amount. This observation was consistent with the fact that with high metal concentrations the number of active sites was also increased [67].

ศูนย์วิจัยทรัพยากร
จุฬาลงกรณ์มหาวิทยาลัย

3.5.6 Effects of solvent

The effect of solvent was studied. The oxidation of ethylbenzene with the $\text{Ni}_{4.8}\text{Al}$ oxide catalyst was performed in CH_3CN and CH_2Cl_2 .

Table 3.13 Effect of types of solvents using $\text{Ni}_{4.8}\text{Al}$ oxide

Solvent	Conversion (%)	Selectivity (%)	
		AP	Others
-	75	98	PE 1%, BZ 1%
CH_2Cl_2	48	98	PE 1%, BZ 1%
CH_3CN	59	95	PE 3%, BZ 1%, BA 1%

Reaction conditions: ethylbenzene 10 mmol, catalyst 0.2 g, TBHP 20 mmol, 130°C , 12 h, solvent 2 mL.

AP = acetophenone, PE = 1-phenylethanol, BZ = benzaldehyde, BA = benzoic acid

When these solvents were used in the oxidation of ethylbenzene, the conversions were low and followed the order $\text{CH}_3\text{CN} > \text{CH}_2\text{Cl}_2$. Interestingly, the conversion was maximized under solvent-free conditions. The decrease in conversion utilizing solvents can be attributed to the blocking of active sites by the solvent molecules, particularly for a polar solvent such as CH_3CN . This result is in agreement with an earlier report by Bhoware and co-workers [8]. When solvents were used, it was found that the ethylbenzene conversion was reduced and followed the order non solvent (36%) > CH_3CN (32%) > CH_2Cl_2 (29%) > $(\text{CH}_3)_2\text{CO}$ (13%) and $\text{C}_2\text{H}_5\text{OH}$ (0.8%), using cobalt-containing mesoporous molecular sieves and TBHP at 80°C for 24 h. The main products were acetophenone, benzaldehyde and benzoic acid. Surprisingly, no 1-phenylethanol was observed under these conditions. The same result was reported by George and co-workers [43], who found that the presence of CH_3CN lowered the ethylbenzene conversion compared to the solvent-free system.

จุฬาลงกรณ์มหาวิทยาลัย

3.5.7 Effect of radical scavenger

The effect of hydroquinone, which is a radical scavenger, was investigated. The results collected in Figure 3.20.

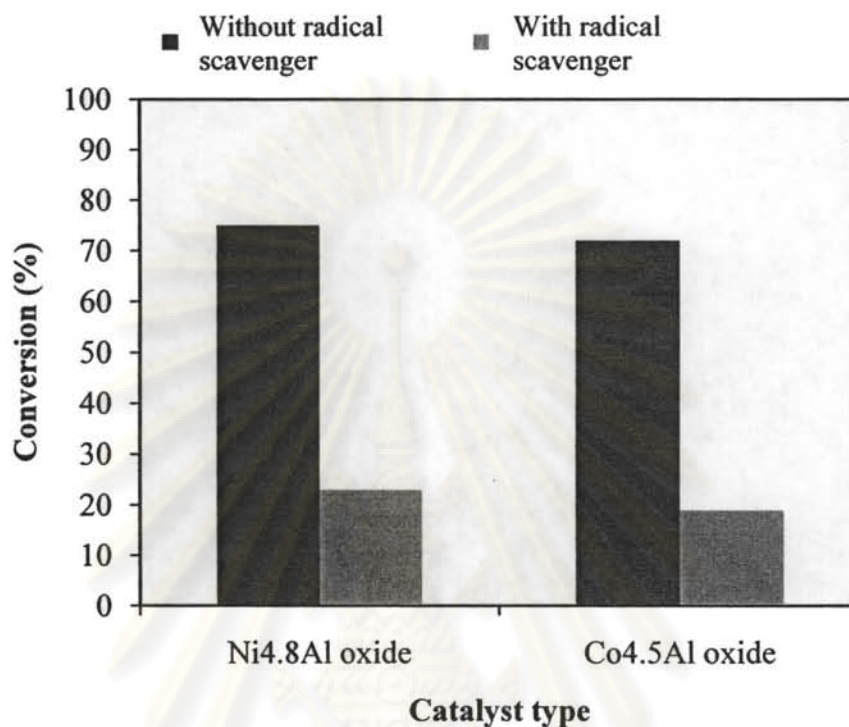


Figure 3.20 Catalytic oxidation of ethylbenzene using binary mixed metal oxide in the presence of radical scavenger.

Reaction conditions: ethylbenzene 10 mmol, catalyst 0.2 g, hydroquinone 10 mmol, TBHP 20 mmol, 130°C, 12 h.

In presence of hydroquinone as radical scavenger ethylbenzene conversion was lower. From Figure 3.20, in case of the Ni_{4.8}Al oxide as catalyst, ethylbenzene conversion decreased from 75% to 23% and for the Co_{4.5}Al oxide from 72% to 19%. From the results obtained it can be concluded that the oxidation of ethylbenzene using TBHP and binary mixed metal oxide as catalyst proceeds by a free radical mechanism [44].

3.6 Oxidation of ethylbenzene with ternary LDH and mixed metal oxide catalysts

The effect of the M^{2+}/M^{3+} mole ratio using CuMgAl as a representative sample was investigated; the catalyst with (Cu+Mg)/Al mole ratio of 4 (79% conversion) gave higher activity than a ratio of 5 (72% conversion). Thus M^{2+}/M^{3+} mole ratio = 4 was used in the further study.

3.6.1 Effect of various catalysts

The $Cu_{1.0}Mg_{2.9}Al$ oxide gave higher activity than its precursor, $Cu_{1.0}Mg_{2.9}Al$ LDH with 70% conversion of ethylbenzene. Thus in the next experiment, only ternary mixed metal oxide catalysts were studied and the results collected in Table 3.14.

Table 3.14 Catalytic oxidation of ethylbenzene using ternary mixed metal oxide catalysts

Catalyst	Conversion (%)	Selectivity (%)	
		AP	Others
$Cu_{1.0}Mg_{2.9}Al$ oxide	79	92	PE 4%, BZ 1%, BA 3%
$Ni_{0.9}Mg_{2.1}Al$ oxide	73	92	PE 4%, BZ 3%, BA 1%
$Co_{0.8}Mg_{1.6}Al$ oxide	73	91	PE 7%, BZ 1%, BA 1%
$Cr_{0.8}Mg_{2.4}Al$ oxide	67	90	PE 2%, BZ 6%, BA 2%
$Mn_{0.9}Mg_{2.2}Al$ oxide	65	89	PE 4%, BZ 3%, BA 4%

Reaction conditions: ethylbenzene 10 mmol, catalyst 0.2 g, TBHP 20 mmol, 130°C, 12 h.

AP = acetophenone, PE = 1-phenylethanol, BZ = benzaldehyde, BA = benzoic acid

The $Cu_{1.0}Mg_{2.9}Al$ oxide yielded the highest activity, the activity order is $Cu_{1.0}Mg_{2.9}Al > Ni_{0.9}Mg_{2.1}Al = Co_{0.8}Mg_{1.6}Al > Cr_{0.8}Mg_{2.4}Al \sim Mn_{0.9}Mg_{2.2}Al$ oxide. TPR result indicated that the $Cu_{1.0}Mg_{2.9}Al$ oxide showed the highest reducibility. However, the low activity obtained for the $Mn_{0.9}Mg_{1.9}Al$ oxide is likely the result of the presence of some $MnCO_3$ phase. This phase had already been reported to give a negative impact on catalytic activity [37].

3.6.2 Effect of reaction temperature

The reaction temperature was varied in the range of 90-150°C using $\text{Cu}_{1.0}\text{Mg}_{2.9}\text{Al}$ oxide. The results are shown in Figure 3.21.

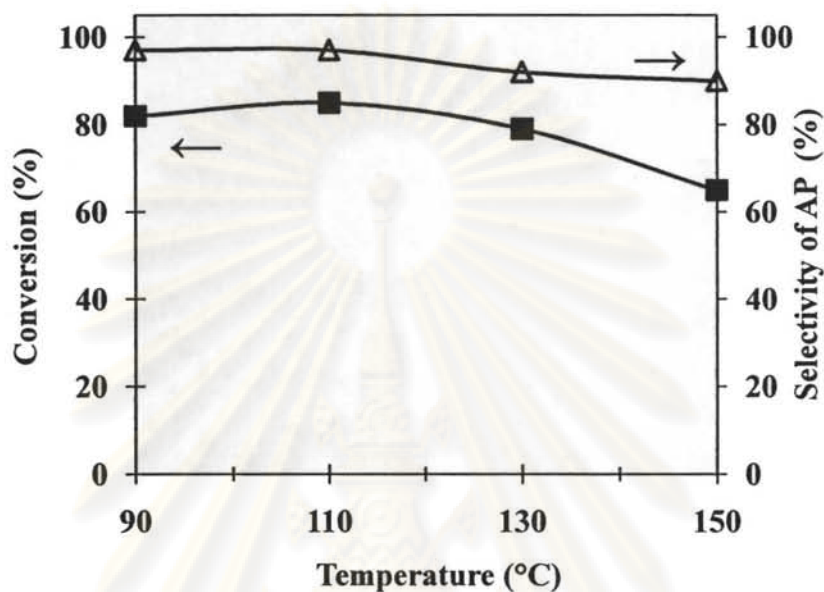


Figure 3.21 Effect of reaction temperature using the $\text{Cu}_{1.0}\text{Mg}_{2.9}\text{Al}$ oxide catalyst. Reaction conditions: ethylbenzene 10 mmol, catalyst 0.2 g, TBHP 20 mmol, 12 h.

The appropriate temperature range for oxidation of ethylbenzene is 90-110°C, which agrees well with TGA results and is consistent with a previous study which reported that these base catalyzed reactions required reaction temperatures below 150°C [29].

ศูนย์วิทยทรัพยากร
จุฬาลงกรณ์มหาวิทยาลัย

3.6.3 Effect of reaction time

Effect of reaction time was observed using $\text{Cu}_{1.0}\text{Mg}_{2.9}\text{Al}$ oxide catalyst, the results as shown in Figure 3.22.

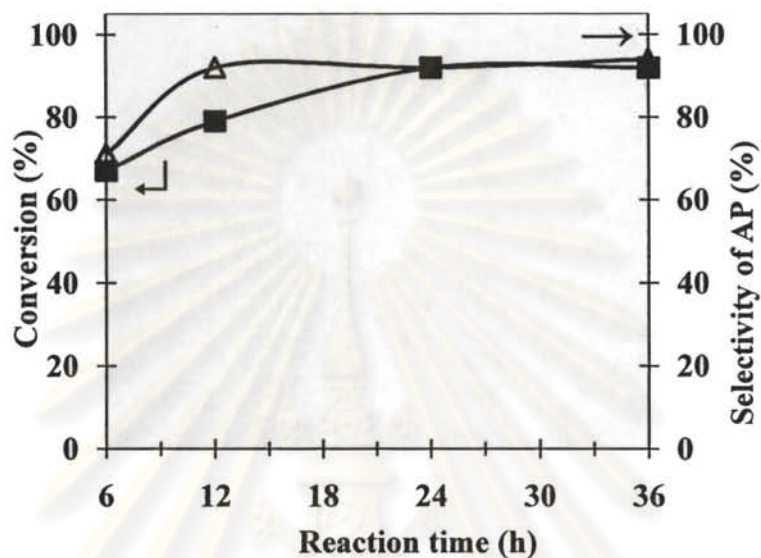


Figure 3.22 Effect of reaction time using $\text{Cu}_{1.0}\text{Mg}_{2.9}\text{Al}$ oxide catalyst.

Reaction conditions: ethylbenzene 10 mmol, TBHP 20 mmol, catalyst 0.2 g, 130°C.

The conversion of ethylbenzene increased with reaction time up to approximately 24 h. As the time increased the selectivity to acetophenone was enhanced from the oxidation of 1-phenylethanol. At longer reaction time of 36 h, benzoic acid (1%) was found from the oxidation of the acetophenone.

ศูนย์วิทยทรัพยากร
จุฬาลงกรณ์มหาวิทยาลัย

3.6.4 Effect of oxidant/substrate mole ratio

The effect of the amount of oxidant and substrate mole ratios (O/S) was studied using $\text{Cu}_{1.0}\text{Mg}_{2.9}\text{Al}$ oxide catalyst. The concentration of TBHP in the reaction was studied in terms of O/S ratio in the range of 1-5. The results are collected in Figure 3.23.

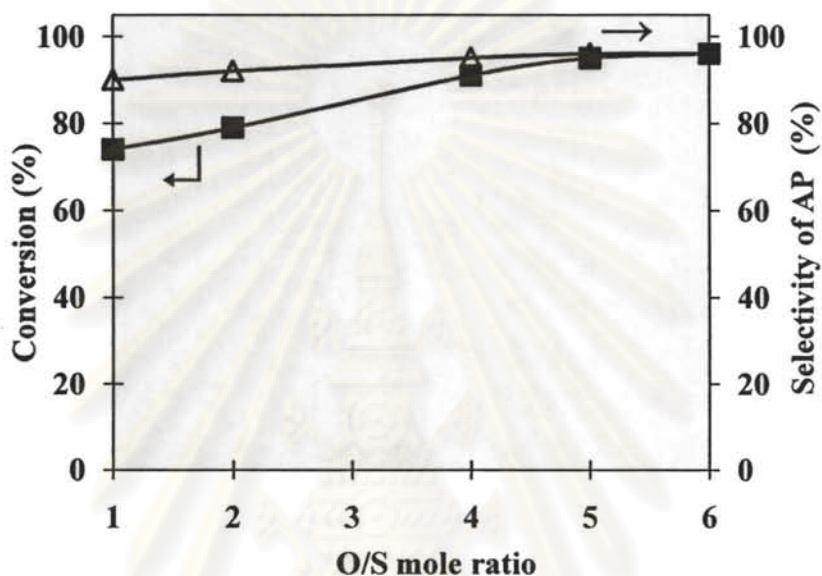


Figure 3.23 Effect of amount of oxidant using $\text{Cu}_{1.0}\text{Mg}_{2.9}\text{Al}$ oxide catalyst.

Reaction conditions: ethylbenzene 10 mmol, catalyst 0.2 g, 130°C, 12 h.

The conversion of ethylbenzene was increased with the TBHP concentration. There was no significant change in conversion and selectivity of acetophenone at the relatively high oxidant/substrate ≥ 4 .

ศูนย์วิทยทรัพยากร
จุฬาลงกรณ์มหาวิทยาลัย

3.6.5 Effect of radical scavenger

The exact mechanism of this reaction is yet unclear; however, the effect of hydroquinone, which is a radical scavenger, is investigated. The results are collected in Figure 3.24.

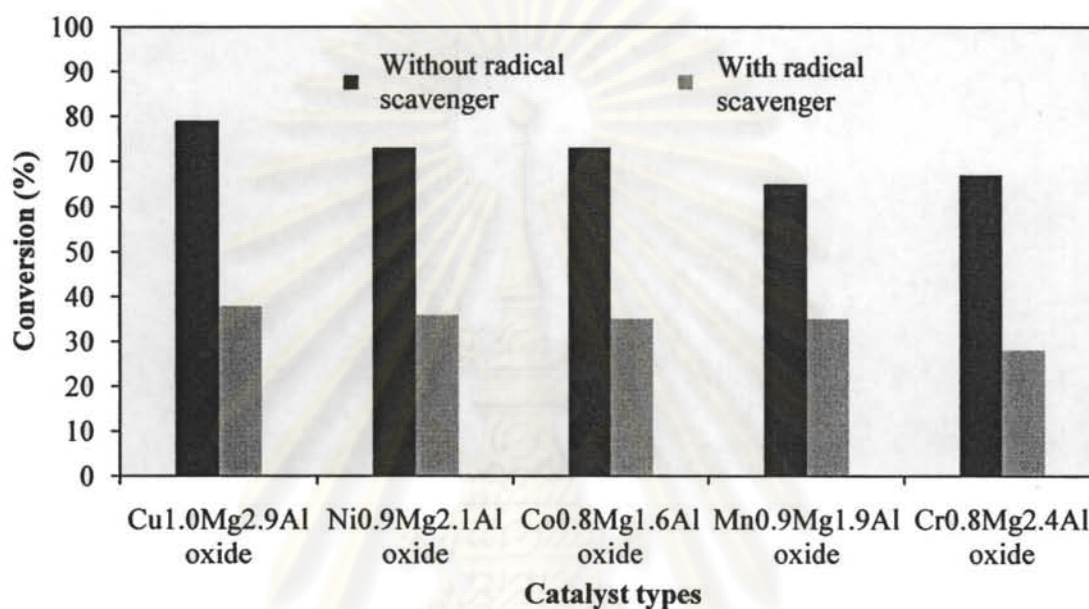


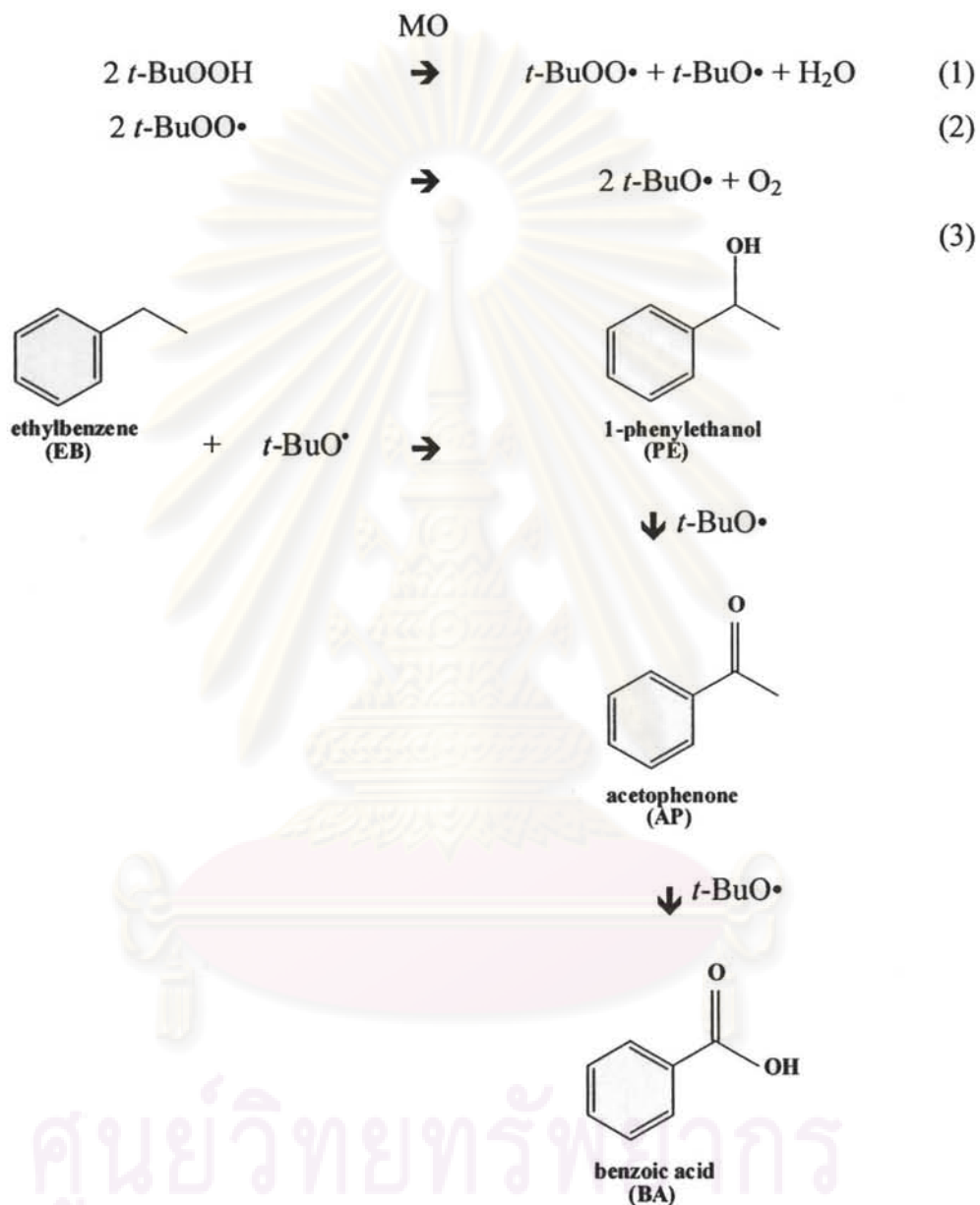
Figure 3.24 Catalytic oxidation of ethylbenzene using ternary mixed metal oxide in the presence of radical scavenger.

Reaction conditions: ethylbenzene 10 mmol, catalyst 0.2 g, hydroquinone 10 mmol, TBHP 20 mmol, 130°C, 12 h.

In the presence of hydroquinone radical scavenger gave lower catalytic activities. From the results obtained it can be concluded that the reaction proceeds via a free radical mechanism. The oxidation of isophorone with a ternary CuMgAl LDH catalyst showed a lower yield of ketoisophorone when 2,6-di-tert-butyl-4-methyl phenol was used as a free radical trap [44].

3.7 Mechanism

The catalytic oxidation of ethylbenzene using mixed metal oxide catalyst by TBHP as oxidant proposed to be as follows.



Scheme 3.3 Proposed mechanism of oxidation of ethylbenzene with mixed metal oxide catalyst using TBHP as oxidant.

3.8 Reusability of catalysts

The catalyst was reused after separation from the liquid reaction mixture by centrifugation followed by washing with the solvent and drying, while avoiding the loss of fine catalyst particles. Then the catalysts were regenerated by calcination in air at 500°C for 5 h.

The spent and reclaimed catalyst was tested in subsequent reactions. The results showed that both the catalysts can be reused with only slight loss of activity from 75% to 70% and 79% to 70%, respectively, from the first to the fourth run. Deactivation of the catalyst probably was due to neutralization of active base sites by the proton released upon TBHP deprotonation. Another possible cause was partial LDH reconstruction caused by the memory effect, particularly in the case of Mg-containing catalyst.

3.9 Heterogeneity of catalysts

The nature of the observed catalysis is truly heterogeneous. In order to find the heterogeneity of the catalyst, a leaching study was carried out using the hot filtrate (catalyst was removed after 6 h) and the amount of metal leached out from the catalyst was also confirmed by ICP analysis. No metal species was found in the filtrate.

3.10 Conclusion

Mixed metal oxide catalysts could catalyze ethylbenzene oxidation in good yield with high selectivity to acetophenone. High catalyst reducibility led to a high catalytic activity in oxidation of ethylbenzene with TBHP. An increase in the conversion of ethylbenzene was observed with increasing TBHP/substrate mole ratios and catalyst amounts. The conversion increased with temperature up to 110°C, whereas a further increase in the reaction temperature to 150°C reduced the conversion of ethylbenzene. The maximum conversion was obtained in non-solvent systems than in acetonitrile or dichloromethane. The catalytic oxidation of ethylbenzene with TBHP using mixed metal oxide occurs via free radical mechanism.

CHAPTER IV

OXIDATION OF ETHYLBENZENE, CYCLOHEXANE AND CYCLOHEXANOL USING POLYOXOMETALATES

In this chapter, the syntheses and characterization of polyoxometalate and transition metal substitution polyoxometalate catalysts are described. These catalysts have been used for the oxidation of hydrocarbons with hydrogen peroxide.

4.1 Introduction

The replacement of traditional, environmentally hazardous and corrosive homogeneous catalysts by heterogeneous catalysts in order to achieve clean technology is one of the goals of society. Among the solid acid catalysts, polyoxometalates (POM) are more efficient and have many other advantages over conventional acid catalysts. The first polyoxometalate, now known as ammonium 12-molybdophosphate, $(\text{NH}_3)_3[\text{PMo}_{12}\text{O}_{40}]$, was the first discovered in 1826 by Berzelius [68] and subsequently introduced to analytical chemistry in 1848 [69].

The applications of polyoxometalates are based on their unique properties, including size, mass, electron and proton transfer tendencies, storage abilities, thermal stabilities, labilities of their lattice oxygen atoms, and high Brønsted acidities of their corresponding acids. As noted above, they have long been used in analytical chemistry, as well as in many pharmaceuticals and in medicinal chemistry. There is a rapidly growing area of polyoxometalate petrochemistry and fine chemical production. Other applications including ion-exchange materials, ion-selective membranes and inorganic resistant materials have also been reported. Catalytic applications of polyoxometalates have been developed in solution as well as in the solid state, as acid and oxidation catalysts. It is evident that research interest in polyoxometalates is very high and still growing [70-72].

In their catalytic chemistry, polyoxometalates are one of the most attractive inorganic modifiers because in crystalline form they have been demonstrated to be highly conductive and thermally stable. There are a large number of different

polyoxometalates, but the most well known and studied are the Keggin type. The basic structural unit of these compounds is the Keggin anion $[XM_{12}O_{40}]^{(n-8)}$, for which n determines the metal oxidation state, X is a central heteroatom (B^{3+} , Si^{4+} or P^{5+}) surrounded by metal M is or an addenda atom (usually Mo^{6+} or W^{6+}) which can be partially replaced by many metal ions, e.g., V^{5+} , Co^{2+} , Zn^{2+} , etc [73-74]. The Keggin structure is composed of a central XO_4 tetrahedron surrounded by twelve edge and corner sharing octahedral metal-oxygen (MO_{12}) units. These compounds are negatively charged, and their electron densities are widely variable depending on the elemental composition and molecular structure.

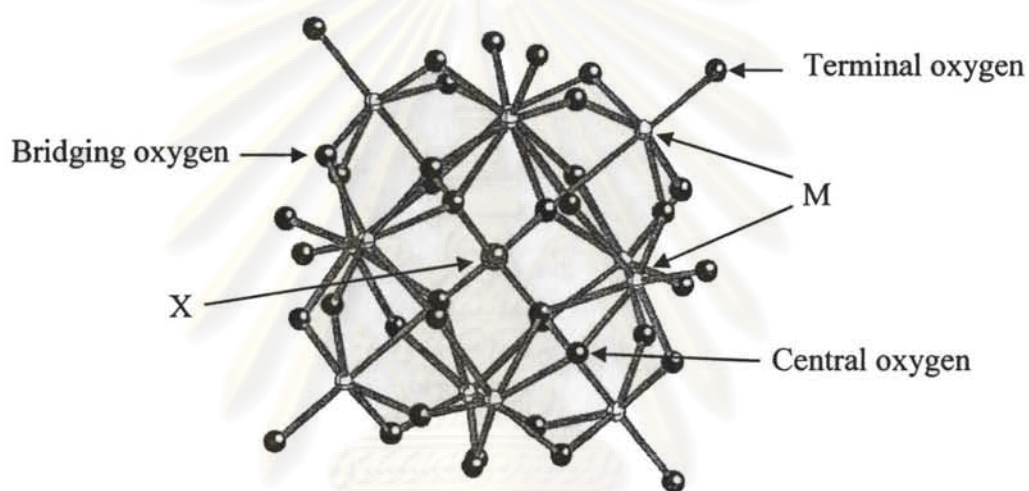


Figure 4.1 Ball-and-stick representation of the Keggin structure [75].

General properties of polyoxometalate compounds are [76-79]:

1. Very high molecular weights (2000 g/mol)
2. Highly colored
3. Highly hydrated
4. Decomposed in strongly basic solutions
5. Thermal stable (depend on the nature of the heteroatom and addenda atom). Complexes containing P as the central atom are generally more stable than the compounds containing Si and W as the addenda atom more stable than Mo.
6. Strong acids, solid heteropolyacids such as $H_3[PW_{12}O_{40}]$ and $H_3[PMo_{12}O_{40}]$ are pure Brønsted acids and are stronger than conventional solid acids such as $SiO_2-Al_2O_3$. The general trend for acid

strength among the common heteropolyacids is as follows $H_3[PW_{12}O_{40}] > H_4[SiW_{12}O_{40}] > H_3[PMo_{12}O_{40}] > H_4[SiMo_{12}O_{40}]$.

- Free acids and most salts of polyoxometalate compounds are soluble in water and organic solvents. Polyoxometalate compounds with large counter cations are less soluble. Cs^+ , Ag^+ , Tl^+ , Hg^{2+} , Pb^{2+} and the larger alkaline earth metal salts are insoluble. The water solubilities of polyoxometalate compounds must be attributed to very low lattice energies and favorable solvation energies of the cations.

Many of the free acids and a few of the salts are very soluble in organic solvents, especially if the latter contain oxygen. Thus, ethers, alcohols and ketones are generally the best solvents. The free acids are insoluble in non-oxygen containing solvents such as benzene, chloroform and carbon disulfide.

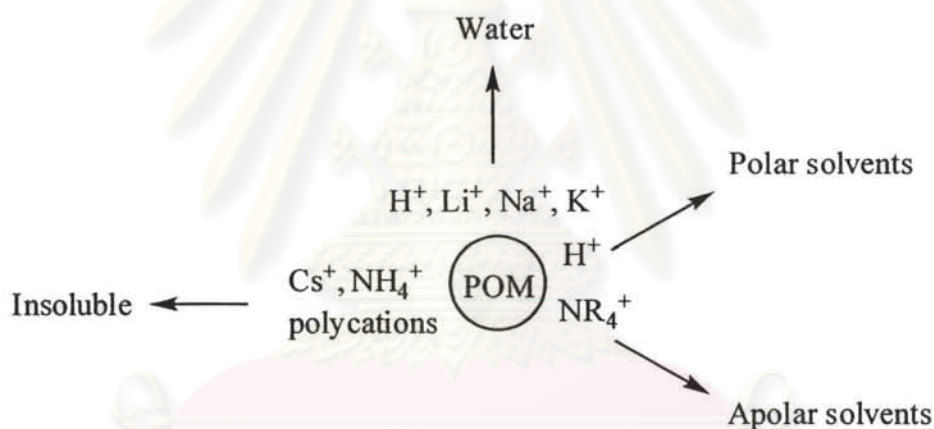


Figure 4.2 Solubility of polyoxometalates as a function of counter cations.

Among hydrocarbons, the oxygenation of alkanes has attracted much attention because they are abundant as resources but low in reactivity. With respect to potential oxidants, fine chemical production allows the choice of various oxygen donors such as peroxides. The global demand for cyclohexane in 2005 was just over 5 million metric tons, driven mainly by nylon feedstocks [64,80-85].

By 2010, global demand for cyclohexane is expected to reach approximately 6 million metric tons, representing an average annual growth rate of 3% during 2005-2010. Global demand in nylon fibers is expected to grow at a 2% annual pace in 2005-2010. China will exhibit the strongest growth for nylon, 3-4% annually, over the next five years. Concerning the source of the cyclohexane, six producers account for

50% of world capacity for cyclohexane: ExxonMobil, Chevron Phillips, Huntsman, Deutsche BP Aktiengesellschaft, ConocoPhillips and Idemitsu Kosan, as shown in Figure 4.3.

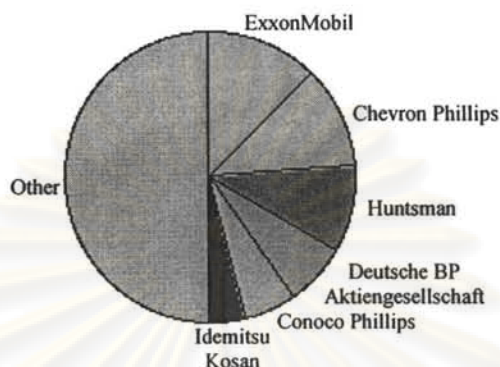


Figure 4.3 Global commercial sources for cyclohexane in 2006 [86].

Practically all cyclohexane is used to make cyclohexanol and cyclohexanone, which, in turn, are used mainly as precursors for adipic acid and caprolactam, respectively. Other uses for cyclohexane include various solvent applications and the production of cyclohexanol and cyclohexanone for nonprecursor uses. The following pie chart shows consumption of cyclohexane by geographic region.

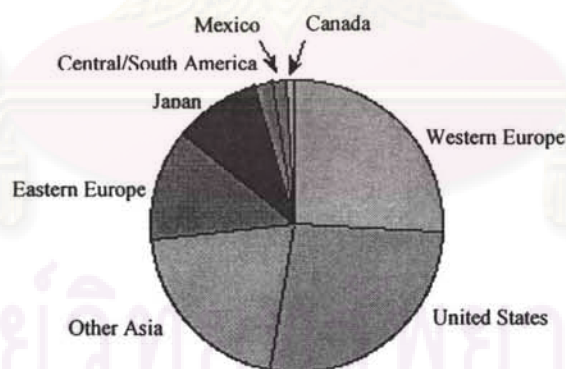
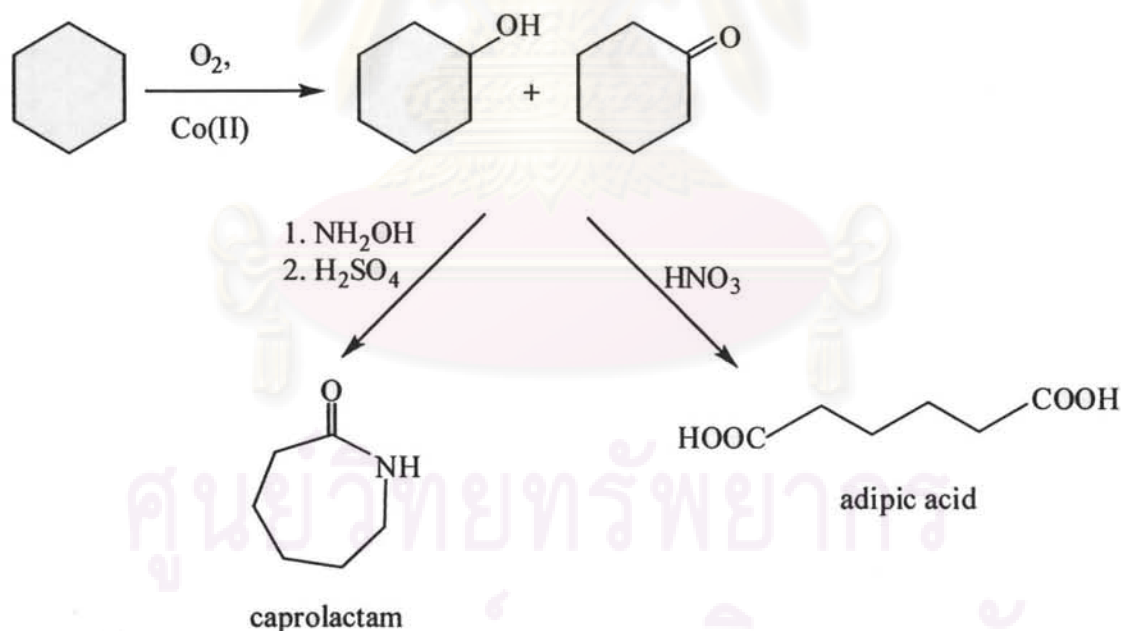


Figure 4.4 Consumption of cyclohexane by region for 2005 [86].

Much of the growth in world demand for cyclohexane will occur in China because of its increased output of nylon fibers, especially for caprolactam/nylon 6 based fibers. Demand for adipic acid is also increasing in China, both as a feedstock for Nylon 6,6 fibers and as a raw material for polyester-based hot melt adhesives for shoe soles. Consumption of cyclohexane is also expected to increase in Taiwan, mainly for nylon fiber production.

In the industrial process, cobalt naphthenate ($\text{Co}(\text{C}_{11}\text{H}_{10}\text{O}_2)_2$) is used for the oxidation of cyclohexane with air (15 atm) at 160°C . However, after 40 min, only 4% of the cyclohexane is converted to oxygenated products, with 80% selectivity towards cyclohexanone and cyclohexanol [7]. The oxidation of cyclohexane into cyclohexanone and cyclohexanol is a process of industrial importance. Over one billion tons of cyclohexanone and cyclohexanol are produced each year worldwide, which are mostly used in the manufacture of Nylon 6 and Nylon 6,6.

The productions of caprolactam and adipic acid is another interesting industrial processes (Scheme 4.1). The goal of many researchers is to produce only cyclohexanone and cyclohexanol with high conversion of cyclohexane and high yields, while using weak oxidants such as O_2 or H_2O_2 . The reaction should be carried out under mild conditions, at room temperature and pressure. However, cyclohexane contains only rather inert C-H bonds and thus only conversions of cyclohexane are to be expected.



Scheme 4.1 Oxidation of cyclohexane to adipic acid and caprolactam [7].

4.2 Literature reviews

Many publications have appeared on the use of polyoxometalates in catalytic oxidations with various substrates, and are described below.

4.2.1 Oxidation of hydrocarbons using polyoxometalate catalysts

In 1996, Matsumoto, *et al.* [78] reported the oxidation of cyclohexane using 80% TBHP with alkyl ammonium salts (Q) of mixed addenda silicotungstates, $(Q[SiW_{11}MO_{39}])$, for which $M = Co^{2+}$, Fe^{3+} or Ru^{3+} , generally in benzene (for $Q_6[SiW_{11}CoO_{39}]$ 1,2-dichloroethane was used), for 2 h at 60°C. The product yields decreased in the order: $Q_6[SiW_{11}CoO_{39}] > Q_5[SiW_{11}RuO_{39}] \geq Q_5[SiW_{11}FeO_{39}]$. Cyclohexanol was the main product and cyclohexanone being formed as a product of a secondary reaction of cyclohexanol.

In 1997, Mizuno, *et al.* [69] studied the liquid-phase oxidation of hydrocarbons by $[(n-C_4H_9)N]_4H_6[PW_9O_{37}\{Fe_2Ni(OAc)_3\}]$ using molecular oxygen as oxidant at 82°C. The conversion of ethylbenzene was 17% in 91 h, with acetophenone being the main product with 73% selectivity. For cyclohexane, conversion was very low (0.36%) and cyclohexanone was the main product with 83% selectivity. However, the catalytic oxidation of cyclohexane with this catalyst in CH_3CN using H_2O_2 as oxidant at 50°C for 118 h gave a higher conversion of 9.6%.

In 1999 Mizuno, *et al.* [87] reported the oxidation of cyclohexane using the *tetra*-butyl ammonium salts of silicotungstates with H_2O_2 as oxidant in CH_3CN at 32°C for 96 h. The initial rate and cyclohexane conversion were observed to follow the order $[(n-C_4H_9)_4N]_6[SiW_{10}Fe(H_2O)_2O_{38}]$ (25.3%) $>$ $[(n-C_4H_9)_4N]_7[SiW_9Fe(H_2O)_3O_{37}]$ (1.0%) $>$ $[(n-C_4H_9)_4N]_5[SiW_{10}Fe(H_2O)_2O_{38}]$ (0.4%) $>$ $[(n-C_4H_9)_4N]_4[SiW_{12}O_{40}]$ (0.1%). The cyclohexanone/cyclohexanol mole ratio equaled 2.

In 2000, Langpape, *et al.* [88] studied the catalytic oxidation of isobutane by heteropolymolybdates combined with various cations: $H_3[PMo_{12}O_{40}]$, $Fe_{0.85}H_{0.45}[PMo_{12}O_{40}]$, $Cs_2Fe_{0.2}H_{0.4}[PMo_{12}O_{40}]$ and $Cs_2H_1[PMo_{12}O_{40}]$. The feed composition mixture contained oxygen, isobutene, nitrogen and helium, in a

33.4:17.2:10.1:40.5 kPa ratio and with a total flow rate of 6 cm³/sec at 340°C. The activities for the oxidation of isobutane decreased in the order Cs₂H[PMo₁₂O₄₀] ≥ Cs₂Fe_{0.2}H_{0.4}[PMo₁₂O₄₀] > H₃[PMo₁₂O₄₀] > Fe_{0.85}H_{0.45}[PMo₁₂O₄₀], and the conversions were 4 - 7%. Methacrylic acid and methacrolein were the main products.

In 2001, Okuhara, *et al.* [89] reported the oxidation of methane (30.8 mmol, 50 atm) catalyzed by vanadium-containing polyoxomolybdates with hydrogen peroxide in fluorinated acid anhydrides [(CF₃CO)₂O] at 80°C for 24 h. The conversions decreased in the order H₄[PW₁₁VO₄₀] > H₅[SiMo₁₁VO₄₀] > H₄[PMo₁₁VO₄₀] > H₅[PMo₁₀V₂O₄₀] > H₃[PMo₁₂O₄₀] > H₆[PMo₉V₃O₄₀], with conversions ranging from 2.7-10.2%. The H₄[PW₁₁VO₄₀] catalyst gave acetic acid as the main product with a 23% selectivity.

In 2002, Nowinska, *et al.* [64] described the oxydehydrogenation of propane by Fe²⁺, Fe³⁺ and Mn²⁺ modified potassium salts of [PW₁₁MO₃₉]^{x-} and M_xK_{5-x}[PW₁₁MO₃₉]. The iron-modified tungstophosphoric anions were unstable under their conditions, with the air:propane feed composition being 25:1 at 50 and 160°C. The catalytic activities and selectivities were significantly dependent on the solution pH used for partial degradation in the preparation step. At a pH of 2, the highest conversion, 45% with 59% selectivity to propene, was found. The unmodified tungstophosphoric acid did not show any oxidative activity. The principal result was that Mn²⁺ incorporation into the Keggin structure led to higher reduction temperatures than their parents, but also enhanced the stabilities of the catalysts.

In 2004, Balula, *et al.* [80] prepared *tetra*-butylammonium salts of polyoxometalates, [XW₁₁M(H₂O)O₃₉]^{p-}, with X = P or Si and M = Fe³⁺ or Mn³⁺. The catalysts were used for the oxidation of cyclooctane with H₂O₂ in acetonitrile. An excess of H₂O₂ afforded higher selectivities for cyclooctyl hydroperoxide. For reactions performed with a H₂O₂/cyclooctane ratio of 2.0, the amount of H₂O₂ in solution decreased more rapidly in the presence of [(*n*-C₄H₉)₄N]₄[PW₁₁Fe(H₂O)O₃₉] than [(*n*-C₄H₉)₄N]₄H₄[SiW₁₁O₃₉]. The main products were cyclooctyl hydroperoxide and cyclooctanone, while cyclooctanol was detected in low yields. The cyclooctyl

hydroperoxide/cyclooctanone ratio, calculated after 9 h of reaction, varied between 0.4 and 1.7, being smaller than 1 for reactions with $[(n\text{-C}_4\text{H}_9)_4\text{N}]_3[\text{PW}_{12}\text{O}_{40}]$, $[(n\text{-C}_4\text{H}_9)_4\text{N}]_4[\text{PW}_{11}\text{VO}_{40}]$, $[(n\text{-C}_4\text{H}_9)_4\text{N}]_4[\text{PW}_{11}\text{Mn}(\text{H}_2\text{O})\text{O}_{39}]$ and $[(n\text{-C}_4\text{H}_9)_4\text{N}]_4\text{H}[\text{SiW}_{11}\text{Fe}(\text{H}_2\text{O})\text{O}_{39}]$. Under these conditions, the lowest selectivities for the hydroperoxide were observed for the $[(n\text{-C}_4\text{H}_9)_4\text{N}]_4[\text{PW}_{11}\text{Mn}(\text{H}_2\text{O})\text{O}_{39}]$ and $[(n\text{-C}_4\text{H}_9)_4\text{N}]_4\text{H}[\text{SiW}_{11}\text{Mn}(\text{H}_2\text{O})\text{O}_{39}]$ polyoxoanions, and the highest selectivities for $[(n\text{-C}_4\text{H}_9)_4\text{N}]_4\text{H}_4[\text{SiW}_{11}\text{O}_{39}]$.

In 2006, Li, *et al.* [81] studied the partial oxidation of propane by $\text{H}_3[\text{PMo}_{12}\text{O}_{40}]$, $\text{H}(\text{VO})[\text{PMo}_{12}\text{O}_{40}]$ and $\text{H}_4[\text{PMo}_{11}\text{VO}_{40}]$. The reaction was studied at 400°C with the propane: molecular oxygen: helium feed composition being 17:30:53 (flow rate 15 mL/min). The highest conversions of propane were observed over $\text{H}(\text{VO})[\text{PMo}_{12}\text{O}_{40}]$ at 53.7%. The effect of Cs^+ substitution for H^+ was observed at 420°C, with the propane: molecular oxygen: helium feed composition being 10:20:70. The activity decreased in the order $\text{Cs}_{2.5}\text{H}_{1.5}[\text{PMo}_{11}\text{VO}_{40}] > \text{Cs}_{2.5}\text{H}_{1.1}(\text{VO})_{0.2}[\text{PMo}_{11}\text{VO}_{40}] > \text{Cs}_{2.5}\text{H}_{0.1}(\text{VO})_{0.2}[\text{PMo}_{12}\text{O}_{40}] > \text{Cs}_{2.5}\text{H}_{0.5}[\text{PMo}_{12}\text{O}_{40}]$, with conversions of 46.2, 43.6, 40.6 and 24.2%, respectively.

4.2.2 Oxidations of other substrates

Polyoxometalates were also used for the catalytic oxidations of other substrates, and some key publications are described below.

In 1993, Atlamsani, *et al.* [82] reported the catalytic oxidation of 2-methylcyclohexanone and cyclohexanone using $\text{H}_5[\text{PMo}_{10}\text{V}_2\text{O}_{40}]$ and $\text{H}_4[\text{PMo}_8\text{V}_4\text{O}_{40}]$ by molecular oxygen (1 atm) at 70°. The $\text{H}_4[\text{PMo}_8\text{V}_4\text{O}_{40}]$ catalyst gave a higher activity than $\text{H}_5[\text{PMo}_{10}\text{V}_2\text{O}_{40}]$. The oxidation of cyclohexanone was carried out in different solvents and *tert*-butyl alcohol (90%) gave a higher conversion over acetonitrile (85%), ethanol (65%) and acetic acid (54%).

In 2003, Etienne, *et al.* [83] reported the preparation of Fe-doped $\text{K}(\text{NH}_4)_2[\text{PMo}_{12}\text{O}_{40}]$ with an Fe/P atomic ratio ranging from 0 - 1.5. The catalysts were used for the oxidation of isobutane. The catalysts were calcined at 350°C before use. The mol% feed composition was isobutane 26: molecular oxygen 13, steam 12, with the balance being helium. It was found that when the Fe/P atomic ratio increased

from 0.5 to 1.5, the conversion of isobutane increased from 6.1 to 11.4% but the selectivity to methacrylic acid was reduced from 32 to 22%.

In 2004, Kholdeeva, *et al.* [84] reported the aerobic oxidation of isobutyraldehyde with $[(n\text{-C}_4\text{H}_9)_4\text{N}]_4\text{H}[\text{PW}_{11}\text{CoO}_{39}]$ and $[(n\text{-C}_4\text{H}_9)_4\text{N}]_5[\text{PW}_{11}\text{CoO}_{39}]$ as catalysts. The reactions were carried out in acetonitrile, under 1 atm air for 6 h at 20°C. The results showed that the catalyst with a proton counter cation, $[(n\text{-C}_4\text{H}_9)_4\text{N}]_4\text{H}[\text{PW}_{11}\text{CoO}_{39}]$, has a higher activity than $[(n\text{-C}_4\text{H}_9)_4\text{N}]_5[\text{PW}_{11}\text{CoO}_{39}]$ (94 and 71% conversions) with a 54% selectivity for isobutyric acid.

In 2006, Oxana, *et al.* [85] published a study dealing with the catalytic oxidation of α -pinene by Zr-substituted polyoxometalates, including $[(n\text{-C}_4\text{H}_9)_4\text{N}]_7\text{H}[\text{PW}_{11}\text{ZrO}_{39}(\mu\text{-OH})_2]$, $[(n\text{-C}_4\text{H}_9)_4\text{N}]_8[\text{PW}_{11}\text{ZrO}_{39}(\mu\text{-OH})_2]$, and $[(n\text{-C}_4\text{H}_9)_4\text{N}]_9[(\text{PW}_{11}\text{ZrO}_{39})_2(\mu\text{-OH})(\mu\text{-O})]$ using H_2O_2 as the oxidant. The reactions were carried out in acetonitrile at 30°C for 1 h, with the substrate: H_2O_2 :catalyst molar ratio being 0.1:0.12:0.0025. The catalytic activities decreased in the order $[(n\text{-C}_4\text{H}_9)_4\text{N}]_7\text{H}[\text{PW}_{11}\text{ZrO}_{39}(\mu\text{-OH})_2] > [(n\text{-C}_4\text{H}_9)_4\text{N}]_8[\text{PW}_{11}\text{ZrO}_{39}(\mu\text{-OH})_2] > [(n\text{-C}_4\text{H}_9)_4\text{N}]_9[(\text{PW}_{11}\text{ZrO}_{39})_2(\mu\text{-OH})(\mu\text{-O})]$ (conversions of 40, 25 and 7%, respectively), yielding verbenol and verbenone as the major products.

In 2007, Bonchio, *et al.* [90] reported the oxidation of *cis*-cyclooctene by oxygen in 1,2-dichloroethane at 75°C for 300 h using *tetra*-heptylammonium (THA) salts of transition metal-substituted polyoxotungstates, $\text{THA}_n[\text{Fe}_4(\text{H}_2\text{O}(\text{XW}_9\text{O}_{33})_2)]^{n-}$, as catalysts, for which $\text{M} = \text{Sb}^{3+}$, As^{3+} , Se^{4+} and Te^{4+} . The conversions of *cis*-cyclooctene followed the order $\text{THA}_6[\beta\text{-Fe}_4(\text{H}_2\text{O})_{10}(\text{SbW}_9\text{O}_{33})_2]$ (68%) $>$ $\text{THA}_4[\beta\text{-Fe}_4(\text{H}_2\text{O})_{10}(\text{TeW}_9\text{O}_{33})_2]$ (58%) $>$ $\text{THA}_6[\beta\text{-Fe}_4(\text{H}_2\text{O})_{10}(\text{AsW}_9\text{O}_{33})_2]$ (51%) and $\text{THA}_4[\beta\text{-Fe}_4(\text{H}_2\text{O})_{10}(\text{SeW}_9\text{O}_{33})_2]$ (40%). The major product was cyclooctene oxide, >59 - 66%.

In 2008, Mirkhani, *et al.* [91] published a study on the oxidation of alkanes (cyclohexane, cyclooctane and ethylbenzene) with H_2O_2 using $\text{M}(\text{salen})\text{-K}_8[\text{SiW}_{11}\text{O}_{39}]$ (salen = $\text{N,N}'$ -ethylenebis(salicylimine)) catalysts for which $\text{M} = \text{Co}^{2+}$, Ni^{2+} , Fe^{3+} and Mn^{3+} , at 80°C for 5 h in acetonitrile. $\text{Fe}^{3+}(\text{salen})\text{-K}_8[\text{SiW}_{11}\text{O}_{39}]$ catalyst gave the highest activity, which was much higher than that for $\text{Fe}^{3+}(\text{salen})\text{Cl}$. The major products were ketones with selectivities $> 90\%$ and conversions $> 50\%$ for all substrates.

Several literature reports, deal with the catalytic oxidation of alcohols and hydrocarbons with mono-substituted polyoxometalates. Therefore, the catalytic oxidation of hydrocarbons using mono-substituted polyoxometalates is interesting. Especially using an environmentally friendly oxidant such as hydrogen peroxide



ศูนย์วิทยทรัพยากร
จุฬาลงกรณ์มหาวิทยาลัย

4.3 Preparation of catalysts

Polyoxometalate catalysts with different cations were prepared by the methods described in the literatures.

4.3.1 Disodium salts of molybdophosphoric and tungstophosphoric acids: $\text{Na}_2\text{H}[\text{PMo}_{12}\text{O}_{40}]$ and $\text{Na}_2\text{H}[\text{PW}_{12}\text{O}_{40}]$ [92]

To a solution of disodium molybdate dihydrate, $\text{Na}_2\text{MoO}_4 \cdot 2\text{H}_2\text{O}$ (14.46 g, 0.07 mol), or sodium tungsten dihydrate, $\text{Na}_2\text{WO}_4 \cdot 2\text{H}_2\text{O}$ (19.46 g, 0.06 mol), were added successively to 0.40 mL of 85% H_3PO_4 and 15 mL of 70% HClO_4 . A precipitate formed from the yellow (for Mo catalyst) or white (for W catalyst) solution. After the mixture was cooled to room temperature, the powder (greenish for Mo catalyst, white for W catalyst) was filtered and dried in vacuum. The powders were recrystallized from a 1:5 (v/v) diethyl ether:water. The product yields were 5.23 g for $\text{Na}_2\text{H}[\text{PMo}_{12}\text{O}_{40}]$ and 5.34 g. for $\text{Na}_2\text{H}[\text{PW}_{12}\text{O}_{40}]$.

$\text{Na}_2\text{H}[\text{PMo}_{12}\text{O}_{40}]$

UV-vis λ_{max} (CH_3CN): 310 nm

Anal. (Mo%): Found: 2.86; Calculated: 2.96

XRD: 2θ : 8.5°, 9.6°, 23.6°, 29.4°

$\text{Na}_2\text{H}[\text{PW}_{12}\text{O}_{40}]$

UV-vis λ_{max} (CH_3CN): 270 nm

Anal. (W%): Found: 1.86; Calculated: 1.91

XRD: 2θ : 10.0°, 15.4°, 18.3°, 25.7°

4.3.2 Molybdophosphoric and tungstophosphoric acids: $\text{H}_3[\text{PMo}_{12}\text{O}_{40}]$ and $\text{H}_3[\text{PW}_{12}\text{O}_{40}]$ [92-93]

A solution of $\text{Na}_2\text{H}[\text{PMo}_{12}\text{O}_{40}]$ (10.0 g) or $\text{Na}_2\text{H}[\text{PW}_{12}\text{O}_{40}]$ (15.0 g) was acidified with 12 mol/dm³ HCl to pH = 1 and extracted by 20 mL diethyl ether. The precipitate which formed was filtered and dried in vacuum to give yellow (Mo catalyst) and white (W catalyst) powder, respectively.

H₃[PMo₁₂O₄₀]UV-vis λ_{\max} (CH₃CN): 312 nmXRD: 2θ : 8.4°, 9.9°, 25.1°, 28.0° (JCPDF 43-0317)**H₃[PW₁₂O₄₀]**UV-vis λ_{\max} (CH₃CN): 271 nmXRD: 2θ : 8.0°, 9.2°, 23.0°, 26.0° (JCPDF 50-0656)**4.3.3 Tetrabutyl ammonium salts of molybdophosphate and tungstophosphate: [(n-C₄H₉)₄N]₃[PMo₁₂O₄₀] and [(n-C₄H₉)₄N]₃[PW₁₂O₄₀] [94]**

0.5 g of Na₂MoO₄ · 2H₂O or Na₂WO₄ · 2H₂O was dissolved in 5 mL water, 0.2 mL of 85% H₃PO₄ and 0.5 mL of concentrated sulfuric acid were then added, and the resulting suspension was stirred at room temperature for 12 h. Addition of 3 mL of water yielded a clear solution to which 0.14 g of (n-C₄H₉)₄NBr was added immediately. After 15 min of stirring, the resulting precipitate was filtered off, washed with water, ethanol, and ether, and dried in vacuum to give light green (Mo catalyst) and white (W catalyst) crystals.

[(n-C₄H₉)₄N]₃[PMo₁₂O₄₀]UV-vis λ_{\max} (CH₃CN): 310 nmXRD: 2θ : 10.3°, 15.2°, 18.8°, 23.7°**[(n-C₄H₉)₄N]₃[PW₁₂O₄₀]**UV-vis λ_{\max} (CH₃CN): 265 nmXRD: 2θ : 10.2°, 15.0°, 18.3°, 23.6°

**4.3.4 11-Tungsto-1-vanadophosphate: $[(n\text{-C}_4\text{H}_9)_4\text{N}]_4[\text{PW}_{11}\text{VO}_{40}]$
 10-Tungsto-2-vanadophosphate: $[(n\text{-C}_4\text{H}_9)_4\text{N}]_5[\text{PW}_{10}\text{V}_2\text{O}_{40}]$ and
 9-Tungsto-3-vanadophosphate: $[(n\text{-C}_4\text{H}_9)_4\text{N}]_6[\text{PW}_9\text{V}_3\text{O}_{40}]$ [95]**

First, a stock solution of V(V) was prepared by dissolving 6 g NH_4VO_3 and 4 g NaOH in 100 mL of water. $\text{NaH}_2\text{PO}_4 \cdot 2\text{H}_2\text{O}$ (0.19 g) was added to a solution of 4.12 g of $\text{Na}_2\text{WO}_4 \cdot 2\text{H}_2\text{O}$ in 150 mL of water, followed by the addition of 22 mL of conc. HCl. After stirring, 5.0 mL, 20 mL and 80 mL portions of the V(V) stock solution were added for the $[(n\text{-C}_4\text{H}_9)_4\text{N}]_4[\text{PW}_{11}\text{VO}_{40}]$, $[(n\text{-C}_4\text{H}_9)_4\text{N}]_5[\text{PW}_{10}\text{V}_2\text{O}_{40}]$ and $[(n\text{-C}_4\text{H}_9)_4\text{N}]_6[\text{PW}_9\text{V}_3\text{O}_{40}]$ respectively. Finally, a solution of $(n\text{-C}_4\text{H}_9)_4\text{NBr}$ was added dropwise with stirring after heating at 70°C for 24 h. The precipitated salts were filtered off, washed with water, ethanol and dried in vacuum at 50°C . The compounds were recrystallized from acetonitrile to give yellow crystals; the product yields $[(n\text{-C}_4\text{H}_9)_4\text{N}]_4[\text{PW}_{11}\text{VO}_{40}]$, $[(n\text{-C}_4\text{H}_9)_4\text{N}]_5[\text{PW}_{10}\text{V}_2\text{O}_{40}]$ and $[(n\text{-C}_4\text{H}_9)_4\text{N}]_6[\text{PW}_9\text{V}_3\text{O}_{40}]$ were 5.32, 5.19 and 5.06 g, respectively.

$[(n\text{-C}_4\text{H}_9)_4\text{N}]_4[\text{PW}_{11}\text{VO}_{40}]$

UV-vis λ_{max} (CH_3CN): 261, 470 nm

Anal. (V%): Found: 1.29, Calculated 1.37

XRD: 2θ : 6.6° , 7.6° , 12.1° , 23.5° , 30.0°

$[(n\text{-C}_4\text{H}_9)_4\text{N}]_5[\text{PW}_{10}\text{V}_2\text{O}_{40}]$

UV-vis λ_{max} (CH_3CN): 250, 463 nm

Anal. (V%): Found: 2.76, Calculated 2.84

XRD: 2θ : 6.6° , 7.6° , 12.1° , 23.5° , 30.0°

$[(n\text{-C}_4\text{H}_9)_4\text{N}]_6[\text{PW}_9\text{V}_3\text{O}_{40}]$

UV-vis λ_{max} (CH_3CN): 245, 443 nm

Anal. (V%): Found: 3.75, Calculated 3.88

XRD: 2θ : 6.6° , 7.6° , 12.1° , 23.5° , 30.0°

**4.3.5 $[(n\text{-C}_4\text{H}_9)_4\text{N}]_4\text{H}[\text{PW}_{11}\text{M}(\text{H}_2\text{O})\text{O}_{39}]$ where M = Mn, Co, Cu, Cr or Ni
[96-97]**

$[(n\text{-C}_4\text{H}_9)_4\text{N}]_4\text{H}[\text{PW}_{11}\text{Co}(\text{H}_2\text{O})\text{O}_{39}]$ was prepared by mixing Na_2HPO_4 (9.1 mmol), $\text{Na}_2\text{WO}_4 \cdot 2\text{H}_2\text{O}$ (100 mmol) and after that the nitrate salt of the appropriate metal ion (12 mmol) in 200 mL of water, and the pH was adjusted to 5 with concentrated nitric acid. An aqueous solution of $[(n\text{-C}_4\text{H}_9)_4\text{N}]\text{Br}$ (45 mmol) in 20 mL was added dropwise, with stirring at 80°C . The precipitated salts were filtered off, washed with water and ethanol, and dried in vacuum at 50°C . The compounds were recrystallized from acetonitrile to give orange, pink and light green crystals.

$[(n\text{-C}_4\text{H}_9)_4\text{N}]_4\text{H}[\text{PW}_{11}\text{Ni}(\text{H}_2\text{O})\text{O}_{39}]$

UV-vis λ_{max} (CH_3CN): 256, 416 nm

Anal. (Ni%): Found 1.59, Calculated 1.57

$[(n\text{-C}_4\text{H}_9)_4\text{N}]_4\text{H}[\text{PW}_{11}\text{Co}(\text{H}_2\text{O})\text{O}_{39}]$

UV-vis λ_{max} (CH_3CN): 254, 474 nm

Anal. (Co%): Found 1.54, Calculated 1.73

$[(n\text{-C}_4\text{H}_9)_4\text{N}]_4\text{H}[\text{PW}_{11}\text{Mn}(\text{H}_2\text{O})\text{O}_{39}]$ [98]

UV-vis λ_{max} (CH_3CN): 261, 379 nm

Anal. (Mn%): Found 1.22, Calculated 1.46

$[(n\text{-C}_4\text{H}_9)_4\text{N}]_4\text{H}[\text{PW}_{11}\text{CuO}_{39}]$

UV-vis λ_{max} (CH_3CN): 261, 625 nm

Anal. (Cu %): Found 1.62, Calculated 1.71

$[(n\text{-C}_4\text{H}_9)_4\text{N}]_4[\text{PW}_{11}\text{Cr}(\text{H}_2\text{O})\text{O}_{39}]$

UV-vis λ_{max} (CH_3CN): 256, 626 nm

Anal. (Cr %): Found 1.50, Calculated 1.67

XRD patterns of $[(n\text{-C}_4\text{H}_9)_4\text{N}]_4\text{H}[\text{PW}_{11}\text{M}(\text{H}_2\text{O})\text{O}_{39}]$, (M= Cu, Mn, Co, Cr and Ni) show similar diffraction peaks at; $2\theta = 8.3^\circ$, 9.0° , 27.8° and 29.1° [99].

4.4 Catalyst characterization

The polyoxometalate catalysts were characterized spectroscopically by FTIR, XRD, TGA, NH₃-TPD and H₂-TPR techniques, and the results are given below.

4.4.1 Fourier transform infrared spectroscopy (FTIR)

Keggin-type polyoxotungstates give characteristic infrared bands in the 1100-700 cm⁻¹ region [90, 92]. The results are collected in Table 4.1.

Table 4.1 FTIR spectra of polyoxometalates

Catalyst	Wavenumber (cm ⁻¹)			
	ν_{as} P-O	ν_{as} M = O _t	ν_{as} M -O _b -M	ν_{as} M-O _c -M
H ₃ [PMo ₁₂ O ₄₀]	1064	964	867	788
H ₃ [PW ₁₂ O ₄₀]	1080	988	890	805
Na ₂ H[PMo ₁₂ O ₄₀]	1063	970	860	787
Na ₂ H[PW ₁₂ O ₄₀]	1077	983	889	789
[(<i>n</i> -C ₄ H ₉) ₄ N] ₃ [PMo ₁₂ O ₄₀]	1070	965	870	804
[(<i>n</i> -C ₄ H ₉) ₄ N] ₃ [PW ₁₂ O ₄₀]	1080	978	895	813
[(<i>n</i> -C ₄ H ₉) ₄ N] ₄ [PW ₁₁ VO ₄₀]	1073,1095	965	886	809
[(<i>n</i> -C ₄ H ₉) ₄ N] ₅ [PW ₁₀ V ₂ O ₄₀]	1065,1093	962	886	808
[(<i>n</i> -C ₄ H ₉) ₄ N] ₆ [PW ₉ V ₃ O ₄₀]	1065,1093	960	882	808
[(<i>n</i> -C ₄ H ₉) ₄ N] ₄ H[PW ₁₁ Ni(H ₂ O)O ₃₉]	1065	969	887	812
[(<i>n</i> -C ₄ H ₉) ₄ N] ₄ H[PW ₁₁ Co(H ₂ O)O ₃₉]	1063	965	887	811
[(<i>n</i> -C ₄ H ₉) ₄ N] ₄ H[PW ₁₁ Mn(H ₂ O)O ₃₉]	1073,1057	967	887	818
[(<i>n</i> -C ₄ H ₉) ₄ N] ₄ H[PW ₁₁ CuO ₃₉]	1101,1067	966	887	816
[(<i>n</i> -C ₄ H ₉) ₄ N] ₄ [PW ₁₁ Cr(H ₂ O)O ₃₉]	1086,1051	965	885	815

t = terminal, b = in corner shared octahedral, c = in edge shared octahedral

ศูนย์วิจัยทรัพยากร
จุฬาลงกรณ์มหาวิทยาลัย

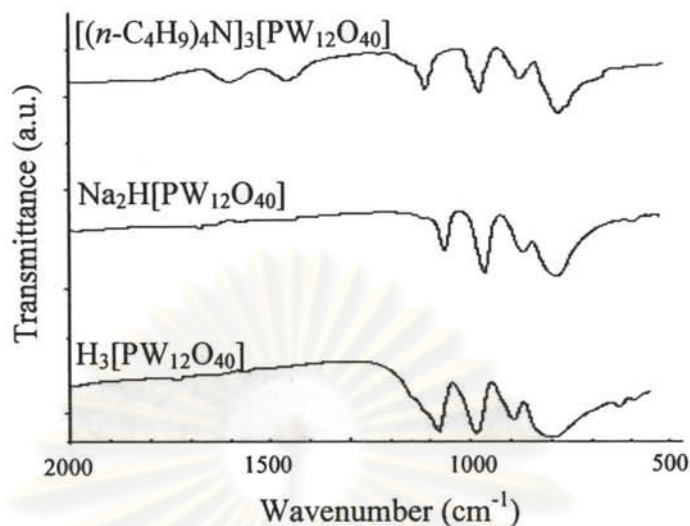


Figure 4.5 FTIR spectra of $\text{H}_3[\text{PW}_{12}\text{O}_{40}]$, $\text{Na}_2\text{H}[\text{PW}_{12}\text{O}_{40}]$ and $[(n\text{-C}_4\text{H}_9)_4\text{N}]_3[\text{PW}_{12}\text{O}_{40}]$.

The FTIR (KBr) results for $\text{H}_3[\text{PMo}_{12}\text{O}_{40}]$, $\text{H}_3[\text{PW}_{12}\text{O}_{40}]$, $\text{Na}_2\text{H}[\text{PMo}_{12}\text{O}_{40}]$ and $\text{Na}_2\text{H}[\text{PW}_{12}\text{O}_{40}]$ (Figure 4.6) show similar four band patterns consistent with the literature [94]. The catalysts containing Mo have lower frequencies than the catalysts containing W. The vibration frequencies of catalysts have previously been shown to depend on the nature of the cation.

The P-O bands appear in the range of $1057\text{-}1080\text{ cm}^{-1}$. It happens that this environment is distorted upon substitution of vanadium into the primary structure of Keggin POMs [100]. The bands at $960\text{-}988\text{ cm}^{-1}$ may be associated with the terminal $(\text{Mo,W})=\text{O}$ bonds. The inter-octahedral (oxygen connecting two WO_6 octahedra in a triad) $\text{W-O}_b\text{-W}$ bands appeared in the range of $867\text{-}887\text{ cm}^{-1}$, and the $\text{W-O}_c\text{-W(V)}$ bands appeared at $787\text{-}818\text{ cm}^{-1}$, which comprise the fingerprint region of Keggin POMs [101]. It is noteworthy that each IR band in the series of $[(n\text{-C}_4\text{H}_9)_4\text{N}]_{4+x}[\text{PW}_{12-x}\text{V}_x\text{O}_{40}]$ catalysts shifted to a lower wave number with increasing vanadium substitution, in particular for the assigned W-O_d vibration, in good agreement with previous results [92].

The FTIR spectra of the tetrabutylammonium salts of transition metal-substituted polyoxotungstates show absorption bands which are slightly shifted to lower wave numbers compared to the Na^+ or H^+ salts, due to the weaker of interactions with their cations [99-103]. The P-O band values found for $[(n\text{-}$

$C_4H_9)_4N)_4H[PW_{11}CuO_{39}]$ are higher, indicating that the distortion of the environment around copper in this anion is more pronounced than for the other metals [102]. The FTIR data indicate that all of the catalysts have Keggin structure frameworks.

4.4.2 Nitrogen adsorption (Brunauer-Emmett-Teller method (BET))

As it is known that salts of $[PW_{12}O_{40}]^{n-}$ with the cations like Na^+ or H^+ have low surface areas ($< 10 \text{ m}^2/\text{g}$) [102-103], the BET surface areas for some representative new catalysts were determined. The results are shown in Table 4.2.

Table 4.2 Surface area measurements of polyoxometalates

Catalyst	Surface area (m^2/g)	Pore volume (cm^3/g)	Mean pore diameter (nm)
$[(n-C_4H_9)_4N]_3[PMo_{12}O_{40}]$	3.3	2.8	33.0
$[(n-C_4H_9)_4N]_3[PW_{12}O_{40}]$	5.3	0.2	67.3
$[(n-C_4H_9)_4N]_4[PW_{11}VO_{40}]$	3.3	0.1	60.3
$[(n-C_4H_9)_4N]_5[PW_{10}V_2O_{40}]$	5.1	4.8	37.5

The Tetrabutylammonium salt catalysts gave surface areas in the range of 3.3-5.3 m^2/g . The catalysts with tetrabutylammonium as the cation possessed larger BET surface areas than the analogous acid and sodium salts.

ศูนย์วิทยทรัพยากร
จุฬาลงกรณ์มหาวิทยาลัย

4.4.3 Thermogravimetric analysis

Thermogravimetric results for the phosphorus-containing species indicated that the compounds decomposed according to the equation:



for which $M = \text{Mo}$ or W and $n = 4$.

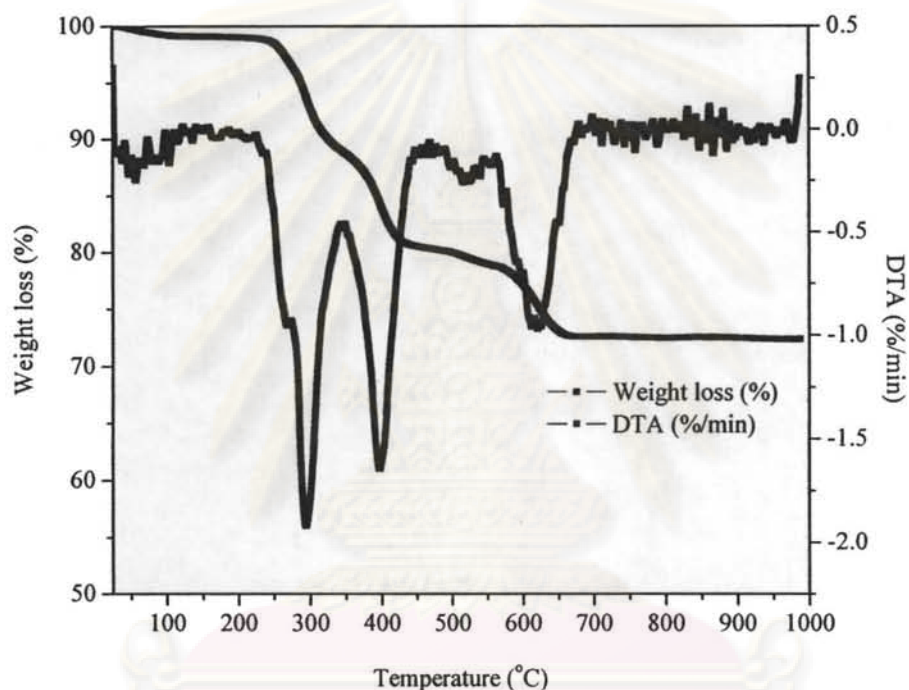


Figure 4.6 Thermogram of the $[(n\text{-C}_4\text{H}_9)_4\text{N}]_4\text{H}[\text{PW}_{11}\text{Co}(\text{H}_2\text{O})\text{O}_{39}]$ catalyst.

The thermogram of $[(n\text{-C}_4\text{H}_9)_4\text{N}]_4\text{H}[\text{PW}_{11}\text{Co}(\text{H}_2\text{O})\text{O}_{39}]$ catalyst exhibits three main ranges of weight loss as seen in Figure 4.7. The first one at *ca.* 160-350°C (1%) is due to the loss of physisorbed water and the second one at *ca.* 350-450°C (27%) corresponds to the loss of waters of hydration and due to the decomposition of the organic part [99]. At temperature above 450°C, it was the decomposition of mono-substituted polyoxometalate to correspond metal oxide. For the other compounds, the similar results were obtained as collected in Table 4.3.

Table 4.3 Decomposition temperatures and percentage mass loss

Catalyst	Decomposition temperature (°C)	Mass loss (%)
$[(n-C_4H_9)_4N]_3[PMo_{12}O_{40}]$	152-610	28.9
$[(n-C_4H_9)_4N]_3[PW_{12}O_{40}]$	154-650	20.7
$[(n-C_4H_9)_4N]_4H[PW_{11}Ni(H_2O)O_{39}]$	187-648	28.1
$[(n-C_4H_9)_4N]_4H[PW_{11}Mn(H_2O)O_{39}]$	150-595	26.3
$[(n-C_4H_9)_4N]_4H[PW_{11}Co(H_2O)O_{39}]$	167-607	27.6

4.4.4 Temperature program desorption (NH₃-TPD)

Temperature-programmed desorption of ammonia was used to investigate the acidities of the catalysts, and the results are as shown in Table 4.4. The temperature ranges were used to identify acid strength; weak acid sites appearing in the range 100-300°C whereas strong acids will appear above 500°C.

Table 4.4 Acidity of polyoxometalates

Catalyst	Acidity distribution (mmol of NH ₃ /g of catalyst)		
	Total	Weak	Strong
H ₃ [PMo ₁₂ O ₄₀]	2.4	1.3	1.2
H ₃ [PW ₁₂ O ₄₀]	2.6	1.4	1.2
Na ₂ H[PMo ₁₂ O ₄₀]	2.3	1.0	1.3
Na ₂ H[PW ₁₂ O ₄₀]	2.3	1.0	1.3
$[(n-C_4H_9)_4N]_3[PW_{12}O_{40}]$	1.7	1.0	0.8
$[(n-C_4H_9)_4N]_4[PW_{11}VO_{40}]$	1.7	1.0	0.7
$[(n-C_4H_9)_4N]_5[PW_{10}V_2O_{40}]$	1.0	0.1	0.9
$[(n-C_4H_9)_4N]_4H[PW_{11}Mn(H_2O)O_{39}]$	1.7	0.3	1.4
$[(n-C_4H_9)_4N]_4H[PW_{11}Co(H_2O)O_{39}]$	2.1	0.5	1.6
$[(n-C_4H_9)_4N]_4H[PW_{11}Ni(H_2O)O_{39}]$	1.4	0.3	1.1

From these results, the total acidity was maximized with H⁺ was the counter ion and weak acidity or Brønsted acidity was also height. The acidities of

polyoxotungstates are greater than those of polyoxomolybdates, in agreement with the higher negative charge on the oxygen atoms in polyoxomolybdates as compared to polyoxotungstates. In the series of tetrabutylammonium salts, when transition metals were substituted for a W atom, the total acidity decreased. In particular, in the case of $[(n\text{-C}_4\text{H}_9)_4\text{N}]_5[\text{PW}_{10}\text{V}_2\text{O}_{40}]$, when two V atoms were replaced with two W atoms, the total acidity clearly decreased.

4.4.5 Temperature program reduction (H₂-TPR)

The reduction temperatures of the catalysts were observed by H₂-TPR, the results being shown in Table 4.5.

Table 4.5 TPR of various polyoxometalates

Catalyst	TPR (°C)
$[(n\text{-C}_4\text{H}_9)_4\text{N}]_3[\text{PW}_{12}\text{O}_{40}]$	505-610, 615-650
$[(n\text{-C}_4\text{H}_9)_4\text{N}]_4[\text{PW}_{11}\text{VO}_{40}]$	570-585, 650-660
$[(n\text{-C}_4\text{H}_9)_4\text{N}]_5[\text{PW}_{10}\text{V}_2\text{O}_{40}]$	463-580, 590-685
$[(n\text{-C}_4\text{H}_9)_4\text{N}]_6[\text{PW}_9\text{V}_3\text{O}_{40}]$	443-585, 590-675
$[(n\text{-C}_4\text{H}_9)_4\text{N}]_4\text{H}[\text{PW}_{11}\text{Ni}(\text{H}_2\text{O})\text{O}_{39}]$	580-590, 610-620
$[(n\text{-C}_4\text{H}_9)_4\text{N}]_4\text{H}[\text{PW}_{11}\text{Mn}(\text{H}_2\text{O})\text{O}_{39}]$	575-585, 595-610
$[(n\text{-C}_4\text{H}_9)_4\text{N}]_4\text{H}[\text{PW}_{11}\text{Co}(\text{H}_2\text{O})\text{O}_{39}]$	585-595, 610-625

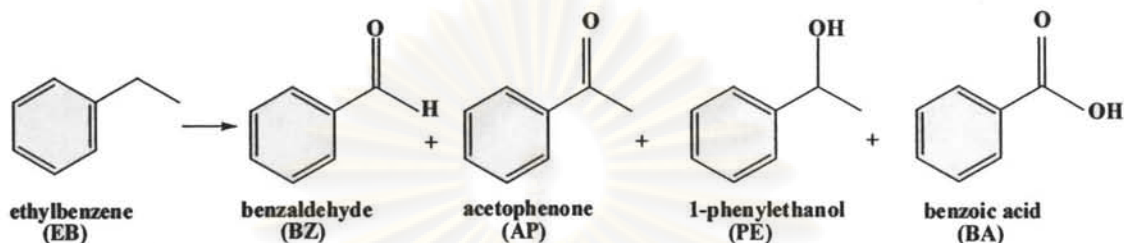
These results are in good agreement with earlier reports [103] that substitution of W⁶⁺ sites by V⁴⁺, Ni²⁺, Mn²⁺ and Co²⁺ in the $[\text{PW}_{12}\text{O}_{40}]^{3-}$ anion tends to decrease the reduction temperature. The lower electronegativities of the substituted transition metals in the polyoxoanions thus tended to higher reducibilities of the catalysts.

4.4.6 Solubilities of the catalysts

Acidic and sodium salts of polyoxometalates are soluble in water and acetonitrile. The catalysts with the tetrabutylammonium cation are soluble in acetonitrile.

4.5 Oxidation of ethylbenzene

The catalytic oxidation of ethylbenzene was studied using mono-substituted polyoxometalates. The effects of temperature, effect of solvent, reaction time, types of catalyst, oxidant per substrate mole ratio (O/S), substrate per catalyst mole ratio (S/C) and catalyst reusabilities were investigated.



Scheme 4.2 Reaction scheme for ethylbenzene oxidation.

The catalyst, substrate and oxidant were placed in a round bottom flask equipped with a condenser in a silicone oil bath. The reaction mixture was heated to the desired temperature for the given reaction time. After the desired time, the catalyst was filtered from the reaction mixture. The liquid mixture was placed into a 25% H₂SO₄ solution and extracted with diethyl ether. The mixture was neutralized with saturated NaHCO₃ solution and dried with anhydrous Na₂SO₄. The oxygenated products and recovered substrate in the liquid mixture were qualitatively analyzed by gas chromatography using an internal standard. The mass balances of all samples were in the range of 95-105%, except for the case of cyclohexane, when it ranged from 87-99%.

ศูนย์วิทยทรัพยากร
จุฬาลงกรณ์มหาวิทยาลัย

4.5.1 Effect of temperature in solvent-free systems

The effects of temperature on activities and product selectivities were observed in the range of 33 to 100°C using $[(n\text{-C}_4\text{H}_9)_4\text{N}]_4\text{H}[\text{PW}_{11}\text{Co}(\text{H}_2\text{O})\text{O}_{39}]$ as the catalyst.

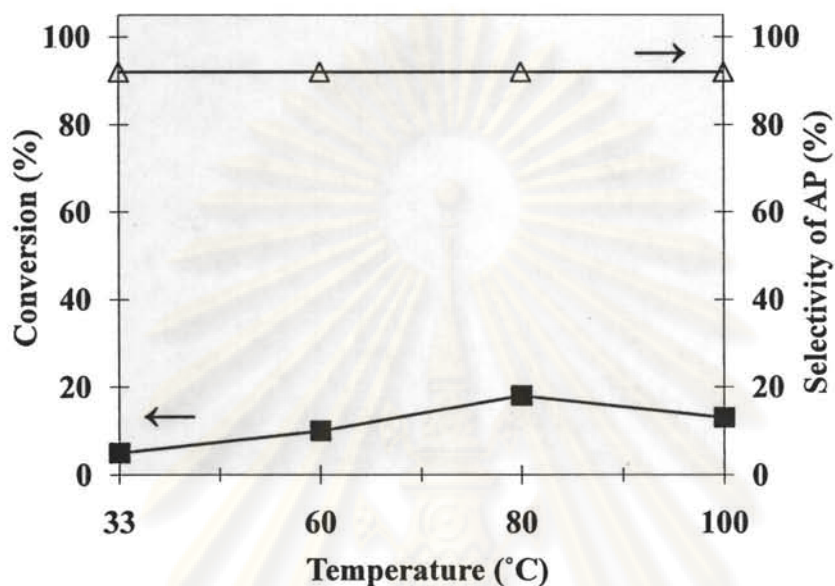


Figure 4.7 Effect of reaction temperature on conversion and selectivity.
Reaction conditions: ethylbenzene 1 mmol, catalyst 0.01 mmol (0.037 g), H_2O_2 10 mmol, 24 h.

When the reaction temperature increased, the conversion of ethylbenzene was enhanced. The maximum temperature utilized was 80°C, and the temperature did not affect acetophenone selectivity over all temperature range.

ศูนย์วิทยทรัพยากร
จุฬาลงกรณ์มหาวิทยาลัย

4.5.2 Effect of types of substituted metal in ethylbenzene oxidation

The effects of metal incorporation in mono-substituted polyoxotungstate catalysts were studied and the results are collected in Table 4.6.

Table 4.6 Effect of types of substituted metal in ethylbenzene oxidation

Catalyst	Conversion (%)	Product selectivity (%)	
		acetophenone	1-phenylethanol
$[(n\text{-C}_4\text{H}_9)_4\text{N}]_4\text{H}[\text{PW}_{11}\text{Ni}(\text{H}_2\text{O})\text{O}_{39}]$	10	95	5
$[(n\text{-C}_4\text{H}_9)_4\text{N}]_4\text{H}[\text{PW}_{11}\text{Mn}(\text{H}_2\text{O})\text{O}_{39}]$	16	98	2
$[(n\text{-C}_4\text{H}_9)_4\text{N}]_4\text{H}[\text{PW}_{11}\text{CuO}_{39}]$	19	91	9
$[(n\text{-C}_4\text{H}_9)_4\text{N}]_4\text{H}[\text{PW}_{11}\text{Co}(\text{H}_2\text{O})\text{O}_{39}]$	18	92	8
$[(n\text{-C}_4\text{H}_9)_4\text{N}]_4\text{H}[\text{PW}_{11}\text{Co}(\text{H}_2\text{O})\text{O}_{39}]^{\text{a}}$	33	92	8

Reaction conditions: ethylbenzene 1 mmol, catalyst 0.01 mmol (0.037 g), H_2O_2 10 mmol, 80°C , 24 h.

^a in CH_3CN 5 mL

When the reaction was conducted without a catalyst, no product was observed. In the solvent-free systems, $[(n\text{-C}_4\text{H}_9)_4\text{N}]_4\text{H}[\text{PW}_{11}\text{CuO}_{39}]$ and $[(n\text{-C}_4\text{H}_9)_4\text{N}]_4\text{H}[\text{PW}_{11}\text{Co}(\text{H}_2\text{O})\text{O}_{39}]$ catalysts gave higher ethylbenzene conversions but lower acetophenone selectivity. No benzoic acid formation was observed for any of the catalysts. Because of the low yield of oxygenated products in the solvent-free system, a solvent such as acetonitrile it was used as solvent since it can dissolve tetrabutylammonium salt of polyoxotungstate. However, $[(n\text{-C}_4\text{H}_9)_4\text{N}]_4[\text{PW}_{11}\text{Cr}(\text{H}_2\text{O})\text{O}_{39}]$ showed no activity in this system.

The higher catalytic reactivities in acetonitrile media using the $[(n\text{-C}_4\text{H}_9)_4\text{N}]_4\text{H}[\text{PW}_{11}\text{Co}(\text{H}_2\text{O})\text{O}_{39}]$ catalyst is attributed to the polarity of the solvent, which by dissolution of catalyst to form homogeneous liquid system, thereby promoting mass transfer [104]. The results showed that substitutions by transition metal enhance catalytic activity.

4.5.3 Effect of reaction time on the oxidation of ethylbenzene

The effect of reaction time was investigated in the range of 12 to 72 h using $[(n\text{-C}_4\text{H}_9)_4\text{N}]_4\text{H}[\text{PW}_{11}\text{Co}(\text{H}_2\text{O})\text{O}_{39}]$, with H_2O_2 as the oxidant, and the results are collected in Figure 4.8.

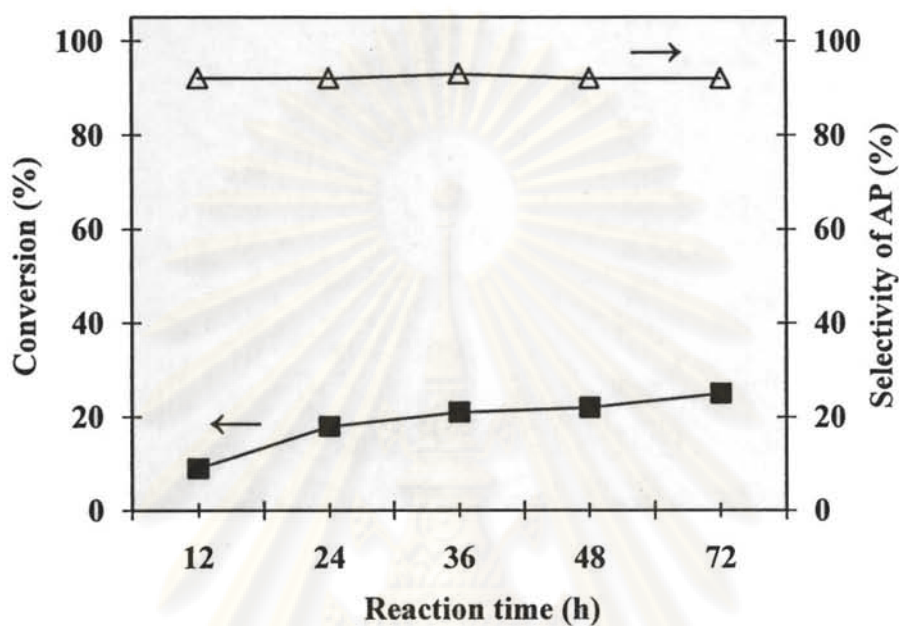


Figure 4.8 Effect of reaction time on ethylbenzene conversion and product selectivity.

Reaction conditions: ethylbenzene 1 mmol, catalyst 0.01 mmol (0.037 g), H_2O_2 10 mmol, 80°C .

Conversion of ethylbenzene increased rapidly at the first 24 h but then leveled off and ethylbenzene conversion remained almost constant. This might be due to the fact that the H_2O_2 had already decomposed in early stage and reaction was limited by lack of oxidizing agent. After a reaction time of 72 h, a small amount of benzoic acid was observed and might be from further oxidation of 1-phenylethanol.

จุฬาลงกรณ์มหาวิทยาลัย

4.5.4 Effects of oxidant per substrate mole ratio (O/S) and substrate per catalyst mole ratios (S/C)

The effects of oxidant/substrate and substrate/catalyst concentration ratios were studied, and the results are collected and described in Table 4.7.

Table 4.7 Effect of O/S and S/C mole ratios using $[(n\text{-C}_4\text{H}_9)_4\text{N}]_4\text{H}[\text{PW}_{11}\text{Co}(\text{H}_2\text{O})\text{O}_{39}]$ catalyst

O/S	S/C	Conversion (%)	Product selectivity (%)		
			acetophenone	1-phenylethanol	benzoic acid
10	100	18	93	7	-
20	50	27	93	7	-
20	100	19	90	9	1

Reaction conditions: ethylbenzene 1 mmol, catalyst 0.01-0.02 mmol (0.037-0.074 g), H_2O_2 10-20 mmol, 80°C, 24 h.

The results showed that the conversion of ethylbenzene and the distribution of the products depended on the concentrations of catalyst and oxidant. When the catalyst amount was increased (S/C = 50), the ethylbenzene conversion was enhanced from 19% to 27% with constant selectivity for acetophenone. However, when the oxidant amounts were increased acetophenone but higher 1-phenylethanol selectivities were observed.

4.5.5 Reusability of catalysts

At the end of the reaction, the $[(n\text{-C}_4\text{H}_9)_4\text{N}]_4\text{H}[\text{PW}_{11}\text{Co}(\text{H}_2\text{O})\text{O}_{39}]$ catalyst was separated by filtration. The absorbed hydrogen peroxide was removed by several washes with a large amount of water and subsequent heating at 110°C for 2 h. The catalyst was then used in another reaction. The results showed that the catalyst can be used four times with only a slight loss in activity (from 18% to 13%), which did not cause a change in AP selectivity (92%).

4.5.6 Effects of reaction conditions

To investigate mechanism of ethylbenzene oxidation with H_2O_2 catalyzed by $[(n\text{-C}_4\text{H}_9)_4\text{N}]_4\text{H}[\text{PW}_{11}\text{Co}(\text{H}_2\text{O})\text{O}_{39}]$, experiments were conducted under nitrogen atmosphere, in the dark and with radical scavenger (iodine). The results are given in Table 4.8.

Table 4.8 Oxidation of ethylbenzene at various conditions

Condition	Conversion (%)	Product selectivity (%)		
		acetophenone	1-phenylethanol	benzoic acid
in air	18	93	7	-
in nitrogen	18	92	8	-
in the dark	21	93	7	-
in of iodine (1 mmol)	-	-	-	-

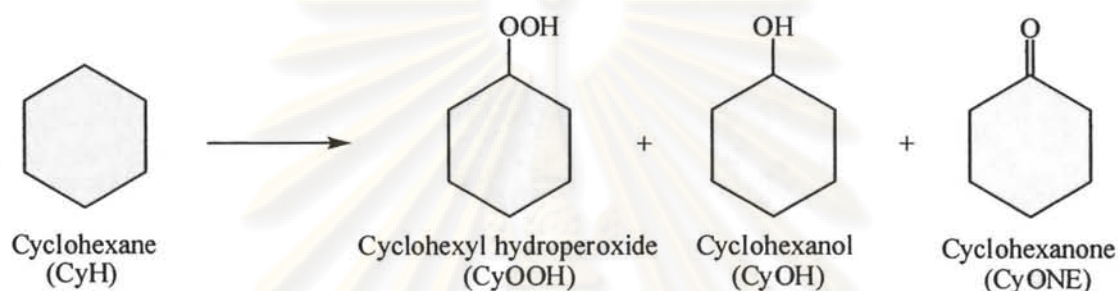
Reaction conditions: ethylbenzene 1 mmol, catalyst 0.01 mmol (0.037 g), H_2O_2 10 mmol, 80°C , 24 h.

When the catalytic oxidation was conducted under nitrogen atmosphere, a similar result as that in air was obtained. There was no reaction was observed when radical scavenger (iodine) was added. The conversion was increased in the dark and inhibited by iodine which acts as a radical trap. Thus it can be concluded that catalytic oxidation of ethylbenzene by H_2O_2 was a radical process mechanism.

ศูนย์วิทยทรัพยากร
จุฬาลงกรณ์มหาวิทยาลัย

4.6 Oxidation of cyclohexane

The prepared mono-substituted polyoxometalate catalysts were studied for the oxidation of cyclohexane to cyclohexanone and cyclohexanol using H_2O_2 as the oxidant. First of all, the effect of oxidant was investigated using either the oxygen molecule itself or H_2O_2 . The results showed that using the oxygen molecule at a pressure of 3 atm can allow for some catalyzed oxidation of cyclohexane, but only to the extent of 1 mol% at 80°C in CH_3CN for 12 h.



Scheme 4.2 Reaction scheme for cyclohexane oxidation and the products found in this study.

The catalytic oxidations of cyclohexane were monitored as functions of the types of metal, oxidant/substrate mole ratio (O/S) and substrate/catalyst mole ratio (S/C).

4.6.1 Effect of types of substituted metal in cyclohexane oxidation

The catalytic activities of the various mono-substituted Keggin compounds in homogeneous and biphasic system were studied in the pressure reactor. The results are collected in Table 4.9.

Table 4.9 Effect of types of substituted metal in cyclohexane oxidation

Catalyst	Product (mol%) ^a		CyONE+CyOH (mol%) ^a	CyONE/CyOH
	CyONE	CyOH		
$[(n\text{-C}_4\text{H}_9)_4\text{N}]_4\text{H}[\text{PW}_{11}\text{Ni}(\text{H}_2\text{O})\text{O}_{39}]$	3.4	2.5	5.9	1.4
$[(n\text{-C}_4\text{H}_9)_4\text{N}]_4\text{H}[\text{PW}_{11}\text{Co}(\text{H}_2\text{O})\text{O}_{39}]$	2.9	4.1	7.0	0.7
$[(n\text{-C}_4\text{H}_9)_4\text{N}]_4\text{H}[\text{PW}_{11}\text{Mn}(\text{H}_2\text{O})\text{O}_{39}]$	4.1	3.8	7.9	1.1
$[(n\text{-C}_4\text{H}_9)_4\text{N}]_4\text{H}[\text{PW}_{11}\text{CuO}_{39}]$	4.2	7.0	11.2	0.6

Reaction conditions: cyclohexane 18.5 mmol, catalyst 0.04 mmol (0.148 g), H_2O_2 39.5 mmol, CH_3CN 5 mL, 80°C , 12 h.

CyONE = cyclohexanone

CyOH = cyclohexanol

CyOOH = cyclohexyl hydroperoxide

^a based on substrate

The phosphotungstate anion with incorporated Cu^{2+} was preferable for cyclohexane oxidation than the other catalysts. $[(n\text{-C}_4\text{H}_9)_4\text{N}]_4\text{H}[\text{PW}_{11}\text{CuO}_{39}]$ as catalyst gave the highest CyONE+CyOH content (11.2%), with no cyclohexyl hydroperoxide observed. In this result, larger amounts of CyONE+CyOH were obtained than in the previous report by Simões and co-workers [96]. In this study, we found that the Mn-containing catalyst, $[(n\text{-C}_4\text{H}_9)_4\text{N}]_4\text{H}[\text{PW}_{11}\text{Mn}(\text{H}_2\text{O})\text{O}_{39}]$, gave low activities for cyclohexane oxidation. This result is in good agreement with a report by Nowinska and coworkers [64], who additionally found that $\text{K}_5[\text{PW}_{11}\text{MnO}_{39}]$ and $\text{Mn}_{2.5}[\text{PW}_{11}\text{MnO}_{39}]$ showed low oxidative activities for propane oxidation.

4.6.2 Effect of O/S and S/C mole ratios

In this study the reaction conditions having S/C and O/S ratios of 463 and 2.0, respectively, were not optimal, giving low yields of cyclohexanone and cyclohexanol. However, the next experiment was designed to optimize the oxidation of cyclohexane, using $[(n\text{-C}_4\text{H}_9)_4\text{N}]_4\text{H}[\text{PW}_{11}\text{CuO}_{39}]$ and H_2O_2 in the hope of increasing the yield of products.

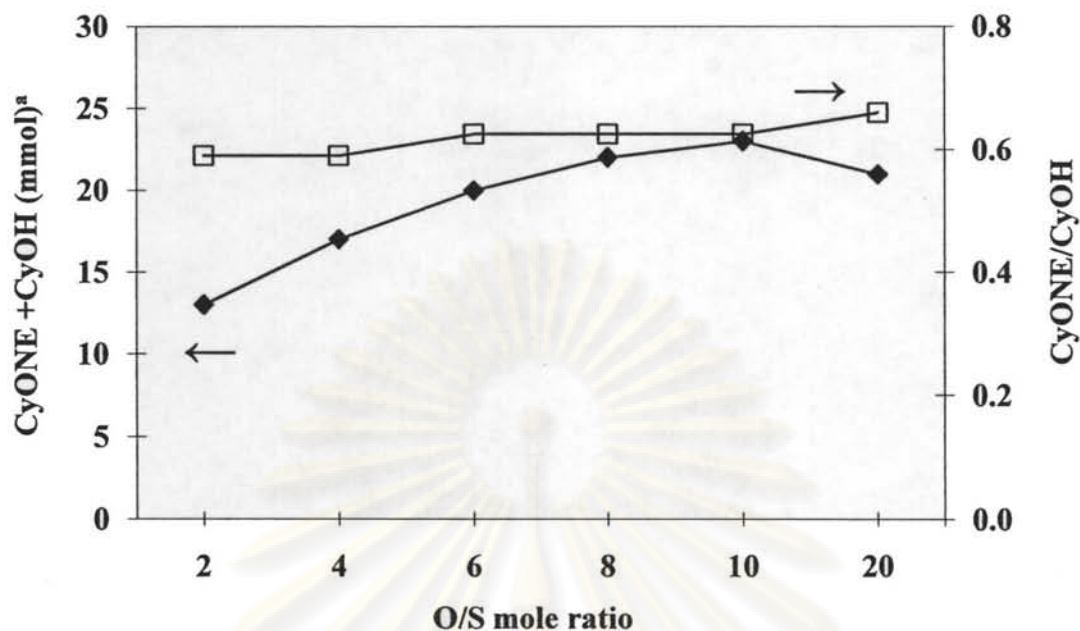


Figure 4.9 Effect of O/S molar ratio to cyclohexane conversion using $[(n\text{-C}_4\text{H}_9)_4\text{N}]_4\text{H}[\text{PW}_{11}\text{CuO}_{39}]$.

Reaction conditions: cyclohexane 18.5 mmol, catalyst 0.04 mmol (0.148 g), CH_3CN 5 mL, 80°C , 12 h.

^a based on substrate

Since H_2O_2 acts as the oxidant in the conversion of cyclohexane, it is thus natural that no CyOH and CyONE are obtained without H_2O_2 . The results showed no significant dependence of product selectivity on the O/S mole ratio. In this study, increases in the H_2O_2 concentration could be made in order to gain higher yields of the desired products, without apparent formation of CyOOH, which could be assayed through its reduction by PPh_3 , and quantified the amount from the increase of the CyOH content.

ศูนย์วิจัยทรัพยากร
จุฬาลงกรณ์มหาวิทยาลัย

4.6.3 Effect of amount of catalyst

The effect of the amount of catalyst in the cyclohexane was investigated in the range of 0.04-0.14 g, and the results are as shown in Figure 4.10.

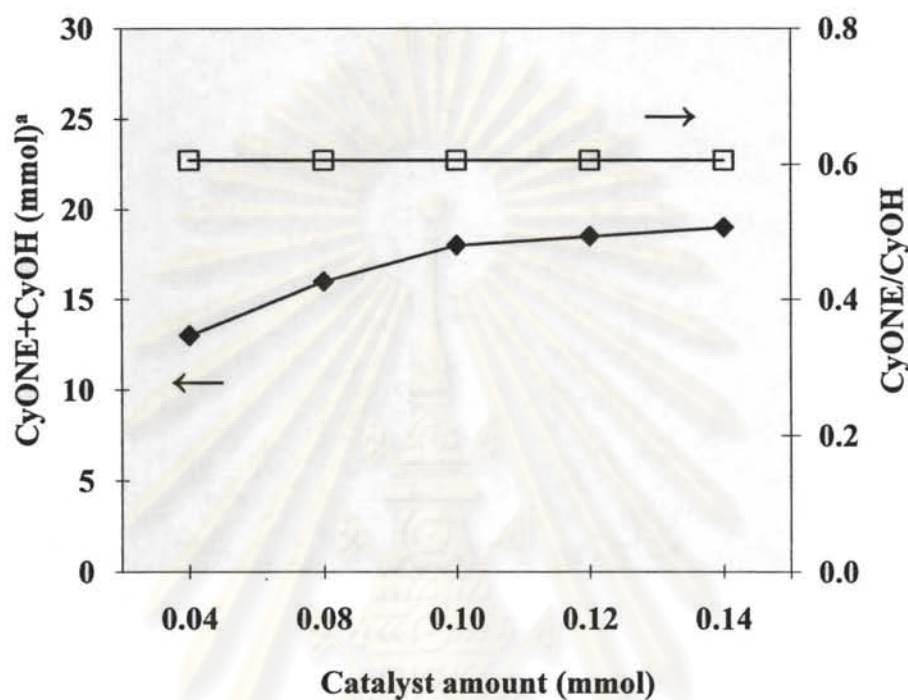


Figure 4.10 Effect of catalyst amount for cyclohexane conversion using $[(n\text{-C}_4\text{H}_9)_4\text{N}]_4\text{H}[\text{PW}_{11}\text{CuO}_{39}]$.
 Reaction conditions: cyclohexane 18.5 mmol, H_2O_2 39.5 mmol, CH_3CN 5 mL, 80°C , 12 h.
^a based on substrate

A higher catalyst amount enhanced the product yield with no significant change in the CyONE/CyOH ratio. However, with 0.12 and 0.14 mmol of catalyst, the catalyst did not completely dissolve in the reaction mixture. The reaction was thus taking place in both heterogeneous and homogeneous phases, and as a result, little enhancement in cyclohexane conversion was observed. In addition, cyclohexanol is more active than cyclohexane in the presence of more catalyst (more active sites), and thus cyclohexanol can be converted to cyclohexanone easily, as described previously by Tian and co-workers [105].

4.6.4 Effect of reaction time in cyclohexane oxidation

Oxidation reactions using H_2O_2 as the oxidant are time dependent and thus the effects of reaction time on the catalyst performance and product selectivity were investigated. Since cyclohexanol and cyclohexanone are more reactive than cyclohexane, which can lead to further undesired oxidation processes, the reaction time could not be extended without leading to unfavorable results. The reaction time was therefore limited to the range of 3-24 h.

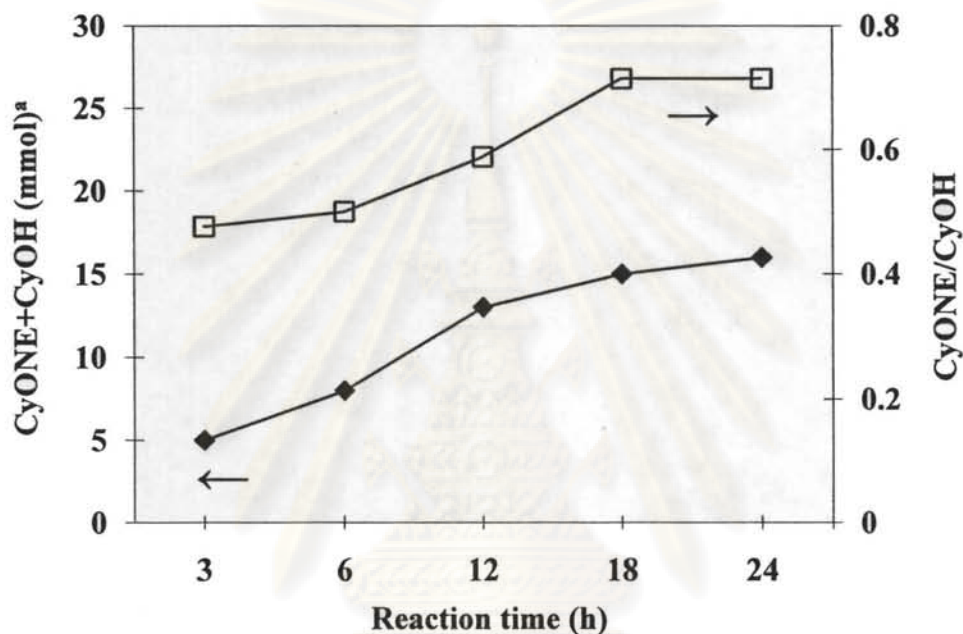


Figure 4.11 Effect of reaction time using $[(n\text{-C}_4\text{H}_9)_4\text{N}]_4\text{H}[\text{PW}_{11}\text{CuO}_{39}]$.
Reaction conditions: cyclohexane 18.5 mmol, catalyst 0.04 mmol (0.148 g), H_2O_2 39.5 mmol, CH_3CN 5 mL, 80°C .

Figure 4.11 shows the effects of the reaction time on the catalytic oxidation of cyclohexane over $[(n\text{-C}_4\text{H}_9)_4\text{N}]_4\text{H}[\text{PW}_{11}\text{CuO}_{39}]$ using H_2O_2 as oxidant. The results indicated that the total yield increased with reaction time until 18 h. Increasing the reaction time further only slightly affected the amounts of cyclohexanone and cyclohexanol because some oxidant is consumed during the 18 h reaction period. However, the CyONE/CyOH ratio decreased significantly after 6 h, and the relative increase in cyclohexanone product perhaps can be attributed to the partial oxidation of cyclohexanol. After about 24 h the reaction practically stopped, because of the consumption of the hydrogen peroxide; however, further addition of H_2O_2 led to further oxidation of cyclohexane. Thus, the catalyst proved to be still active.

4.7 Stability of the catalyst

After the reaction the used catalyst was separated and washed with water and dried, then it was characterization with XRD. The XRD patterns of the catalyst before and after reaction were compared in Figure 4.12.

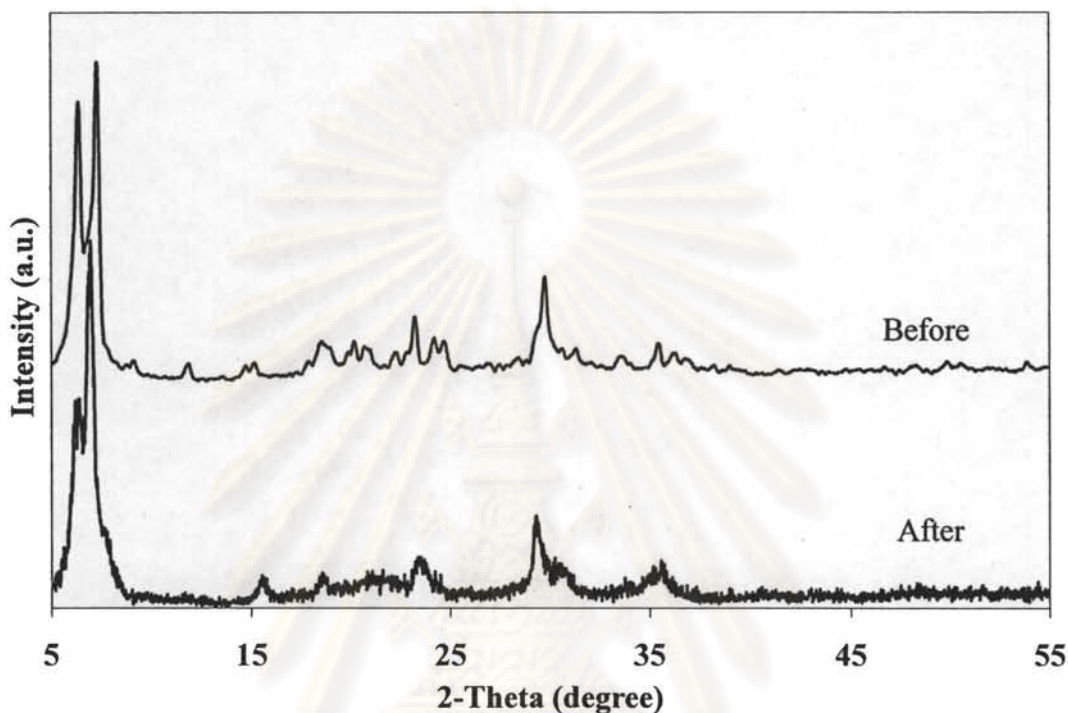


Figure 4.12 XRD patterns of $[(n\text{-C}_4\text{H}_9)_4\text{N}]_4\text{H}[\text{PW}_{11}\text{Co}(\text{H}_2\text{O})\text{O}_{39}]$, before and after reaction in catalytic oxidation of cyclohexane.

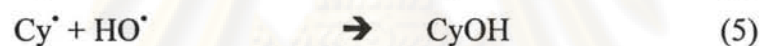
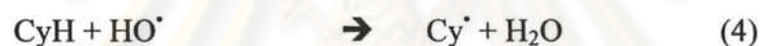
XRD patterns indicated that $[(n\text{-C}_4\text{H}_9)_4\text{N}]_4\text{H}[\text{PW}_{11}\text{Co}(\text{H}_2\text{O})\text{O}_{39}]$ catalyst did not show significant differences of characteristic peaks before and after use.

4.8 Mechanism of cyclohexane oxidation with POMs

The experiments with $[(n\text{-C}_4\text{H}_9)_4\text{N}]_4\text{H}[\text{PW}_{11}\text{CuO}_{39}]$ were repeated under an atmosphere of nitrogen. The results were not different from those obtained in air in agreement with previous report of Bulula and co-worker [80], using $[(n\text{-C}_4\text{H}_9)_4\text{N}]_4[\text{PW}_{11}\text{Fe}(\text{H}_2\text{O})\text{O}_{39}]$ in cyclooctane oxidation with H_2O_2 . The experiment was also performed in the presence of iodine, a well-known radical scavenger and the oxidation of cyclohexane did not occur [96].

In this case, the first step was assumed to be the coordination of H_2O_2 molecule to metal (M), followed by the formation of $\text{HOO}\cdot$. The $\text{HO}\cdot$ radicals were then generated by a reaction similar to that of Eq. (3), with reoxidation of metal.

Catalytic oxidation of cyclohexane using H_2O_2 as oxidant was conducted by radical mechanism. The steps were described below. First of all, hydrogen peroxide was decomposed to radical in (1-2) at metal (M). $\text{Cy}\cdot$ radical was created in step (4) and it was changed to CyOH in step (5). $\text{Cy}\cdot$ was reacted with molecular oxygen (6) and it was changed to CyOOH by reacted with proton in step (7). Finally, CyONE was formed by further oxidation of CyOH (8).



4.9 Oxidation of cyclohexanol

4.9.1 Oxidation of primary alcohols to carboxylic acid

The conversion of primary alcohols into carboxylic acids is not a difficult task. Often, the same oxidant that has been used to oxidized alcohols to aldehydes is applicable for the oxidation to acids when used in appropriate amounts, in different solvents, at higher temperatures, or at longer reaction times. An example is the oxidation of primary alcohols with air or oxygen with platinum-on-charcoal or platinum dioxide as catalyst.

4.9.2 Oxidation of secondary alcohols to ketones

All oxidants used for the oxidation of primary alcohols to aldehydes can be applied to secondary alcohols. Because the products, ketones, are much less sensitive to overoxidation than aldehydes, more intensive reaction conditions, such as an excess of the oxidant, higher temperatures, or longer reaction times, can be used.

Secondary alcohols are converted into ketones in 70-98% isolated yields when refluxed with Raney nickel in benzene for 1-24 h with azeotropic removal of water. The addition of 1-octene as a hydrogen acceptor does not affect the yields. Primary alcohols, under such reaction conditions, usually suffer decarbonylation and yield hydrocarbons with one less carbon. Catalytic oxidation is affected by passing oxygen through solutions of alcohols in the presence of metal catalysts.

4.9.3 Oxidation of secondary alcohols to carboxylic acids

The treatment of secondary alcohols with powerful oxidants such as nitric acid, chromium trioxide, or potassium permanganate results not only in oxidation to ketones but also in subsequent oxidation of the ketones to carboxylic acids. Thus cyclohexanol gives adipic acid, 4-isopropylcyclohexanol gives β -isopropyladipic acid, and 2-methylcyclohexanol gives 6-ketoeanthoic (δ -acetylvaleric or heptanon-6-oic) acid.

4.10 Literature reviews

Many publications have appeared on the use of polyoxometalates in catalytic oxidations of alcohols, and are described below.

In 1997, Neumann *et al.* [76] studied the catalytic oxidation of cyclohexanol using $\text{Na}_{11}[\text{Ru}_2\text{Zn}_3\text{W}_{19}\text{O}_{68}]$. The reaction was carried out in 30% H_2O_2 at 25°C for 2 h, 5% conversion of cyclohexanol was obtained with 100% selectivity of cyclohexanone.

In 2000, Yang *et al.* [77] reported the preparation of $\text{Cs}_n\text{H}_{4-n}[\text{PMo}_{11}\text{VO}_{40}]$, $n \geq 3$. These catalysts were used in oxidation of ethanol to acetaldehyde, ethylene and diethyl ether, the feed gas consisted of ethanol 13%, oxygen 30% in nitrogen balance

(flow rate 15 mL/min) at 250°C. For the Cs_n salt in which $n < 3$, acetaldehyde was the main product (> 95%). For $n = 2-3$, ethylene and diethyl ether selectivity were increased, while acetaldehyde selectivity was decreased (< 40%).

In 2005, Wang *et al.* [106] studied the catalytic oxidation of alcohols using $Na_6[SiW_{11}M(H_2O)O_{40}] \cdot 12H_2O$ (where $M = V^{4+}, Cr^{6+}, Mn^{4+}, Fe^{3+}, Co^{2+}, Ni^{2+}, Cu^{2+}$ and Zn^{2+}). The reaction was carried out in water with H_2O_2 :substrate = 1.5, substrate:catalyst = 670 at 90°C. The activity order was: $Zn^{2+} > Mn^{4+} + M^{4+} + Mn^{6+} > Fe^{3+} + Fe^{2+} > Co^{2+} > Cu^{2+}$. It was found that benzyl alcohol and cyclohexanol was converted to benzoic acid and cyclohexanone with 100% conversion and 100% selectivity in 2 and 7 h, respectively. The catalyst could be reused without loss of activity.

In 2007, Weng *et al.* [107] reported the catalytic oxidation of benzyl alcohol by H_2O_2 in dimethyl acetate and acetonitrile with quaternary ammonium salts; $[C_7H_7N(CH_3)_3]^+$ and $[CH_3(C_{15}H_{30})C_5H_5N]^+$ of polyoxotungstate anions; $[PW_{12}O_{40}]^{3-}$, $[PW_{11}O_{39}]^{7-}$, $[PW_9O_{40}]^{9-}$, $[P_2W_{18}O_{62}]^{6-}$, $[SiW_{11}O_{39}]^{8-}$ and $[SiW_{10}O_{36}]^{8-}$. It was found that the activity of the catalysts with lacunary structure ($W^{6+} < 12$ atoms) was higher than those with complete structure. The reaction catalyzed by the catalysts with P was faster than those with Si^{4+} . The catalyst can be reused with slight decrease in activity (83.5% conversion in the third run) compared to 86.2%.

In 2008, Egusquiza *et al.* [108] reported the catalytic oxidation of 2-naphthol to 1, 2-naphthoquinone by H_2O_2 using $K_{10}[(PW_9O_{34})_2M_4(H_2O)_2]$ catalyst, where $M = Co^{2+}, Zn^{2+}$ or Mn^{2+} . The activity order was: $Co^{2+} > Mn^{2+} > Zn^{2+}$. The conversion was higher in acetonitrile than acetone. For Co catalyst, the yields of 1, 2 naphthoquinone were 89% in acetonitrile in 20 min at 80°C and 94% in acetone in 1 h at 56°C.

The above reviewed literature, deal with the catalytic oxidation of alcohols and hydrocarbons with mono-substituted polyoxometalate. Using mono-substituted polyoxometalate, molecular oxygen and hydrogen peroxide for oxidation of cyclohexanol and catalytic function of polyoxometalate in the solid-state as well as in solution has attracted much attention in the catalytic research.

In this research, the system consists of environmentally oxidant, hydrogen peroxide to oxidize cyclohexane and cyclohexanol with polyoxometalates and mono-substituted polyoxometalates catalysts.

4.11 Catalytic study

The prepared polyoxometalates as described earlier were used in catalytic oxidation of cyclohexanol with hydrogen peroxide as oxidant. Effect of reaction parameters were studied and presented below.

4.11.1 Effect of reaction temperature

Effect of temperature on the yield of cyclohexanol was studied by varying the temperature between 50 and 110°C, while other parameters were kept constant.

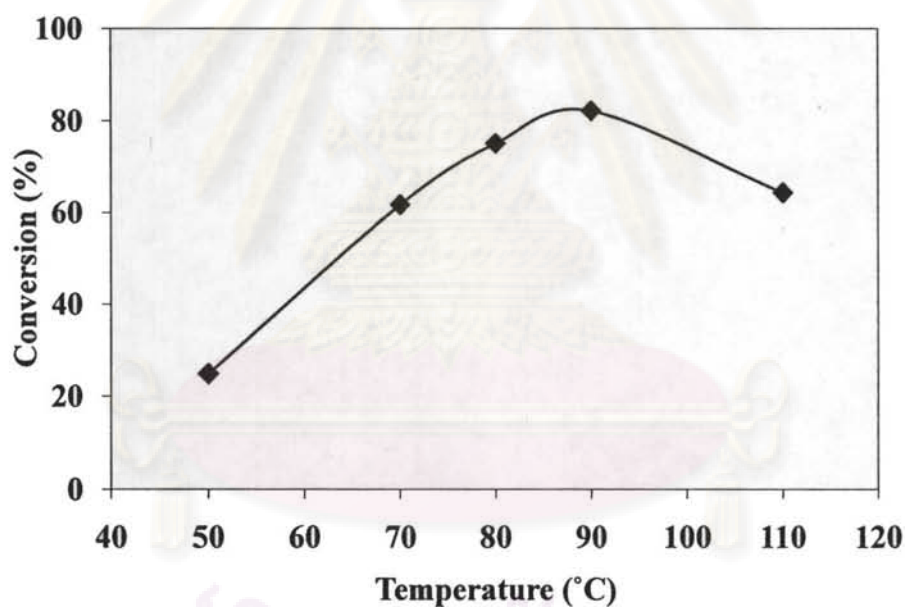


Figure 4.14 Effect of reaction temperature using $[(n\text{-C}_4\text{H}_9)_4\text{N}]_3[\text{PW}_{12}\text{O}_{40}]$.

Reaction conditions: cyclohexanol 6.7 mmol, catalyst 0.01 mmol, 90°C, 7 h.

Conversion of cyclohexanol increased with the reaction temperature up to 90°C and the conversion of cyclohexanol was decreased at 110°C. This may be due to faster rate of H_2O_2 decomposition [85]. Therefore temperature at 90°C was used for further study.

4.11.2 Effect of types of catalyst

The activity of various polyoxometalates catalysts in oxidation of cyclohexanol with hydrogen peroxide as oxidant was investigated and compared under the same reaction condition. The results are shown in Table 4.10.

Table 4.10 Oxidation of cyclohexanol with hydrogen peroxide

Catalyst	Conversion (%)	TON ^a
H ₃ [PMo ₁₂ O ₄₀]	19	127
H ₃ [PW ₁₂ O ₄₀]	48	321
Na ₂ H[PMo ₁₂ O ₄₀]	25	168
Na ₂ H[PW ₁₂ O ₄₀]	56	375
[(<i>n</i> -C ₄ H ₉) ₄ N] ₃ [PMo ₁₂ O ₄₀]	30	201
[(<i>n</i> -C ₄ H ₉) ₄ N] ₃ [PW ₁₂ O ₄₀]	82	549
[(<i>n</i> -C ₄ H ₉) ₄ N] ₄ [PW ₁₁ VO ₄₀]	96	643
[(<i>n</i> -C ₄ H ₉) ₄ N] ₅ [PW ₁₀ V ₂ O ₄₀]	58	389
[(<i>n</i> -C ₄ H ₉) ₄ N] ₆ [PW ₉ V ₃ O ₄₀]	60	402
[(<i>n</i> -C ₄ H ₉) ₄ N] ₄ H[PW ₁₁ Co(H ₂ O)O ₃₉]	91	610
[(<i>n</i> -C ₄ H ₉) ₄ N] ₄ H[PW ₁₁ Ni(H ₂ O)O ₃₉]	99	663
[(<i>n</i> -C ₄ H ₉) ₄ N] ₄ H[PW ₁₁ Mn(H ₂ O)O ₃₉]	89	596

Reaction conditions: cyclohexanol 6.7 mmol, catalyst 10 μmol, 90°C, 7 h.

^aTON = turnover number = mmol of products/mmol of catalyst

It was observed that W-POM has higher activity than Mo-POM in every series, due to the higher acid strengths of polyoxotungstate [77,106]. These catalytic activity orders are corresponding to acidity of the polyoxometalate and salt effect. H₃[PW₁₂O₄₀] is more acidic than H₃[PMo₁₂O₄₀].

Among various salts, tetrabutylammonium salt which it was not dissolved in the reaction mixture showed the activity in the order; [(*n*-C₄H₉)₄N]₃[PW₁₂O₄₀] > Na₂H[PW₁₂O₄₀] > H₃[PW₁₂O₄₀]. This might be due to the reaction was carried out in biphasic system (solvent-free), tetrabutylammonium salts can be solvated by the substrate molecules and function as phase transfer catalyst between organic and

can be solvated by the substrate molecules and function as phase transfer catalyst between organic and aqueous phase. Thus, tetrabutylammonium salt showed the highest catalytic activity in this system. POM could catalyze in aqueous phase.

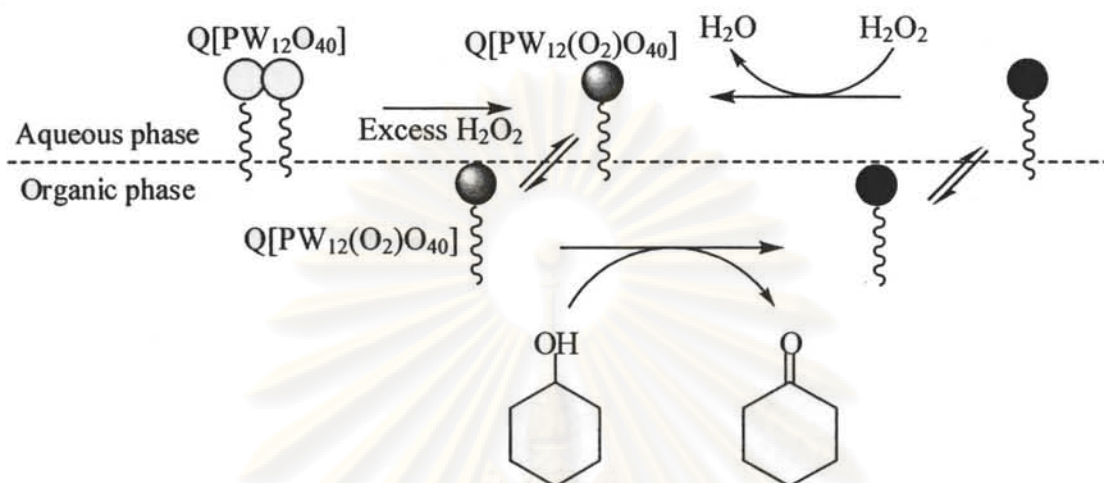


Figure 4.15 Phase transfer catalysis mechanism [104].

As suggested in many publications [104], the oxidation of alcohols with phase transfer catalyst may be depicted as a catalytic cycle, as seen in Figure 4.15. This cycle consists of four basic steps:

1. In the presence of H_2O_2 , $[(n\text{-C}_4\text{H}_9)_4\text{N}]_3[\text{PW}_{12}\text{O}_{40}]$ or tetrabutylammonium salt, the metal precursor is oxidized and dissociated to form peroxometal anion, $[\text{PW}_{12}(\text{O}_2)\text{O}_{40}]^{3-}$.
2. Tetrabutylammonium salts with large lipophilic cation can function as phase transfer catalyst and transfer the peroxometal into organic phase.
3. In organic phase, alcohols are oxidized by peroxometal complex and form oxygenated product.
4. The reduced oxo species returns to aqueous phase and restores the catalytic cycle.

The replacement of W^{6+} atoms by V^{5+} to form $[(n\text{-C}_4\text{H}_9)_4\text{N}]_{3+x}[\text{PW}_{12-x}\text{V}_x\text{O}_{40}]$ led to higher cyclohexanol conversion. However the conversions of cyclohexanol over $[(n\text{-C}_4\text{H}_9)_4\text{N}]_{3+x}[\text{PW}_{12-x}\text{V}_x\text{O}_{40}]$ catalysts decreased with more vanadium substitution $[(n\text{-C}_4\text{H}_9)_4\text{N}]_4[\text{PW}_{11}\text{VO}_{40}] > [(n\text{-C}_4\text{H}_9)_4\text{N}]_5[\text{PW}_{10}\text{V}_2\text{O}_{40}] \leq [(n\text{-C}_4\text{H}_9)_4\text{N}]_6[\text{PW}_9\text{V}_3\text{O}_{40}]$. This could be due to wider ligand-to-metal charge transfer (LMCT) band gap which led to decrease in the catalytic activity [109] or due to the

poor stabilities of the corresponding peroxo intermediate species in the oxygen transfer reaction [110].

Mono-substitution W^{6+} atom in polyoxotungstate anions with transition metals such as Co, Ni and Mn achieved high conversion and comparatively high selectivity. This might be due to the increasing of the reducibility property of the catalyst, the activity was decreased in the order; $[(n-C_4H_9)_4N]_4H[PW_{11}Ni(H_2O)O_{39}] > [(n-C_4H_9)_4N]_4H[PW_{11}Co(H_2O)O_{39}] > [(n-C_4H_9)_4N]_4H[PW_{11}Mn(H_2O)O_{39}]$.

4.12 Conclusion

Mono-substituted polyoxometalate catalysts could catalyze the ethylbenzene and cyclohexane oxidation efficiently using hydrogen peroxide as oxidant. $[(n-C_4H_9)_4N]_4H[PW_{11}CuO_{39}]$ and $[(n-C_4H_9)_4N]_4H[PW_{11}Co(H_2O)O_{39}]$ performed the high activity. The amount of alcohol and ketone increased with hydrogen peroxide concentration, catalyst amount and reaction time. Polyoxotungstate gave higher catalytic activity in cyclohexanol oxidation than polyoxomolybdate. Tetrabutylammonium salt showed the highest activity, the catalytic activity decreased in the order; $[(n-C_4H_9)_4N]_3[PW_{12}O_{40}] > Na_2H[PW_{12}O_{40}] > H_3[PW_{12}O_{40}]$ at $110^\circ C$. Tetrabutylammonium salt was the suitable cations in this system compared with sodium and acid salts due to this cation function as phase transfer catalyst. Mono-substituted polyoxotungstate catalyst with Ni, Co and Mn showed higher activity than their parent.

ศูนย์วิจัยทรัพยากร
จุฬาลงกรณ์มหาวิทยาลัย

CHAPTER V

OXIDATION OF CYCLOHEXANE USING TRANSITION METAL-INCORPORATED XEROGEL CATALYSTS

In this chapter, metal-incorporated xerogel catalysts were synthesized and used in hydrocarbon oxidations with TBHP, molecular oxygen and air.

5.1 Introduction

The development of heterogeneous catalysts for the selective oxidation of hydrocarbons is a current challenge and has been studied extensively in recent years. Due to environmental and economic concerns, the development of highly efficient catalytic processes, which minimize the formation of side products and residues, is quite desirable. An interesting approach is supporting catalytically active metals on molecular sieves or related systems, thus enhancing the selectivity because the well-defined porous systems have been successfully applied as heterogeneous oxidation catalysts in the liquid phase. Furthermore, various transition metals, e.g. Mn, Zr, Cr, Fe, Ni and Cu, have been incorporated into zeolites, silicalites, silicon aluminium phosphates (SAPOs) or aluminium phosphates (AlPOs) and used in oxidation reactions. However, the use of these materials as oxidation catalysts is restricted because of relatively low activity or of metal leaching from the molecular sieves. On the other hand, transition metals such as vanadium, when incorporated into xerogels, have been studied in cyclohexane oxidation and showed to have considerable selectivity and activity [111]. Because of their excellent properties, silicon oxide based materials that have hydrophobic character favor the adsorption of hydrocarbons such as cyclohexane. The hydrophobicity of these supports results in a low affinity for oxidation products, which are expelled from the catalytically active sites as soon as they are formed. Thus, over-oxidation of the products is reduced and high selectivities are maintained [112-113].

5.1.1 Sol-gel process

The sol-gel process is particularly suitable for the preparation of oxide glasses and it is therefore of scientific and technological interest to study the structural developments occurring at various stages of the entire sol-gel to glass process and

investigate the factors influencing its structure and properties as shown in Figure 5.1 [114-115].

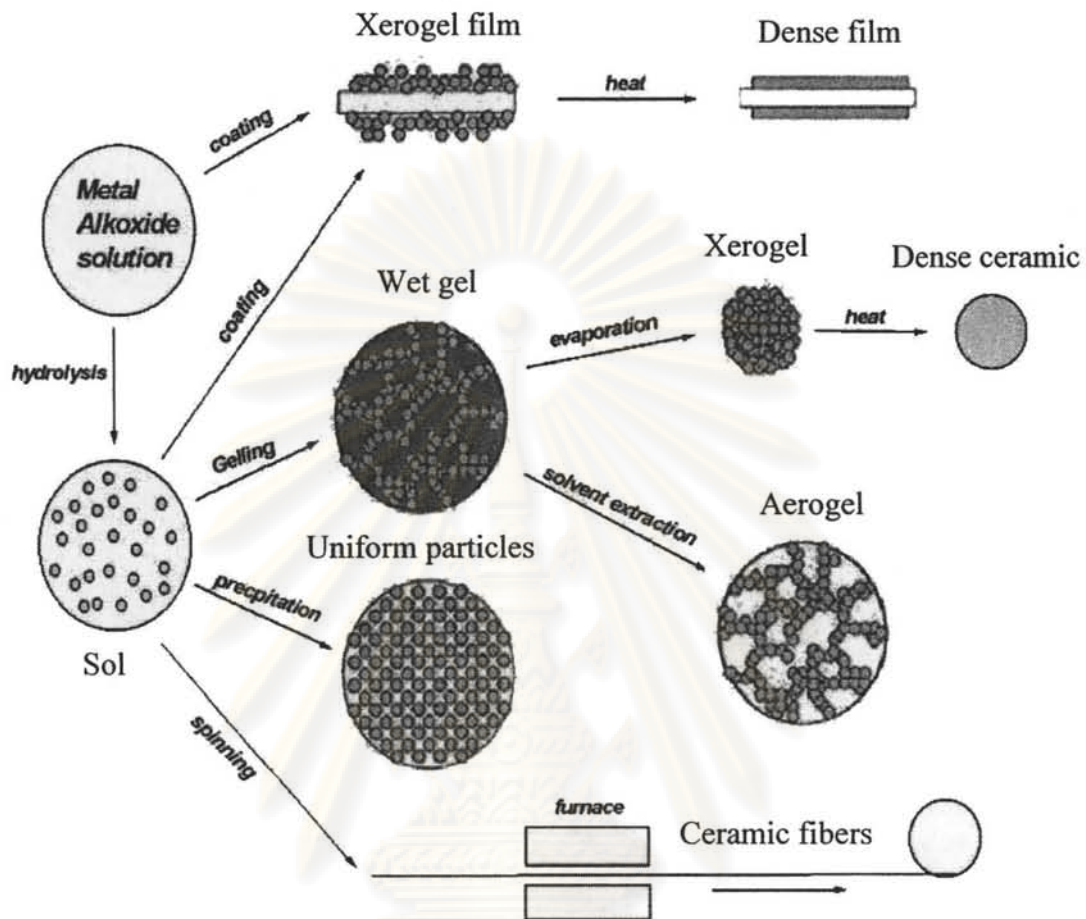


Figure 5.1 Sol-gel process and products [116].

The sol-gel process can be divided into the following steps: formation of a solution, gelation, aging, drying and densification. In the preparation of silica materials, one starts with an appropriate alkoxide, tetramethyl orthosilicate (TMOS) or tetraethyl orthosilicate (TEOS), which is mixed with water or solvent, such as methanol and ethanol? Hydrolysis leads to the formation of silanol groups (Si-OH). These species are intermediates as they react further by condensation to form siloxane groups (Si-O-Si). As the hydrolysis and condensation reactions continue, viscosity increases until the “sol” ceases to flow and forms a “gel”. The reactions are summarized in equation below [116].



When a wet gel is formed, the gel is converted into dense ceramic or glass particles by drying and heat-treatment. If the liquid in the wet gel is removed under supercritical conditions, a highly porous and extremely low density material called an aerogel forms. However, xerogels can be obtained by slowly drying a wet gel at a low temperature.

The parameters which influence the hydrolysis and condensation reactions in the sol-gel process include the reactivity of metal alkoxide, water/alkoxide ratio, solution pH, temperature and nature of the solvent.

In this chapter, silicates containing different types of transition metals such as Ni, Co, Cu, Mn and Cr were synthesized by sol-gel methods and the applications of these materials as catalysts in the oxidation of cyclohexane are presented. These catalysts are used in oxidation of hydrocarbons with TBPH and oxygen. The parameters such as amount of oxidant, types of metal, reaction time and types of solvent are investigated.

5.2 Literatures review

Some literature reports on the catalytic oxidation activities of the metal-incorporated xerogels are as follows.

In 2001, Jin *et al.* [112] reported the preparation of WO_3/SiO_2 catalysts by an alkoxide-sol-gel method using TEOS as the network-forming reagent. Sodium tungstate was added from 10-30 wt% into the alkoxide gel and it was calcined at 550°C . The 15 wt% WO_3/SiO_2 catalyst showed high catalytic activity (100% conversion) in the oxidation of cyclopentene to glutaraldehyde by H_2O_2 in *tert*-butyl ethanol at 35°C for 24 h.

In 2003, Riberio *et al.* [113] published catalytic oxidation activity of fructose to 2, 5-furandicarboxylic acid and 5-hydroxymethoyfurfural using cobalt acetylacetonate ($\text{Co}(\text{acac})_3$) in xerogel as the catalyst in air (20 atm) at 160°C for 65 min and water as solvent. Conversion was 46% with 83 and 17% selectivity of 2,5-furandicarboxylic acid and 5-hydroxymethoyfurfural.

In 2004 Daparkar *et al.* [114] reported the synthesis of the mesoporous material MCM-41 containing vanadium (3.3 wt %) in the framework. The catalyst was used in the oxidation of cyclohexane in the presence of acetic acid and methyl ethyl ketone (MEK) at 100°C using H₂O₂ as oxidant. They found that methyl ethyl ketone worked as an initiator, giving 100% conversion in 12 h with 90% selectivity of cyclohexanol.

In 2005 Zhou *et al.* [115] reported the preparation of nanocrystalline cobalt oxide (50 nm) by precipitation of cobalt nitrate with N-cetyl-N,N,N-trimethyl ammonium bromide. The catalyst was used in the oxidation of cyclohexane in oxygen at 120°C for 6 h. The conversion of cyclohexane was 8%, the main products being cyclohexanol and cyclohexanone (minor products were cyclohexene and adipic acid).

In 2006 Anand *et al.* [116], reported transition metal incorporation into the framework of a three-dimensional mesoporous silicate (M-TUD-1; M = Ti, Co, Fe and Cr). These catalysts were used in cyclohexane oxidation with TBHP, with the ratio of TBHP/cyclohexane equal to 0.5, at 70°C for 18 h. Cr- and Co-TUD-1 gave the highest activities, 13.5 and 9.5%. Cyclohexanone was the main product with more than 90% selectivity (minor products were cyclohexanol, cyclohexene and adipic acid).

In 2007 Ebadi *et al.* [117], prepared 5% wt. metallophthalocyanine supported on alumina materials (MPc/ γ -Al₂O₃; M = Co, Fe and Mn). These catalyzed oxidation of cyclohexane with air (1 atm, 30 mL/min) at 340°C for 3 h. The order of catalytic activities is: CoPc/ γ -Al₂O₃ > FePc/ γ -Al₂O₃ > MnPc/ γ -Al₂O₃. The CoPc/ γ -Al₂O₃ catalyst gave 33% conversion of cyclohexane with 37% selectivity of cyclohexanol and cyclohexanone and 17% of cyclohexene. When they increased the reaction temperature from 340 to 410°C, conversion of cyclohexane and selectivity of cyclohexanone and cyclohexanol decreased due to the lower stability of the catalyst at high temperature.

In 2008 Reddy *et al.* [118], reported the new cobalt encapsulated SBA-15 (2% wt. Co) catalysts were used in liquid phase oxidation of cyclohexane without solvent using oxygen as an oxidant (1 atm) at 160°C. The catalyst showed a 9.4% conversion of cyclohexane and 78% selectivity to cyclohexanone.

In 2008 Wang, *et al.* [4], reported the preparation of metal-containing ZSM-5 (M-ZSM-5) in which M = Ni, Fe, Co, Mn and Cu (2% by weight). These catalysts were used for cyclohexane oxidation with TBHP (85% in aqueous) in an ionic liquid, 1-ethyl-3-methylimidazolium tetrafluoroborate (emim)BF₄, at 90°C for 12 h. Using FeZSM-5, the maximum activity was obtained with 21% conversion of cyclohexane.

In 2008, Chen *et al.* [119], reported cobalt incorporation into the framework of hexagonal mesoporous silica (HMS) modified by organic groups, methyltriethoxysilane (CoMeHMS), propyltrimethoxysilane (CoPrHMS) and phenyltriethoxysilane (CoPhHMS). These catalysts were used for the oxidation of cyclohexane with TBHP and oxygen (1 atm) at 115°C for 6 h. The highest conversion was found with CoPhHMS as catalyst with 7% conversion of cyclohexane.

5.3 Preparation of metal incorporated xerogel catalysts

Metal-incorporated xerogel catalysts were prepared by an acid-catalyzed sol-gel method [120-121] as described below.

To 49 mmol of TEOS and 1 mmol of Co(OAc)₂·4H₂O dissolved in 150 mmol of ethanol, placed in a beaker equipped with an efficient magnetic stirring bar, was added 18 mmol of 8 M HCl over a period of 15 min. The reaction mixture was stirred for 5 min and then allowed to stand at room temperature to remove the volatiles by slow evaporation. The resulting brittle xerogel was subsequently dried at 110°C in air for 24 h and thereafter cooled to room temperature. After that the material (glass like) was crushed and sieved (100 mesh particles). The other catalysts used the same procedure.

5.4 Characterization of metal-incorporated xerogel catalysts

The synthesized catalysts were characterized with various techniques, the results being given below.

5.4.1 Functional group analysis of metal-incorporated xerogel catalysts

FTIR spectra showed the typical peaks for amorphous cobalt on silica xerogel catalysts.

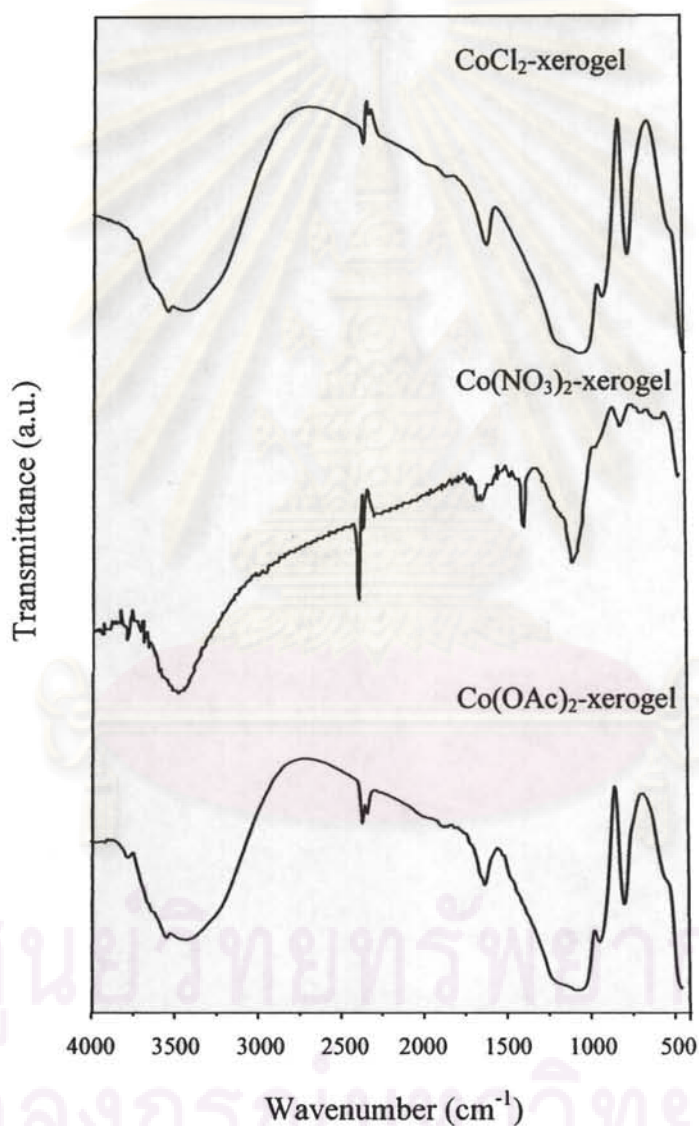


Figure 5.2 FTIR spectra of cobalt incorporated xerogel catalysts.

In Figure 5.2 one can observe a broad band between $3400\text{--}3500\text{ cm}^{-1}$, which is the characteristic stretching vibration range for hydroxyl groups. The typical peaks for amorphous silicate materials prepared via the sol-gel method appeared at 1080, 950

and 790 cm^{-1} . The band at about 1650 cm^{-1} corresponds to the bending mode of the water molecule. In Figure 5.2, for the $\text{Co}(\text{NO}_3)_2$ -xerogel, the sharp band close to 1380 cm^{-1} is due to the presence of NO_3^- ions [120-122]. FTIR spectra of the other samples are shown in appendix G.

5.4.2 Phase analysis of metal-incorporated xerogels

The XRD patterns of the xerogels containing metal salts showed only a broad peak characteristic of amorphous silica.

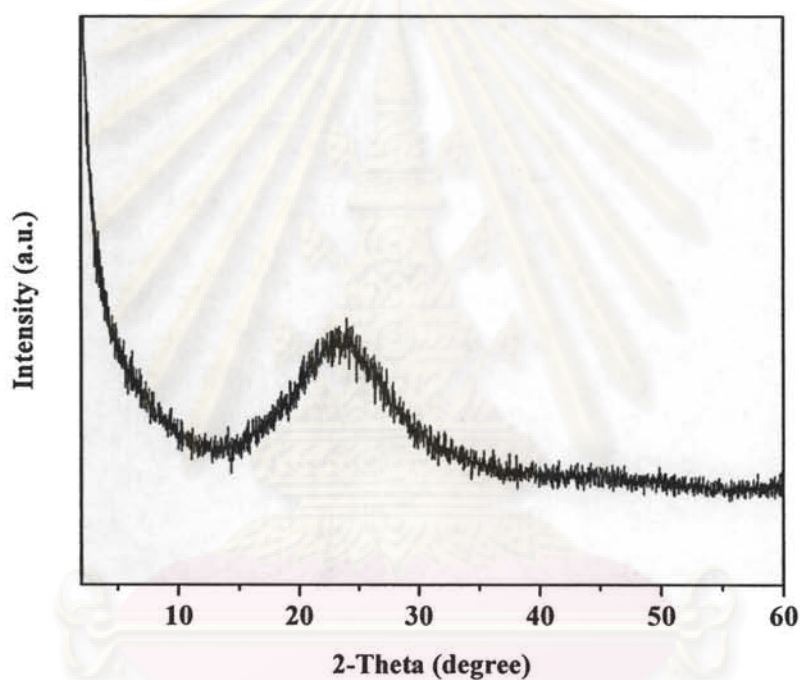


Figure 5.3 XRD pattern of $\text{Co}(\text{OAc})_2$ -xerogel catalysts.

The XRD pattern of metal-incorporated xerogels was obtained, and is shown in Figure 5.3. Only an amorphous phase was observed with no metal phase being apparent, presumably due to the low metal concentration. The XRD patterns of other catalysts have been collected in appendix H.

5.4.3 Diffuse reflectance ultraviolet-visible spectroscopy (DRUV)

The diffuse reflectance spectra of the catalysts were obtained using a UV-visible spectrophotometer to provide more information about the catalysts. The results are given in Table 5.1.

Table 5.1 Absorption bands of metal-incorporated xerogel catalysts

Catalyst	Absorption band (nm)
Ni(NO ₃) ₂ -xerogel	330-375, 500-600
Cr(NO ₃) ₃ -xerogel	420-600
Mn(NO ₃) ₂ -xerogel	250-275
Cu(NO ₃) ₂ -xerogel	420-570
Co(NO ₃) ₂ -xerogel	440-550
Co(OAc) ₂ -xerogel	300-410, 650-800
Co(Cl) ₂ -xerogel	300-410, 720-800
Ni(NO ₃) ₂ -xerogel	330-375, 500-630

The Ni(NO₃)₂-xerogel showed two broad absorption bands between 330-375 nm and a broad band between 500-630 nm, which indicated the presence of Ni²⁺ in the sample [123]. The Cr(NO₃)₃-xerogel showed the absorption band between 420-600 nm, which indicated octahedral coordination of Cr³⁺ in the sample [120]. The Mn(NO₃)₂-xerogel showed peak between 250-275nm, which indicated the presence of Mn²⁺ in the sample [124]. The Cu(NO₃)₂-xerogel exhibited absorptions between 420 and 570 nm, and these absorptions can be assigned to O²⁻ → Cu²⁺ charge transfers [125]. Broad bands between 800 and 1200 nm are typical of d-d transitions of Cu²⁺ in an octahedral or square pyramidal environment. However, these bands are too broad to allow a detailed assignment of the absorptions. The Co(OAc)₂-xerogel and CoCl₂-xerogel showed broad absorption bands between 300-410 and 700-800 nm, which indicated tetrahedral coordination of Co²⁺ [121]. The Co(NO₃)₂-xerogel sample showed an absorption peak at 500-560 nm, revealing octahedral coordination of Co²⁺.

5.4.4 Surface area measurement (Brunauer-Emmett-Teller method (BET))

The surface properties of metal-incorporated xerogels were observed by the nitrogen adsorption technique, after the samples were pretreated at 100°C for 1 h. The results have been collected in Table 5.2.

Table 5.2 Surface analysis of metal-incorporated xerogel catalysts

Catalyst	Surface area (m ² /g)	Pore volume (cm ³ /g)	Mean pore diameter (nm)
Ni(NO ₃) ₂ -xerogel	264	0.1	2.1
Cr(NO ₃) ₃ -xerogel	418	0.2	2.1
Mn(NO ₃) ₂ -xerogel	263	0.1	2.1
Cu(NO ₃) ₂ -xerogel	430	0.1	2.0
Co(NO ₃) ₂ -xerogel	279	0.2	2.2
Co(OAc) ₂ -xerogel	352	0.1	2.0
CoCl ₂ -xerogel	308	0.2	2.1

The results show that all samples have surface areas between about 263-430 m²/g, with no significant differences of their pore volumes and mean pore diameters.

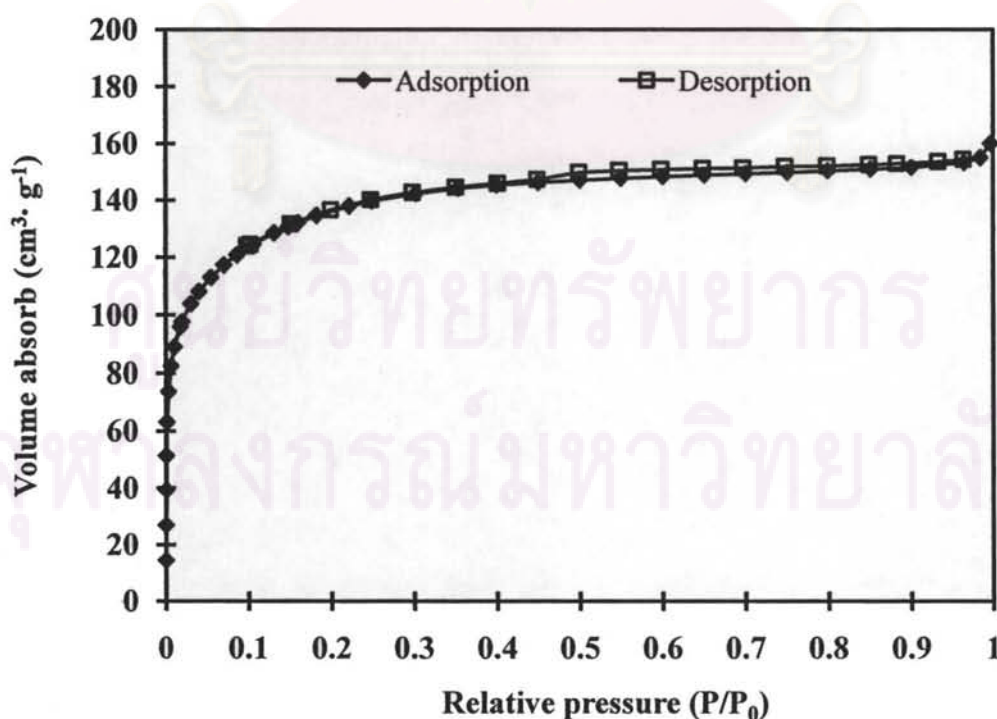


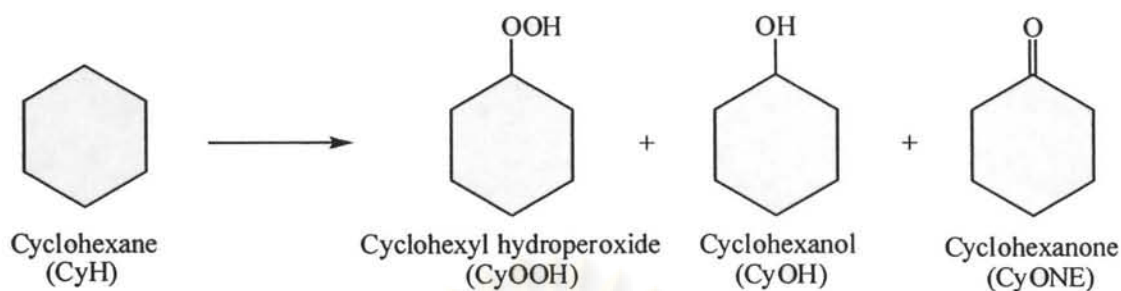
Figure 5.4 Adsorption and desorption isotherm of Co(OAc)₂-xerogel.

The adsorption isotherm is clearly of the Langmuir type indicating fairly small pores and a narrow pore-size distribution, the same result having been found earlier by Neumann and co-workers [126]. In this case $\text{TiO}_2(\text{Cl})$ -xerogel was prepared which a surface area of $750 \text{ m}^2/\text{g}$ and an average pore diameter of 1.5 nm Rogovin and co-workers [121] prepared metal-incorporated xerogel and found the same results; BET measurements showed surface areas of metal-incorporated xerogel were in the range of $650\text{-}750 \text{ m}^2/\text{g}$ with average pore diameters of 1.5 nm.

5.5 Catalytic activity

Metal-incorporated xerogel catalysts were studied with respect to the effect of metal and anion, types of anion, reaction time, air pressure, amount of methyl ethyl ketone, the extent of leaching, and reusability. No leaching of cobalt to the liquid phase was observed when anhydrous *tert*-butyl hydroperoxide was used. Nevertheless, the use of aqueous solutions of H_2O_2 (30%) or *tert*-butyl hydroperoxide (70%) resulted in considerable metal leaching [121]. Thus, in this study 6 M TBHP in decane was used and the results from the catalytic oxidation of cyclohexane using metal-incorporated xerogels are described below.

General oxidation procedure of cyclohexane in Parr reactor with 6 M TBHP in decane is described in details as follow. The catalyst, substrate and oxidant placed in the stainless steel reactor located in the electrical heater. In case of oxidant is air the reactor is purged for 3 times. The stainless steel reactor is heated to the desired temperature and reaction time. After the desired reaction time, the reaction mixture is cooled down and the catalyst is filtered off. The liquid mixture is added 25% H_2SO_4 solution and extract with diethyl ether. The liquid mixture is neutralized with saturated NaHCO_3 solution and dried over Na_2SO_4 anhydrous. The oxygenated products and recovered substrate in a liquid mixture are qualitatively analyzed by gas chromatography using the internal standard method. The mass balance of all samples is in the range 87-99%. The oxygenated products found in this study from the cyclohexane oxidation are shown in Scheme 5.1.



Scheme 5.1 Reaction scheme of cyclohexane oxidation and its products found in this study.

5.5.1 Effect of types of metal

The prepared metal-incorporated xerogels were used for the oxidation of cyclohexane with 6 M TBHP in decane under fixed conditions with a TBHP/cyclohexane mol ratio of 0.65. The results are shown in Table 5.3.

Table 5.3 Oxidation of cyclohexane using metal-incorporated xerogel catalysts

Catalyst	Product (mol%) ^a			CyONE+CyOH (mol%) ^a	CyONE/CyOH
	CyONE	CyOH	CyOOH		
Ni(NO ₃) ₂ -xerogel	7.0	4.3	trace	11.3	1.6
Cr(NO ₃) ₃ -xeroge	7.6	5.4	trace	13.0	1.4
Mn(NO ₃) ₂ -xerogel	10.8	5.4	trace	16.2	2.0
Cu(NO ₃) ₂ -xerogel	12.9	4.3	trace	17.2	3.0
Co(NO ₃) ₂ -xerogel	16.2	5.4	trace	21.6	3.0

Reaction conditions: cyclohexane 18.5 mmol, catalyst 0.05 g, TBHP 12 mmol (6 M in decane), 70°C, 24 h.

CyONE = cyclohexanone

CyOH = cyclohexanol

CyOOH = cyclohexyl hydroperoxide

trace = less than 0.05 mol%

^a based on mole of substrate

The blank experiment without catalyst gave only a negligible amount of cyclohexanone and cyclohexanol. For the oxidation of cyclohexane using metal-incorporated xerogel with TBHP, the Co(NO₃)₂-xerogel gave the highest activity,

with the products yield being 21.6 mol% and CyONE/CyOH ratio being 3.0. These results indicated that cyclohexanone was the main product for all metal-incorporated catalysts. CyOOH was quantitatively reduced by triphenylphosphine (PPh₃) to yield cyclohexanol.

5.5.2 Effect of types of anion

Several types of cobalt salts were studied: chloride, nitrate and acetate, and the results for cyclohexane oxidation have been collected in Table 5.4.

Table 5.4 Oxidation of cyclohexane using cobalt xerogel catalysts

Catalyst	Product (mol%) ^a			CyONE+CyOH (mol%) ^a	CyONE/CyOH
	CyONE	CyOH	CyOOH		
CoCl ₂ -xerogel	11.9	4.9	trace	16.8	2.4
Co(NO ₃) ₂ -xerogel	16.2	5.4	trace	21.6	3.0
Co(OAc) ₂ -xerogel	18.9	7.0	trace	25.9	2.7

Reaction conditions: cyclohexane 18.5 mmol, catalyst 0.05 g, TBHP 12 mmol (6 M in decane), 70°C, 24 h.

CyONE = cyclohexanone

CyOH = cyclohexanol

CyOOH = cyclohexyl hydroperoxide

trace = less than 0.05 mol%

^a based on mole of substrate

Cobalt xerogel catalysts with acetate anion gave the better conversions than those with chloride and nitrate anions; the higher activities of Co(OAc)₂-xerogels were in fact previously reported by Rogovin and coworker [121]. The activity order was Co(OAc)₂-xerogel > Co(NO₃)₂-xerogel > CoCl₂-xerogel.

5.5.3 Effect of reaction time

The Co(OAc)₂-xerogel catalyst was chosen for the study of the effect of the reaction time on the selectivity of cyclohexanone and cyclohexanol in cyclohexane oxidation with 6 M TBHP in decane. The time dependence of the product distributions using Co(OAc)₂-xerogel catalyst are given below.

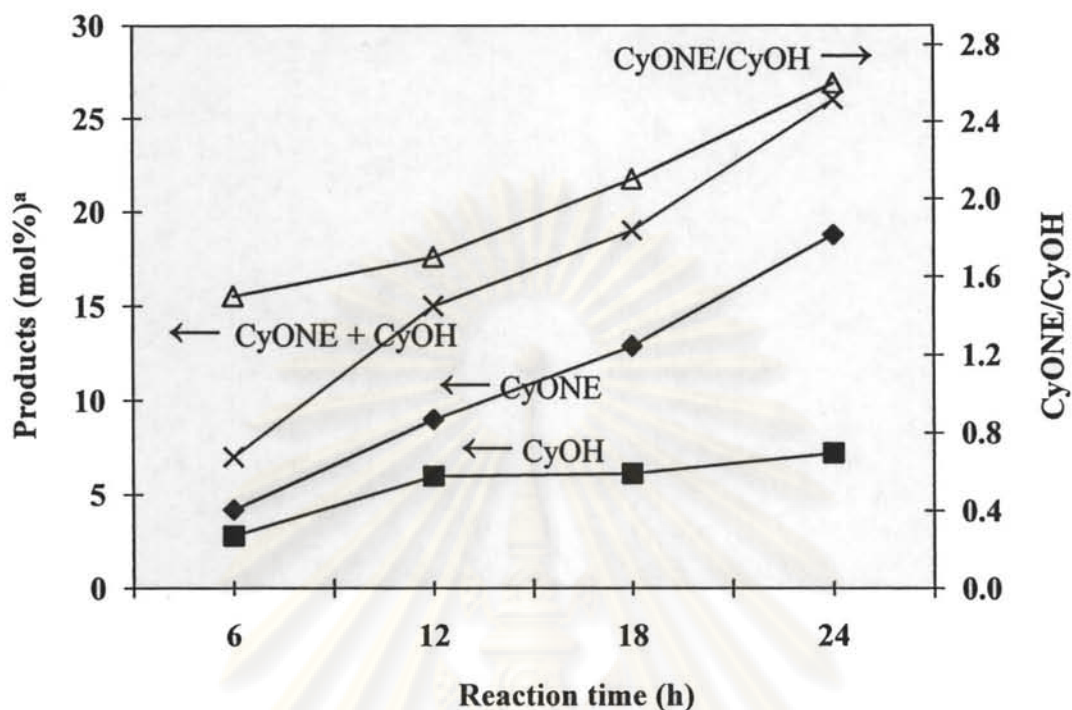


Figure 5.5 Effect of reaction time on cyclohexane oxidation using $\text{Co}(\text{OAc})_2$ -xerogel.

Reaction conditions: cyclohexane 18.5 mmol, catalyst 0.05 mg, TBHP 12 mmol (6 M TBHP in decane, 70°C).

^a based on mole of substrate

The ratio of cyclohexanone and cyclohexanol increased with reaction time. At the beginning (6-12 h), CyONE/CyOH ratio was 1.6 but, beyond 12 h the rate of cyclohexanol production decreased and the ratio of CyONE/CyOH was enhanced. This might be due to cyclohexanol being further oxidized to cyclohexanone.

5.5.4 Effect of air pressure

To combine the effect of oxidant such air in the presence of TBHP in decane was observed in oxidation of cyclohexane. Air pressures of 1, 3 and 5 atm were used, with a fixed amount of TBHP (6 mmol). The results and discussions are provided below.

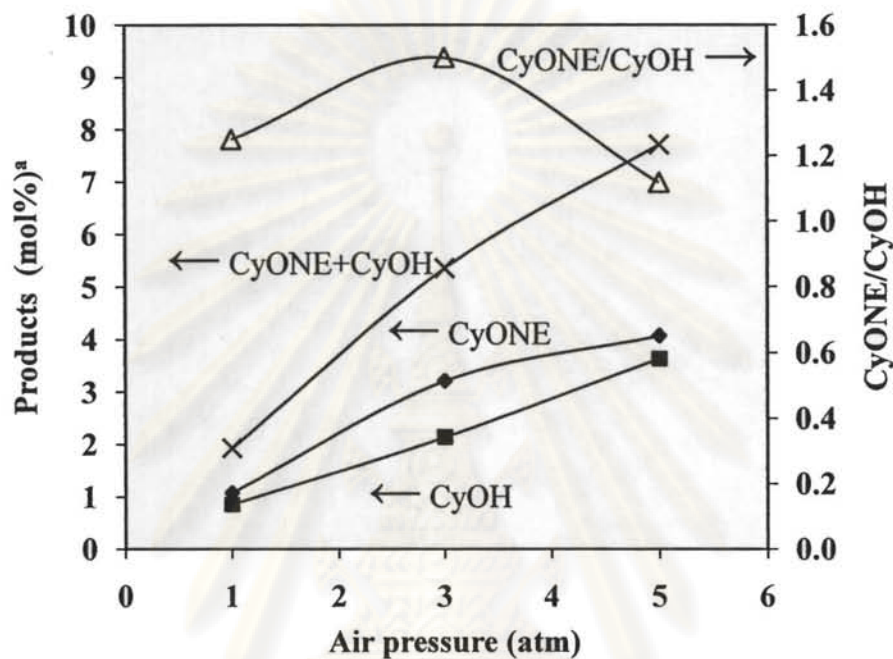


Figure 5.6 Effect of air pressure on cyclohexane oxidation using $\text{Co}(\text{OAc})_2$ -xerogel.

Reaction conditions: cyclohexane 46.9 mmol, catalyst 0.05 g, TBHP 6 mmol (6 M TBHP in decane), MEK 5.6 mmol, 100°C , 6 h.

^a based on mole of substrate

From Figure 5.6, one can observe that a higher amount of cyclohexyl hydroperoxide was produced when the reaction was carried out at high air pressure. The selectivity to products showed a remarkable change with the increase of air pressure. High pressures promoted formation of cyclohexanone as well as cyclohexanol. The maximum CyONE/CyOH ratio was observed at 3 atm. From the result, it can be concluded that air can be used as oxidant with metal-incorporated xerogel catalysts.

5.5.5 Effect of amount of TBHP

To study the effect of the amount of TBHP (6 M in decane) on the cyclohexane oxidation in air, the reactions were done while keeping the other parameters constant. The results and discussion have been collected in Table 5.5.

Table 5.5 Effect of the amount of TBHP in cyclohexane oxidation using $\text{Co}(\text{OAc})_2$ -xerogel

TBHP (mmol)	Product (mol%) ^a			CyONE+CyOH (mol%) ^a	CyONE/CyOH
	CyONE	CyOH	CyOOH		
0.6	0.8	0.8	trace	1.6	1.0
3.0	1.9	1.7	trace	3.6	1.1
6.0	3.2	2.1	trace	5.3	1.5

Reaction conditions: cyclohexane 46.9 mmol, catalyst 0.05 g, TBHP 0.6-6.0 mmol (6 M in decane), MEK 5.6 mmol, air 3 atm, 100°C, 6 h.

CyONE = cyclohexanone

CyOH = cyclohexanol

CyOOH = cyclohexyl hydroperoxide

trace = less than 0.05 mol%

^a based on mole of substrate

When the amount of TBHP was increased, the total product yields increased. More oxidant likely helps in generating more radicals. The selectivity of cyclohexanone increases with an increase in TBHP amount and the selectivity of cyclohexanol decreases, as described earlier by Kumar and co-workers [127]. This might be due to oxidation of cyclohexanol to cyclohexanone in the presence of excess amounts of TBHP.

จุฬาลงกรณ์มหาวิทยาลัย

5.5.6 Effect of amount of methyl ethyl ketone

Methyl ethyl ketone is the initiator in oxidation with air, thus the effect of the amount of methyl ethyl ketone (MEK) is observed for cyclohexane oxidation with TBHP (6 M in decane) and air. The results are in Table 5.6.

Table 5.6 Effect of amount of MEK in cyclohexane oxidation using Co(OAc)₂-xerogel

MEK (mmol)	Products (mol%) ^a			CyONE+CyOH (mol%) ^a	CyONE/CyOH
	CyONE	CyOH	CyOOH		
-	2.6	1.7	trace	4.3	1.5
5.6	3.2	2.1	trace	5.3	1.5
8.4	3.0	2.3	0.2	5.3	1.3
11.2	2.8	1.7	0.2	4.5	1.6

Reaction conditions: cyclohexane 46.9 mmol, catalyst 0.05 g, TBHP 6 mmol (6 M in decane), air 3 atm, 100°C, 6 h.

CyONE = cyclohexanone

CyOH = cyclohexanol

CyOOH = cyclohexyl hydroperoxide

trace = less than 0.05 mol%

^a based on mole of substrate

MEK worked as an initiator in the reaction due to the amount of cyclohexanone and cyclohexanol enhancement when MEK was added. However, the increased amount of MEK did not significantly affect the amount of cyclohexanone and cyclohexanol. A similar result has been described earlier in V-MCM41-catalyzed cyclohexane oxidation with H₂O₂ in acetic acid [128]. In addition, the use of cyclohexanone instead of MEK led to more products yields (cyclohexanone (3.4 mol%) and cyclohexanol (3.0 mol%)), but the lower in cyclohexanone selectivity (CyONE/CyOH = 1.1) was observed [129].

5.5.7 Effect of the amount of catalyst

The amount of $\text{Co}(\text{OAc})_2$ -xerogel catalyst was varied in the range of 25-150 mg for the cyclohexane oxidation with 6 M TBHP in decane and air in the presence of MEK. The results and discussions are given below.

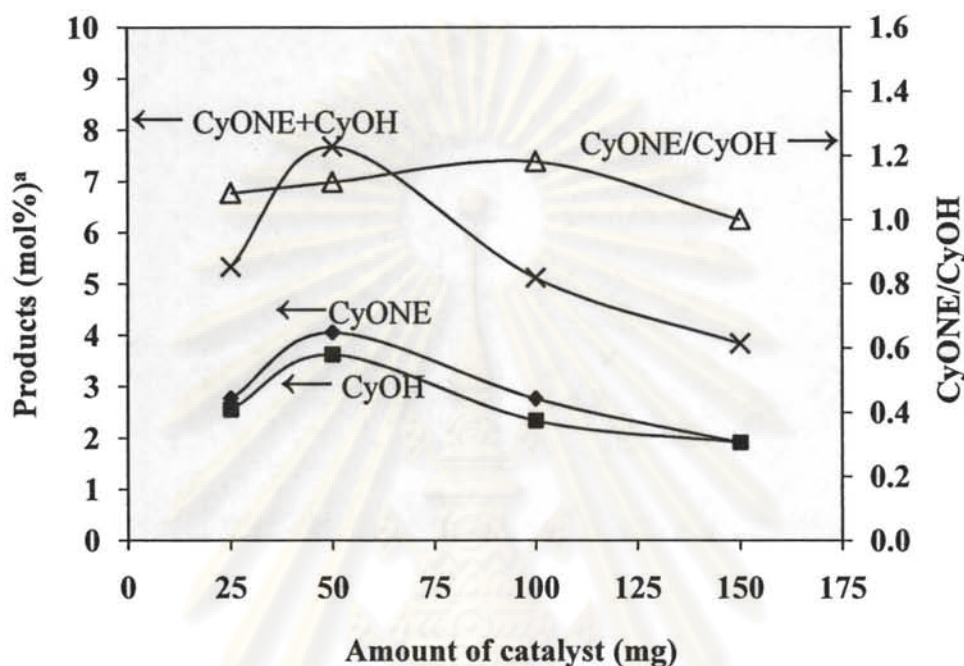


Figure 5.7 Effect of catalyst amount in cyclohexane oxidation using $\text{Co}(\text{OAc})_2$ -xerogel.

Reaction conditions: cyclohexane 46.9 mmol, catalyst 25-150 g, TBHP 6 mmol (6 M in decane), air 3 atm, MEK 5.6 mmol, 100°C, 6 h.

Figure 5.7 shows the effect of catalyst amount on the cyclohexane oxidation reaction. It can be seen that cyclohexanone and cyclohexanol increase with catalyst amount and a maximum point was obtained for 0.05 g of $\text{Co}(\text{OAc})_2$ -xerogel catalyst. However, the observed reduction in desired products may be due to the presence of the excess catalyst.

จุฬาลงกรณ์มหาวิทยาลัย

5.6 Leaching test of metal-incorporated xerogel catalysts

The extent of leaching in the metal-incorporated xerogel catalysts used for cyclohexane oxidation was observed in aqueous solution and decane.

No leaching of cobalt species to the liquid phase was observed for TBHP. Nevertheless, the use of aqueous solutions of 30% H_2O_2 or 70% TBHP resulted in considerable metal leaching [121]. The UV-vis spectra from the leaching test of $Co(OAc)_2$ -xerogel indicated that this catalyst leached cobalt species only into aqueous solutions. However, ICP analysis indicated that the cobalt species concentration in non polar solvent such as decane was very low (less than 0.11 M) thus this catalyst was catalyzed with heterogeneous system using TBHP in decane and least leaching as described above.

5.7 Conclusion

The metal-incorporated xerogel catalysts could catalyze oxidation of cyclohexane in good yields. The $Co(OAc)_2$ -xerogel catalyst was the best catalyst in this study. In TBHP as oxidant more cyclohexanone is observed, the maximum mole ratio of cyclohexanone/cyclohexanol is 2.7, however in TBHP/air/MEK condition found the lower mole ratio of cyclohexanone/cyclohexanol which is 1.6 but the reaction time is shorter than in only TBHP as oxidant for 4 folds. When TBHP in decane was used as oxidant, there was no leaching of the metal into the reaction mixture.

REFERENCES

- 1 Jay, A. and Labinger, J. A. Selective alkane oxidation: hot and cold approaches to a hot problem. J. Mol. Catal. A: Chem. 220 (2004): 27-35.
- 2 Ramanathan, A.; Hamdy, M. S.; Parton, R.; Maschmeyer, T.; Jansen, J. C. and Hanefeld, U. Co-TUD-1 catalysed aerobic oxidation of cyclohexane. Appl. Catal. A: Gen. 355 (2009): 78-82.
- 3 Bond, G. C. Heterogeneous catalysis: principles and applications, 2nd Clarendon Press, Oxford, 1987.
- 4 Wang, J. Y.; Zhao, F. Y.; Liu, R. J. and Hu, Y. Q. Oxidation of cyclohexane catalyzed by metal-containing ZSM-5 in ionic liquid. J. Mol. Catal. A: Chem. 279 (2008): 153-158.
- 5 Hudlicky, M. Oxidation of organic chemistry. Washington DC: ACS Monograph. 186, 1991, p.1.
- 6 Sheldon, R. A. and Kochi, J. K. Metal catalyzed oxidation of organic compounds, Academic Press, New York, 1981 (Chapter 11).
- 7 Schuchardt, U.; Cardoso, D.; Sercheli, R.; Pereira, R.; Cruz, R. S. ; Guerreiro, M. C.; Mandelli, D.; Spinace, E. V. and Pires, E. L. Cyclohexane oxidation continues to be a challenge. Appl. Catal. A: Gen. 211 (2001): 1-17.
- 8 Bhoware, S. S.; Shylesh, S.; Kamble, K. R. and Singh, A. P. Cobalt-containing hexagonal mesoporous molecular sieves (Co-HMS): synthesis, characterization and catalytic activity in the oxidation reaction of ethylbenzene. J. Mol. Catal. A: Chem. 255 (2006): 123-130.
- 9 Xavier, K. O.; Chacko, J. and Yusuff, K. K. M. Zeolite-encapsulated Co(II), Ni(II) and Cu(II) complexes as catalysts for partial oxidation of benzyl alcohol and ethylbenzene. Appl. Catal. A: Gen. 258 (2004): 251-259.
- 10 Basile, F.; Fornasari, G.; Gazzano, M. and Vaccari, A. Synthesis and thermal evolution of hydrotalcite-type compounds containing noble metals. Appl. Clay Sci. 16 (2000): 185-200.
- 11 Cavani, F.; Trifiro, F. and Vaccari, A. Hydrotalcite-type anionic clay: preparation, properties and application. Catal. Today 11 (1991): 173-301.
- 12 Roelofs, J. C. A. A.; Dillen, A. J. and Jong, K. P. Base-catalyzed condensation

- of citral and acetone at low temperature using modified hydrotalcite catalysts. Catal. Today 60 (2000): 297-303.
- 13 Prinetto, F.; Tichit, D.; Teissier, R. and Coq, B. Mg- and Ni-containing layered double hydroxides as soda substitutes in the aldol condensation of acetone. Catal. Today 55 (2000): 103-116.
- 14 Centi, G. and Parathoner, S. Catalysis by layered materials: a review. Microporous Mesoporous Mater. 107 (2008): 3-15.
- 15 Xu, Z. P. and Zeng, H. C. Interconversion of brucite-like and hydrotalcite-like phase in cobalt hydroxide compounds. Chem. Mater. 11 (1999): 67-74.
- 16 Gillman, G. P.; Noble, M. A. and Raven, M. D. Anion substitution of nitrate-saturated layered double hydroxide of Mg and Al. Appl. Clay Sci. 38 (2008): 179-186.
- 17 Rivera, J. A.; Fetter, G.; Jimenez, Y.; Xochipa, M. M. and Bosch, P. Nickel distribution in (Ni,Mg)/Al-layered double hydroxides. Appl. Catal. A: Gen. 316 (2007): 207-211.
- 18 Rives, V. and Ulibarri, M. A. Layered double hydroxides (LDH) intercalated with metal coordination compounds and oxometalates. Coord. Chem. Rev. 181 (1999): 61-120.
- 19 Casenave, S.; Martinez, H.; Guimon, C.; Auroux, A.; Hulea, V.; Cordoneanu, A. and Dumitriu, E. Acid-base properties of Mg-Ni-Al mixed oxides using LDH as precursors. Thermochim. Acta 379 (2001): 85-93.
- 20 Crivello, M.; Perez, C.; Fernandez, J.; Eimer, G.; Herrero, E.; Casuscelli, S. and Rodriguez-Castellon, E. Synthesis and characterization of Cr/Cu/Mg mixed oxides obtained from hydrotalcite-type compounds and their application in the dehydrogenation of isoamylic alcohol. Appl. Catal. A: Gen. 317 (2007): 11-19.
- 21 Carrado, K. A. and Kostapapas, A. Layered double hydroxides (LDHs). Solid State Ion. 26 (1998): 77-86.
- 22 De Roy, A. Lamellar Double Hydroxides. Mol. Cryst. Liq. Cryst. 311 (1998): 173-193.
- 23 Ulibarri, M. A.; Pavlovic, I.; Barriga, C.; Hermosín, M. C. and Cornejo, J. Adsorption of anionic species on hydrotalcite-like compounds: effect of interlayer anion and crystallinity. Appl. Clay Sci. 18 (2001):17-37.
- 24 Cantrell D.G.; Gillie, L. J.; Lee, A. F. and Wilson, K., Structure-reactivity

- correlations in MgAl hydrotalcite catalysts for biodiesel synthesis. Appl. Catal. A: Gen. 287 (2005): 183-190.
- 25 Zhang, H.; Qi, R.; Evans, D. G. and Duan, X. Synthesis and characterization of a novel nano-scale magnetic solid base catalyst involving a layered double hydroxide supported on a ferrite core. J. Solid State Chem. 177 (2004): 772-780.
- 26 Sychev, M.; Prihod'ko, R.; Erdmann, K.; Mangel, A. and Santen, R. A. Hydrotalcites: relation between structural features, basicity and activity in the wittig reaction. Appl. Clay Sci. 18 (2001): 103-110.
- 27 Lucredio, A. F. and Assaf, E. M., Cobalt catalysts prepared from hydrotalcite precursors and tested in methane steam reforming. J. Power Sources 159 (2006): 667-672.
- 28 Corma, A.; Fornes, V.; Rey F.; Cervilla A.; Llopis E. and Ribera, A. Catalytic air oxidation of thiols mediated at a Mo(VI)O₂ complex center intercalated in a Zn(II)-Al(III) layered double hydroxide host. J. Catal. 152 (1995): 237-242.
- 29 Bravo-Suárez, J.; Páez-Mozo, E. A. and Oyama, S. T. Review of the synthesis of layered double hydroxides: a thermodynamic approach. Quim. Nova. 27 (2004): 601-614.
- 30 Barrault, J. ; Derouault, A. ; Courtois, G. ; Maissant, J. M. ; Dupin, J. C. ; Guimon, C. ; Martine, H. and Dumitriu, E. On the catalytic properties of mixed oxides obtained from the Cu-Mg-Al LDH precursors in the process of hydrogenation of the cinnamaldehyde. Appl. Catal. A: Gen. 262 (2004): 43-51.
- 31 <http://abulafia.mt.ic.ac.uk/shannon/ptable.php>, based on R. D. Shannon. Acta Cryst. A32 (1976): 751.
- 32 Yang, W. S.; Kim, Y. M.; Liu, P. K. T.; Sahimi, M. and Tsotsis, T. T. A study by in situ technique of the thermal evolution of the structure of a Mg-Al-CO₃ layered double hydroxide. Chem. Eng. Sci. 57 (2002): 2945-2953.
- 33 Costantino, U.; Marmottini, F.; Nocchetti, M. and Vivani, R. New synthetic routes to hydrotalcite-like anionic clays. Characterization and properties of the obtained compounds. Eur. J. Inorg. Chem. 10 (1998): 1439-1446.
- 34 Kaneda, K.; Yamashita, T.; Matsushita, T. and Ebitani, K. Heterogeneous oxidation of allylic and benzylic alcohols catalyzed by Ru-Al-Mg hydrotalcites in the presence of molecular oxygen. J. Org. Chem. 63 (1998): 1750-1751.

- 35 Bahranowski, K.; Dula, R.; Gasiior, M.; Labanowska, M.; Michalik, A.; Vartikian, L. A. and Serwicka, E. M. Oxidation of aromatic hydrocarbons with hydrogen peroxide over Zn,Cu,Al-layered double hydroxides. Appl. Clay Sci. 93 (2001): 93-101.
- 36 Carpentier, J.; Lamonier, J. F.; Siffert, S.; Zhilinskaya, E. A. and Aboukais, A. characterization of Mg/Al hydrotalcite with interlayer palladium complex for catalytic oxidation of toluene. Appl. Catal. A: Gen. 234 (2002): 91-101.
- 37 Choudhary, V. R.; Indurkar, J. R.; Narkhede, V. S. and Jha, R. MnO_4^{1-} exchanged Mg–Al hydrotalcite: a stable and reusable/environmental-friendly catalyst for selective oxidation by oxygen of ethylbenzene to acetophenone and diphenylmethane to benzophenone. J. Catal. 227 (2004): 257-261.
- 38 Barbosa, C. A. S.; Dias, P. M.; Ferreira, A. M. and Constantino, V. R. L. Mg-Al hydrotalcite-like Compounds containing iron-phthalocyanine complex: effect of aluminium substitution on the complex adsorption features and catalytic activity. Appl. Clay Sci. 28 (2005): 147-158.
- 39 Kawabata, T.; Shinozuka, Y.; Ohishi, Y.; Shishido, T.; Takaki, K. and Takehira, K. Nickel containing Mg-Al hydrotalcite-type anionic clay catalyst for the oxidation of alcohols with molecular oxygen. J. Mol. Catal. A: Chem. 236 (2005): 206-215.
- 40 Jana, S. K.; Wu, P. and Tatsumi, T. NiAl hydrotalcites as an efficient and environmentally friendly solid catalyst for solvent-free liquid-phase selective oxidation of ethylbenzene to acetophenone with 1 atm of molecular oxygen. J. Catal. 240 (2006): 268-274.
- 41 Hulea, V.; Maciucă, A.; Fajula, F. and Dumitriu, E. Catalytic oxidation of thiophenes and thioethers with hydrogen peroxide in the presence of W-containing layered double hydroxides. Appl. Catal. A: Gen. 313 (2006): 200-207.
- 42 Llamas, R.; Jiménez-Sanchidrián, C. and Ruiz, J. R. Heterogeneous Baeyer-Villiger oxidation of ketones with H_2O_2 /nitrile, using Mg/Al hydrotalcite as catalyst. Tetrahedron 63 (2007): 1435-1439.
- 43 George, K and Sugunan, S. Nickel substituted copper chromite spinels: preparation, characterization and catalytic activity in the oxidation reaction of ethylbenzene. Catal. Commun. 9 (2008): 2149-2153.

- 44 Kishore, D. and Rodrigues, A. E. Liquid phase catalytic oxidation of isophorone with tert-butylhydroperoxide over Cu/Co/Fe-MgAl ternary hydrotalcites. Appl. Catal. A: Gen. 345 (2008): 104-111.
- 45 Ferreira, O. P.; Alves, O. L.; Gouveia, D. X.; Souza Filho, A. G.; Paiva, J. A. C. and Filho, J. M. Thermal decomposition and structural reconstruction effect on Mg-Fe-based hydrotalcite compounds. J. Solid State Chem. 177 (2004): 3058-3069.
- 46 Gryglewicz, S. Alkaline-earth metal compounds as alcoholysis catalysts for ester oils synthesis. Appl. Catal. A: Gen. 192 (2000):23-28.
- 47 Holgado, M. J.; Rives, V. and San Roman, M. S. Characterization of Ni-Mg-Al mixed oxides and their catalytic activity in oxidative dehydrogenation of n-butane and propene. Appl. Catal. A: Gen. 214 (2001): 219-228.
- 48 Kruissink, E. C.; Alzamora, L. E.; Orr, S.; Doesburg, E. B. M.; Van Reijen, L. L.; Ross, J. R. H. and Van Veen, G. Preparation of catalysts II, studies in surface science catalysis. Vol. 3, edited by Delmon, B.; Grange, P.; Jacobs, P. A. and Poncelet, G. Elsevier, Amsterdam, 1979 p.143.
- 49 Lwin, Y.; Yarmo, M. A.; Yaakob, Z.; Mohamad, A. B. and Daud, W. R. W. Synthesis and characterization of Cu-Al layered double hydroxides. Mater. Res. Bull. 36 (2001): 193-198. CuAl
- 50 Fornasari, G.; Gazzano, M.; Matteuzzi, D.; Trifirò, F. and Vaccari, A. Structure and reactivity of high-surface-area Ni/Mg/Al mixed oxides. Appl. Clay Sci. 10 (1995): 69-82.
- 51 Alejandre, A.; Medina, F.; Salagre, P.; Correig, X. and Sueiras, J. E. Preparation and study of Cu-Al mixed oxides via hydrotalcite-like precursors. Chem. Mater. 11 (1999): 939-948.
- 52 Yu, J. J.; Jiang, Z.; Zhu, L.; Ping Hao, Z. and Xu, P. Adsorption/desorption studies of NO_x on well-mixed oxides derived from Co-Mg/Al hydrotalcite-like compounds. J. Phys. Chem. B 110 (2006): 4291-4300.
- 53 Kang, M.; Park, E. D.; Kim, J. M. and Yie, J. E. Manganese oxide catalysts for NO_x reduction with NH₃ at low temperatures. Appl. Catal. A: Gen. 327 (2007): 261-269.
- 54 Zhang, X. Y.; Pope, M. T.; Chance, M. R. and Jameson, G. H. High-valent manganese in polyoxotungstates-1. Manganese(IV) Keggin derivatives.

- Polyhedron 14 (1995): 1381-1392.
- 55 Dula, R.; Janik, R.; Machej, T.; Stoch, J.; Grabowski, R. and Serwicka, E.M. Mn-containing catalytic materials for the total combustion of toluene: The role of Mn localization in the structure of LDH precursor. Catal. Today 119 (2007): 327-331.
- 56 Wang, X.; Li, Y. Hydrothermal reduction route to Mn(OH)₂ and MnCO₃ nanocrystals. Materials Chemistry and Physics 82 (2003): 419-422.
- 57 García-García, J. M.; Pérez-Bernal, M. E.; Ruano-Casero, R. J. and Rives, V. Chromium and yttrium-doped magnesium aluminum oxides prepared from layered double hydroxides Solid State Sciences 9 (2007) 1115-1125.
- 58 Raid, M. Influence of magnesium and chromium oxides on the physicochemical properties of γ -alumina. Appl. Catal. A: Gen. 327 (2007): 13-21.
- 59 Rives, V.; Ulibarri, M. A. and Montero, A. Application of temperature-programmed reduction to the characterization of anionic clays. Appl. Clay Sci. 10 (1995): 83-93.
- 60 Biswick, T.; Jones, W.; Pacula, A. and Serwicka, E. Synthesis, characterisation and anion exchange properties of copper, magnesium, zinc and nickel hydroxy nitrates. J. Solid State Chem. 179 (2006): 49-55.
- 61 Lu, Y.; Wei, M.; Yang, L. and Li, C. Synthesis of layered cathode material Li[CoxMn_{1-x}]O₂ from layered double hydroxides precursors. J. Solid State Chem. 180 (2007): 1775-1782.
- 62 Weast, R. C. CRC Handbook of Chemistry and Physics, 58th, Edition, CRC Press, Boca Raton, Cleveland, 1977.
- 63 Marchi, A. J. and Apesteguía, C. R. Impregnation-induced memory effect of thermally activated layered double hydroxides. Appl. Clay Sci. 13 (1998): 35-48.
- 64 Nowinska, K.; Sopa, M.; Waclaw, A. and Szuba, D. Transition metal modified lacunary heteropoly compounds as catalysts for oxidation of light paraffins. Appl. Catal. A: Gen. 225 (2002): 141-151.
- 65 Shylesh, S.; Samuel, P. P. and Singh, A. P. Chromium-containing small pore mesoporous silicas: synthesis, characterization and catalytic behavior in the liquid phase oxidation of cyclohexane. Appl. Catal. A: Gen. 318 (2007): 128-

- 136.
- 66 Hermans, I.; Peeters, J. and Jacobs, P. A. Autoxidation of ethylbenzene: The Mechanism Elucidated. J. Org. Chem. 72 (2007): 3057-3064.
- 67 Singh, P. S.; Kosuge, K.; Ramaswamy, V. and Rao, B. S. Characterization of MeAPO-11s synthesized conventionally and in the presence of fluoride ions and their catalytic properties in the oxidation of ethylbenzene. Appl. Catal. A: Gen. 177 (1999): 149-159.
- 68 Pope, M. T. Heteropoly and isopoly oxometalates; Springer, Berlin, 1983 Pope, M. T.; Polyoxometalates: From Platonic Solids to Ant-Retro Viral Activity; Müller, A., Eds.; Kluwer Academic Publishers: Dordrecht, The Netherlands, 1994.
- 69 Mizuno, N.; Nozaki, C.; Hirose, T.; Tateishi, M. and Iwamoto, M. Liquid-phase oxygenation of hydrocarbons with molecular oxygen catalyzed by Fe₂Ni-substituted Keggin-type. J. Mol. Catal. A: Chem. 117 (1997): 159-168.
- 70 Lee, K.Y.; Mizuno, N.; Okuhara, T. and Misono, M. Catalysis by heteropoly compounds. 13, Bull. Chem. Soc. Jpn. 62 (1989): 1731.
- 71 Bardin, B. B.; Bordawekar, S. V.; Neurock, M. and Davis R. J. Acidity of Keggin-type heteropolycompounds evaluated by catalytic probe reactions, sorption microcalorimetry, and density functional quantum chemical calculations. J. Phys. Chem. B 102 (1998): 10817-10825.
- 72 Kim, Y. S.; Wang, F.; Hickne, M.; Zawodzinski, T. A. and McGrath, J. E., Organic silica/nafiction® composite membrane for direct methanol fuel cells. J. Membr. Sci. 212 (2003): 263-282.
- 73 Bardin, B. B. and Davis, R. J. Characterization of copper and vanadium containing heteropolyacid catalysts for oxidative dehydrogenation of propane. Appl. Catal. A: Gen. 185 (1999): 283-292.
- 74 Duclausaud, H. and Borshch, S. A. Iron-molybdenum electron delocalization in substituted Keggin polyoxoanions. Inorg. Chem. 38 (1999): 3489-3493.
- 75 Misono, M.; Ono, I.; Koyano, G. and Aoshima, A. Heteropolyacids versatile green catalysts usable in a variety of reaction media. Pure Appl. Chem. 72 (2000): 1305-1311.
- 76 Neumann, R.; Kenkin, A. M.; Juwiler, D.; Miller, H. and Gara, M. Catalytic oxidation with hydrogen peroxide catalyzed by 'sandwich' type transition metal

- substituted polyoxometalates. *J. Mol. Catal. A: Chem.* 117 (1997): 169-183.
- 77 Yang, J. I.; Lee, D.; Lee, J.; Hyun, J. C. and Lee, K. Selective and high catalytic activity of $CsnH4-nPMo11VO40$ ($n \geq 3$) for oxidation of ethanol. *Appl. Catal. A: Gen.* 194-195 (2000): 123-127.
- 78 Matsumoto, Y.; Asami, M.; Hashimoto, M. and Misono, M. Alkane oxidation with mixed addenda heteropoly catalysts containing Ru(III) and Rh(III). *J. Mol. Catal. A: Chem.* 114 (1996): 161-168.
- 79 Langpape, M. and Millet, J. M. Effect of iron counter ions on the redox properties of the Keggin-type molybdophosphoric heteropolyacid: part I. An experimental study on isobutane oxidation. *Appl. Catal. A: Gen.* 200 (2000): 89-101.
- 80 Balula, M. S. S.; Santos, I. C. M. S.; Simões, M. M. Q.; Neves, M. G. P. M. S.; Cavaleiro, J. A. S. and Cavaleiro, A. M. V. A comparative study between Keggin-type tungstophosphates and tungstosilicates in the oxidation of cyclooctane with hydrogen peroxide. *J. Mol. Catal. A: Chem.* 222 (2004): 159-165.
- 81 Li, X.; Jing, Z.; Ji, W.; Zhang, Z.; Chen, Y.; Au, C.; Han, S. and Hibst, H. Effect of vanadium substitution in the cesium salts of Keggin-type heteropolyacids on propane partial oxidation. *J. Catal.* 237 (2006): 58-66.
- 82 Atlamsani, A. and Breeault, J. M. Oxidation of 2-methylcyclohexanone and cyclohexanone by dioxygen catalyzed by vanadium-containing heteropolyanions. *J. Org. Chem.* 58 (1993): 5663-5665.
- 83 Etienne, E.; Cavani, F.; Mezzogori, R.; Trifirò, G.; Calestani, G.; Gengembre, L. and Guelton, M. Chemical-physical characterization of Fe-doped, Keggin-type P/Mo polyoxometalates, catalysts for the selective oxidation of isobutane to methacrylic acid. *Appl. Catal. A: Gen.* 256 (2003): 275-290.
- 84 Kholdeeva, O. A.; Vanina, M. P.; Timofeeva, M. N.; Maksimovskaya, R. I.; Trubitsina, T. A.; Melgunov, M. S.; Burgina, E. B.; Mrowiec-Bialon, J.; Jarzebski, A. B. and Hill, C. L. Co-containing polyoxometalate-based heterogeneous catalysts for the selective aerobic oxidation of aldehydes under ambient condition. *J. Catal.* 226 (2004): 363-371.
- 85 Oxana, A. K.; Maksimov, G. M.; Maksimovskaya, R. I.; Vanina, M. P.; Trubitsina, T. A.; Naumov, D. Y.; Kolesov, B. A.; Antonova, N. S., Carbo, J. J.

- and Roblet, J. M. ZrIV-monosubstituted Keggin-type dimeric polyoxometalates: synthesis, characterization, catalysis of H₂O₂-base oxidations, and theoretical study. *Inorg. Chem.* 45 (2006): 7224-7234.
- 86 www.sriconsulting.com. March 2008.
- 87 Mizuno, N.; Kiyoto, I.; Nozaki, C. and Misono, M. Remarkable structure dependence of intrinsic catalytic activity for selective oxidation of hydrocarbons with hydrogen peroxide catalyzed by iron-substituted silicotungstates. *J. Catal.* 181 (1999): 171-174.
- 88 Langpape, M.; Millet, J. M. M.; Uzkan, U. S. and Boudeulle, M. Study of cesium or cesium-transition metal-substituted Keggin-type phosphomolybdic acid as isobutane oxidation catalysts. I. Structural characterization. *J. Catal.* 181 (1999): 80-90.
- 89 Okuhara, T.; Watanabe, H.; Nishimura, T.; Inumaru, K. and Misono, M. Microstructure of cesium hydrogen salts of 12-tungstophosphoric acid relevant to novel acid catalysis. *Chem. Mater.* 12 (2000): 2230-2238.
- 90 Bonchio, M.; Carraro, M.; Farinazzo, A.; Sartorel, A.; Scorrano, G. and Körtz, U. Aerobic oxidation of cis-cyclooctene by iron-substituted polyoxotungstates: evidence for a metal initiated auto-oxidation mechanism. *J. Mol. Catal. A: Chem.* 262 (2007): 36-40.
- 91 Mirkhani, V.; Moghadam, M.; Tangestaninejad, S.; Mohammadpoor-Baltork, I. and Nahid, R. Oxidation of alkanes with hydrogen peroxide catalyzed by Schiff base complexes covalently anchored to polyoxometalate. *Catal. Commun.* 9 (2008): 2171-2124.
- 92 Deltcheff-R, C.; Fournier, M.; Franck, R.; and Thouvenot, R. Vibration investigations of polyoxometalates. 2. Evidence for anion-anion interactions in molybdenum (VI) and tungsten (VI) compounds related to Keggin structure. *Inorg. Chem.* 22 (1983): 207-216.
- 93 Yori, J. C.; Grau, J. M. Benítez, V. M. and Sepúlveda, J. Hydroisomerization-cracking of n-octane on heteropolyacid H₃PW₁₂O₄₀ supported on ZrO₂, SiO₂ and carbon effect of Pt incorporation on catalyst performance. *Appl. Catal. A: Gen.* 286 (2005): 71-78.
- 94 Silviani, E.; and Burns, R. C. Synthesis and characterization of soluble alkali metal, alkaline earth metal and related Keggin-type [PMo₁₂O₄₀]³⁻ salts for

- heterogeneous catalysis reactions. J. Mol. Catal. A: Chem. 219 (2004): 327-342.
- 95 Ueda, T.; Komatsu, M.; and Hojo, M. Spectroscopic and voltammetric studies on the formation of Keggin type V(V)-substituted tungstoarsenate (V) and –phosphate (V) complexes in aqueous and aqueous-organic solutions. Inorg. Chem. Acta 344 (2003): 77-84.
- 96 Simoes, M. M. Q.; Santos, I. C. M. S.; Balula, M. S. S.; Gamelas, J. A. F.; Cavaleiro, A. M. V.; Neves, G. P. M. S.; Cavaleiro, J. A. S. Oxidation of cycloalkanes with hydrogen peroxide in the presence of Keggin-type polyoxotungstates. Catal. Today 91-92 (2004): 211-214.
- 97 Guo, Y. and Hu, C. Heterogeneous photo catalysis by solid polyoxometalates. J. Mol. Catal. A: Chem. 262 (2007): 136-148.
- 98 Limburg, J.; Vrettos, J. S.; Liable-Sands, L. M.; Rheingold, A. L.; Crabtree, R.H. and Brudvig, G.W. A Functional model for O-O bond formation by the O₂-evolving complex in photosystem II. Science 283 (1999): 1524-1527.
- 99 Gamelas, J. A.; Santos, I. C. M. S.; Freire, C.; Castro, B. and Cavaleiro, A. M. V. EPR and electronic spectroscopic studies of Keggin type undecatungstophosphocuprate(II) and undecatungstoborocuprate(II). Polyhedron 18 (1999): 1163-1169.
- 100 Zhou, G.; Yang, X.; Liu, J.; Zhen, K.; Wang, H. and Cheng, T. Structure and catalytic properties of magnesia-supported copper salts of molybdovanadophosphoric acid. J. Phys. Chem. B 110 (2006): 9831-9837.
- 101 Fournier, M.; Franck, R. and Thouvenot, R. Vibrational investigations of polyoxometalates. 2. evidence for anion-anion interactions in molybdenum(VI) and tungsten(VI) compounds related to the Keggin structure. Inorg. Chem. 22 (1983): 207-216.
- 102 Gamelas, J. A. F.; Cavaleiro, A. M. V.; Freire, C. and Castro, B. Synthesis and characterization of polyoxotungstates compounds with complex copper and cobalt cations. J. Coord. Chem. 54 (2001): 35-51.
- 103 Gamelas, J. A. F.; Soares, M. R.; Ferreira, A. and Cavaleiro, A. M. V. Polymorphism in tetra-butylammonium salts of Keggin-type polyoxotungstates. Inorg. Chim. Acta 342(2003):16-22.
- 104 Zhu, W.; Li, H.; He, X.; Zhang, Q.; Shu, H. and Yan, Y. Synthesis of adipic acid catalyzed by surfactant-type peroxotungstates and peroxomolybdates. Catal.

- Commun. 9 (2008): 551-555.
- 105 Tian, P.; Liu, Z.; Wu, Z.; Xu, L. and He, Y. Characterization of metal-containing molecular sieves and their catalytic properties in the selective oxidation of cyclohexane. Catal. Today 93–95 (2004): 735-742.
- 106 Wang, J.; Yan, L.; Li, G.; Wang, X.; Ding, Y., Suo, J. Mono-substituted Keggin-polyoxometalate complexes as effective and recyclable catalyst for the oxidation of alcohols with hydrogen peroxide in biphasic system. Tett. Lett. 46 (2005): 7023-7027.
- 107 Weng, Z. H.; Wang, J. Y. and Jian, X. G. Efficient Oxidation of Benzyl Alcohol with Heteropolytungstate as Reaction-Controlled Phase-Transfer. Catal. Chin. Chem Lett. 18 (2007): 936-938.
- 108 Egusquiza, M. G.; Romanelli, G. P.; Cabello, C. I.; Botto, I. L. and Thomas, H. J. Arene and phenol oxidation with hydrogen peroxide using ‘sandwich’ type substituted polyoxometalates as catalysts. Catal. Commun. 9 (2008): 45-50.
- 109 Ilkenhans, T.; Herzog, B.; Braun, T. and Schlogl, R. The nature of the active phase in the heteropolyacid catalyst $H_4PVMo_{11}O_{40} \cdot 32H_2O$ used for the selective oxidation of isobutyric acid. J. Catal. 153 (1995): 275-292.
- 110 Alekar, N. A.; Indira, V.; Halligudi, S. B.; Srinivas, D.; Gopinathan, S. and Gopinathan, C. Kinetics and mechanism of selective hydroxylation of benzene catalysed by vanadium substituted heteropolymolybdates. J. Mol. Catal. A: Chem. 164 (2000): 181-189.
- 111 Neumann, R. and Levin-Elad, M. Vanadium silicate xerogels in hydrogen peroxide catalyzed oxidations. Appl. Catal. A: Gen. 122 (1995): 85-97.
- 112 Jin, R.; Li, H. and Deng, J. Selective oxidation of cyclopentene to glutaraldehyde by H_2O_2 over the WO_3/SiO_2 catalyst. J. Catal. 203 (2001): 75-81.
- 113 Ribeiro, M. L. and Schuchardt, U. Cooperative effect of cobalt acetylacetonate and silica in the catalytic cyclization and oxidation of fructose to 2,5-furandicarboxylic acid. Catal. Commun. 4 (2003): 83-86.
- 114 Daparkar, S. E.; Sakthivel, A. and Selvam, P. Mesoporous VMCM-41: highly efficient and remarkable catalyst for selective oxidation of cyclohexane to cyclohexanol. J. Mol. Catal. A: Chem. 223 (2004): 241-250.
- 115 Zhou, L.; Xu, J.; Miao, H., Wang, F. and Li, X. Catalytic oxidation of cyclohexane to cyclohexanol and cyclohexanone over Co_3O_4 nanocrystals with

- molecular oxygen. Appl. Catal. A: Gen. 292 (2005): 223-228.
- 116 Anand, R.; Hamdy, M. S.; Gkourgkoulas, P.; Maschmeyer, T.; Jansen, J. C. and Hanefeld, U. Liquid phase oxidation of cyclohexane over transition metal incorporated amorphous 3D-mesoporous silicates. Catal. Today 117 (2006): 279-283.
- 117 Ebadi, A.; Safari, N. and Peyrovi, M. H. Aerobic oxidation of cyclohexane with γ -alumina supported metallophthalocyanines in the gas phase. Appl. Catal. A: Gen. 321 (2007): 135-139.
- 118 Reddy, S. S.; Raju, B. D.; Padmasri, A. H.; Prakash, P. K. S. and Rao, K. S. R. Novel and efficient cobalt encapsulated SBA-15 catalysts for the selective oxidation of cyclohexane. Catal. Today 141 (2009): 61-65.
- 119 Chen, C.; Qiaohong, Z.; Hong, M.; Jin, G.; Zhiqiang, S. and Jie1, X. Catalytic activity of Co-HMS modified by organic groups for cyclohexane oxidation. Chinese J. Catal. 29 (2008): 4-6.
- 120 Cruz, S. R.; Silva, J. M. S.; Arnold, U. and Schuchardt, U. Catalytic activity and stability of a chromium containing delicate in liquid phase cyclohexane oxidation. J. Mol. Catal. A: Chem. 171 (2001): 251-257.
- 121 Rogovin, M. and Neumann, R. Silicate xerogels containing cobalt as heterogeneous catalysts for the side-chain oxidation of alkyl aromatic compounds with *tert*-butyl hydroperoxide. J. Mol. Catal. A: Chem. 138 (1999): 315-318.
- 122 Barbosa, G. N. and Oliveira, H. P. Synthesis and characterization of V_2O_5 - SiO_2 xerogel composites prepared by base catalysed sol-gel method. J. Non-Cryst. Solids 352 (2006): 3009-3014.
- 123 Dunn, B. C.; Covington, D. J.; Cole, P.; Pugmire, R. J.; Meuzelaar, H. L. C.; Ernst, R. D.; Heider, E. C. and Eyring, E. M. Silica xerogel supported cobalt metal Fischer-Tropsch catalysts for syngas to diesel range fuel conversion. Energy & Fuels 18 (2004): 1519-1521.
- 124 Gómez-Guzmán, O.; Martínez-Flores, J. O.; Mayen-Mondragón, R. and Yáñez-Limón, J. M. Synthesis, characterization and local changes induced by argon laser in silica glass xerogel doped with transition metal ions. J. Non-Cryst. Solids 352 (2006): 3437-3443.
- 125 Cruz, R. S.; Silva, J. M. de S.; Arnold, U.; Sercheli, M. S. and Schuchardt, U.

- Copper containing silicates as catalysts for liquid phase cyclohexane oxidation. J. Braz. Chem. Soc. 13 (2002): 170-176.
- 126 Neumann, R. and Levin-Elad, M. Metal oxide (TiO_2 , MoO_3 , WO_3) substituted silicate xerogels as catalysts for the oxidation of hydrocarbons with hydrogen peroxide. J. Catal. 166 (1997): 206-217.
- 127 Kumar, R.; Sithambaram, S. and Suib, S. L. Cyclohexane oxidation catalyzed by manganese oxide octahedral molecular sieves-Effect of acidity of the catalyst. J. Catal. 262 (2009): 304-313.
- 128 Lecloux, A. J. and Pirard, J. P. section 4. Catalysts, surface function high-temperature catalysts through sol-gel synthesis. J. Non-Cryst. Solids 225 (1998): 146-152.
- 129 Lambert, S.; Polard, J.; Pirard, J. and Heinrichs, B. Improvement of metal dispersion in Pd/SiO_2 cogelled xerogel catalysts for 1,2-dichloroethane hydrodechlorination. Appl. Catal. B: Environ. 50 (2004): 127-140.



ศูนย์วิทยทรัพยากร
จุฬาลงกรณ์มหาวิทยาลัย



ศูนย์วิทยทรัพยากร
จุฬาลงกรณ์มหาวิทยาลัย

APPENDIX A

Adsorption and desorption isotherm of LDH and mixed metal oxide

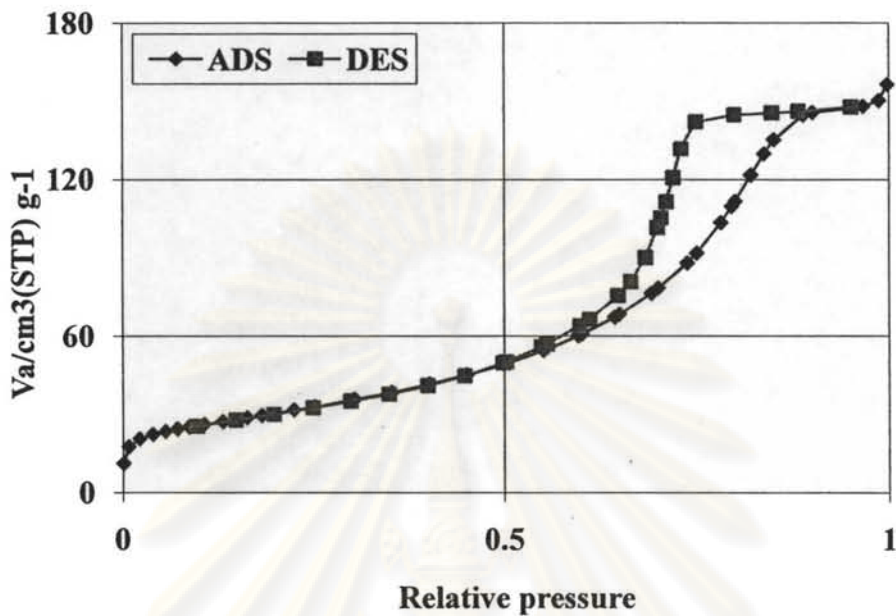


Figure A.1 Adsorption and desorption isotherm of the Ni_{4.8}Al LDH.

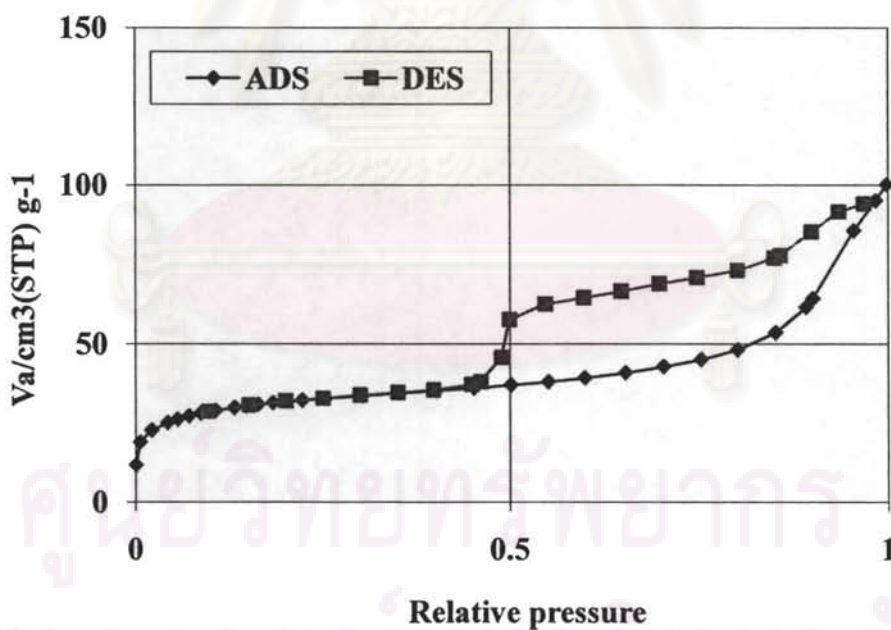


Figure A.2 Adsorption and desorption isotherm of the Cu_{1.0}Mg_{2.9}Al LDH.

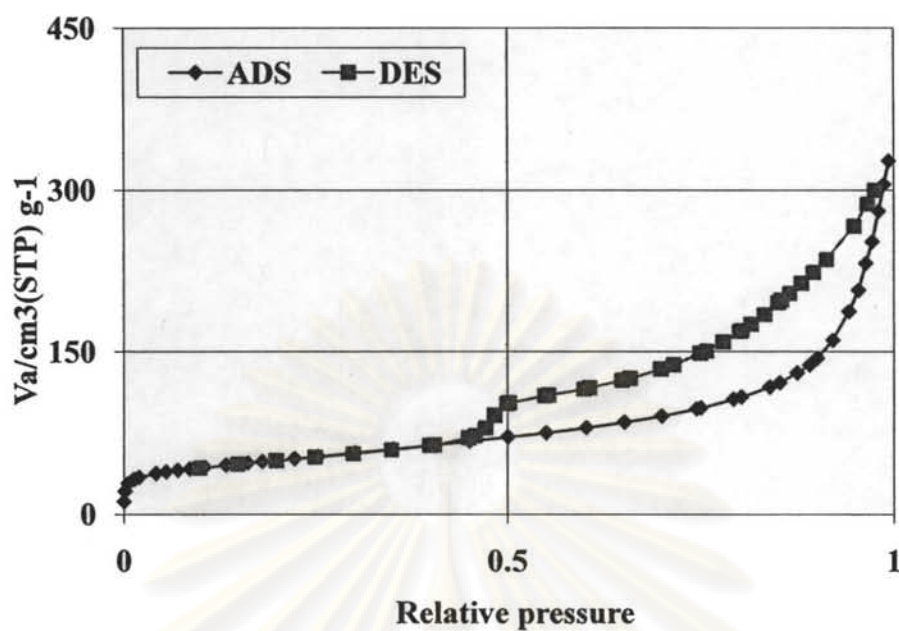


Figure A.3 Adsorption and desorption isotherm of the $\text{Cr}_{0.8}\text{Mg}_{2.4}\text{Al}$ LDH.

ศูนย์วิทยทรัพยากร
จุฬาลงกรณ์มหาวิทยาลัย

APPENDIX B

Fourier Transforms Infrared Spectroscopy (FTIR)

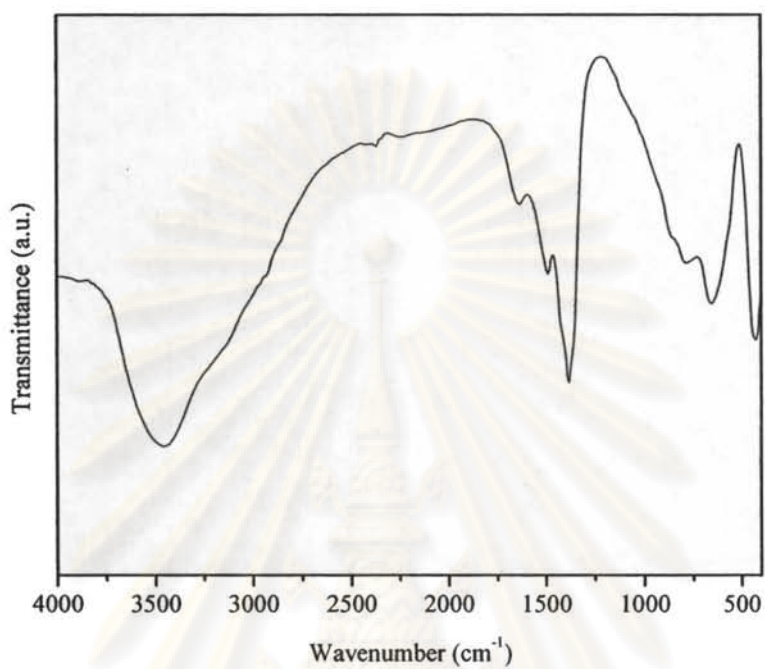


Figure B.1 FTIR spectrum of Ni_{4.9}Al LDH.

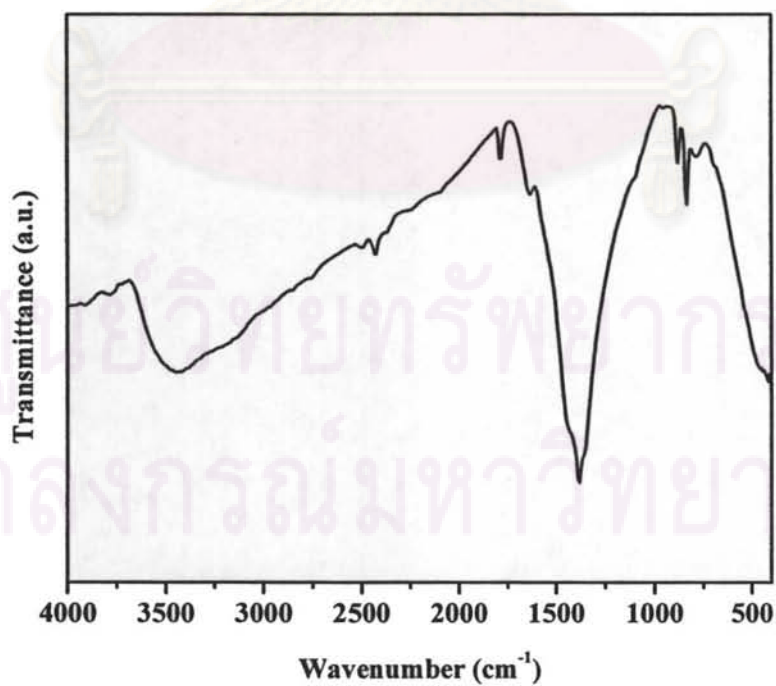


Figure B.2 FTIR spectrum of Co_{4.5}Al oxide.

APPENDIX C
X-ray diffraction (XRD)

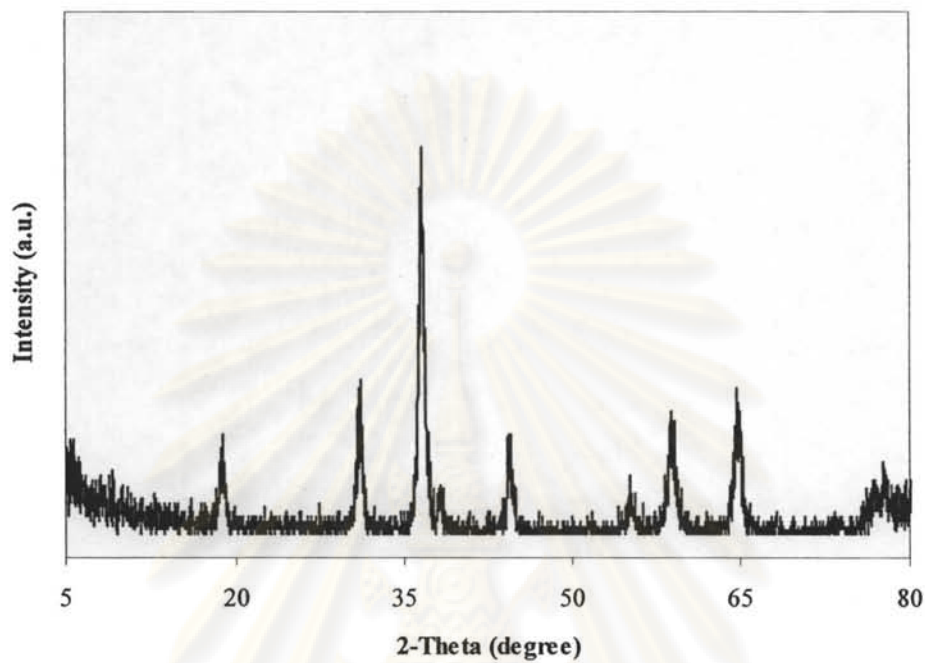


Figure C.1 XRD pattern of $\text{Co}_{4.8}\text{Cr}$ oxide.

ศูนย์วิทยทรัพยากร
จุฬาลงกรณ์มหาวิทยาลัย

APPENDIX D

Diffuse reflectance ultraviolet-visible spectroscopy (DRUV)

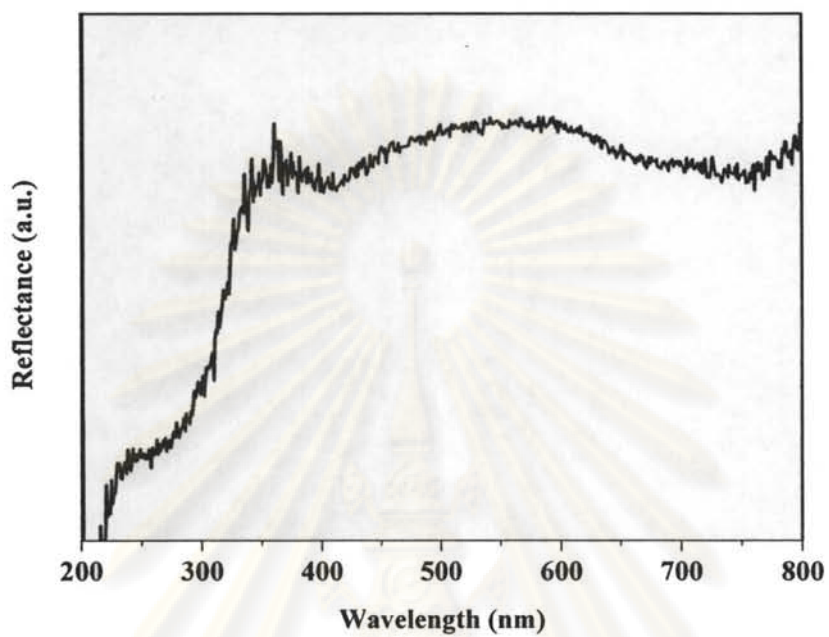


Figure D.1 DRUV spectra of Ni_{4.8}Al oxide.

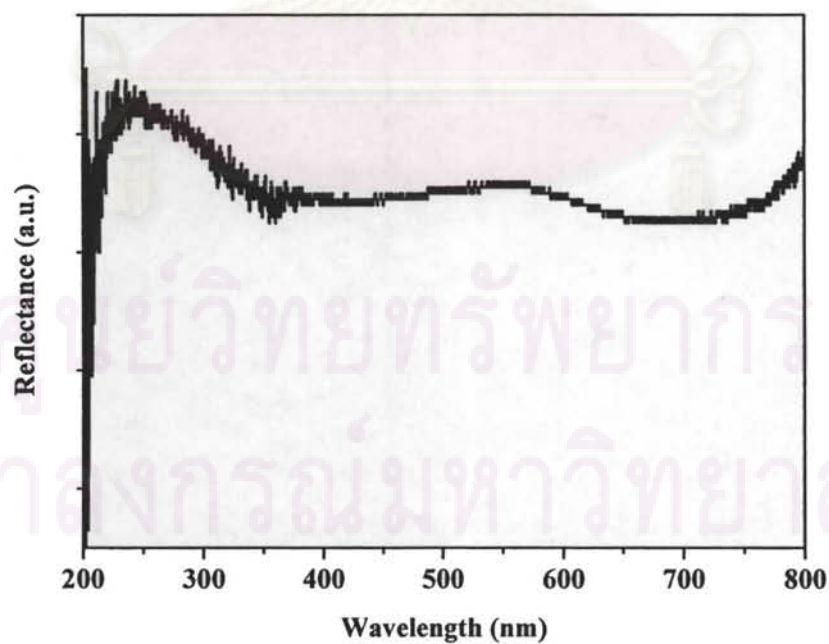


Figure D.2 DRUV spectra of Co_{4.5}Al oxide.

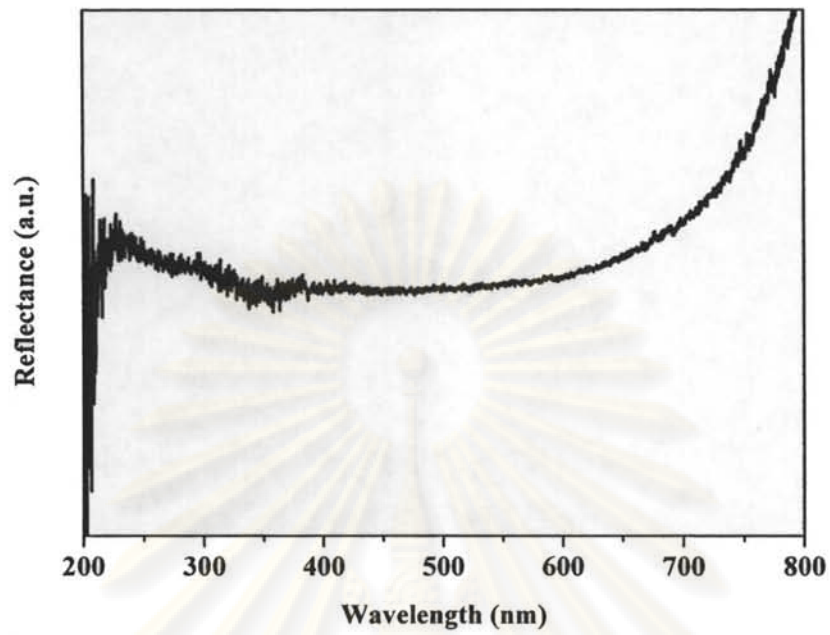


Figure D.3 DRUV spectra of $\text{Cu}_{4.9}\text{Al}$ oxide.

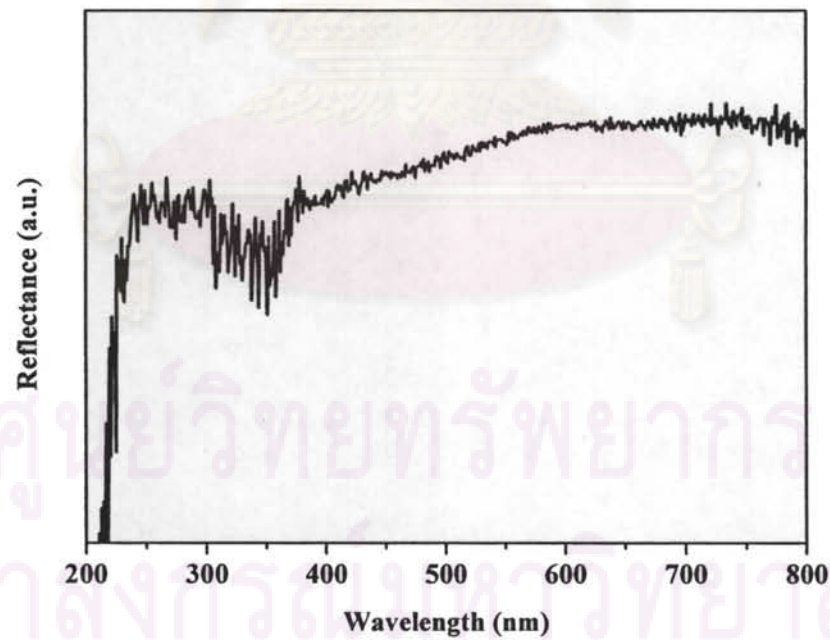


Figure D.4 DRUV spectra of $\text{Ni}_{5.1}\text{Cr}$ oxide.

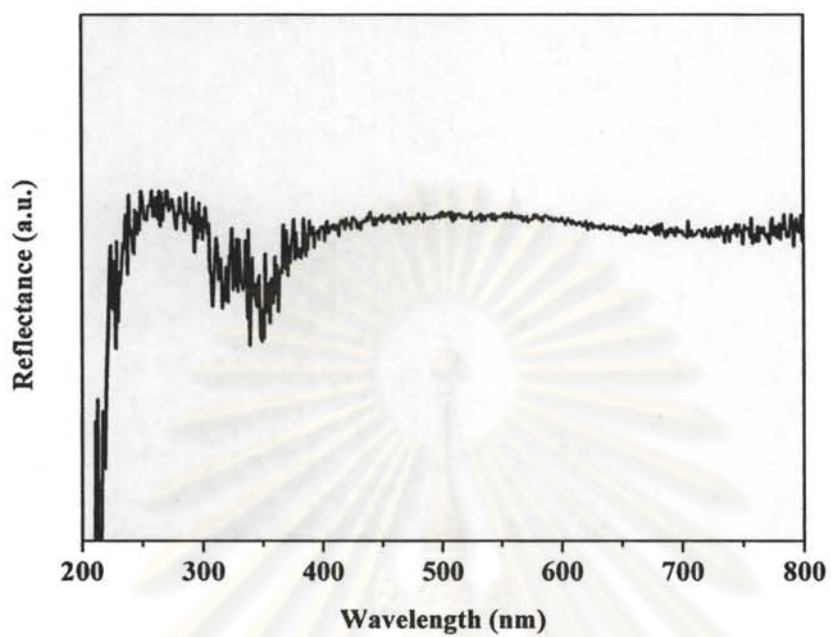


Figure D.5 DRUV spectra of $\text{Co}_{4.8}\text{Cr}$ oxide.

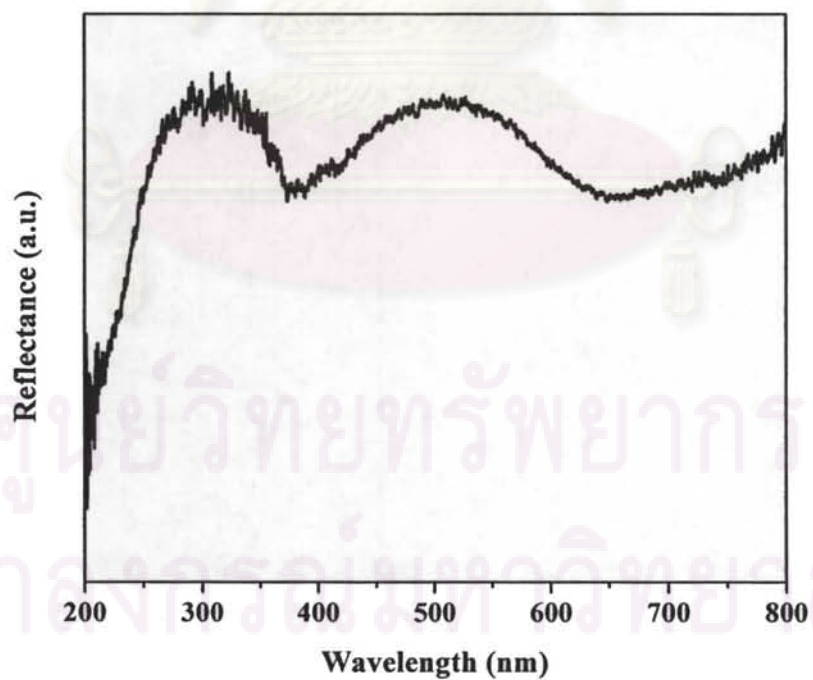


Figure D.6 DRUV spectrum of $\text{Ni}_{0.9}\text{Mg}_{2.1}\text{Al}$ oxide.

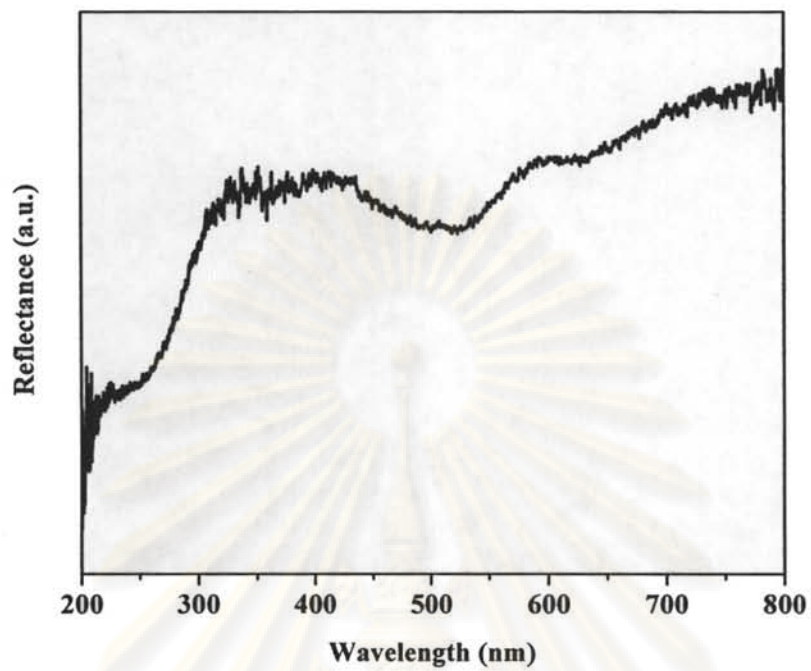


Figure D.7 DRUV spectrum of $\text{Co}_{0.8}\text{Mg}_{1.6}\text{Al}$ oxide.

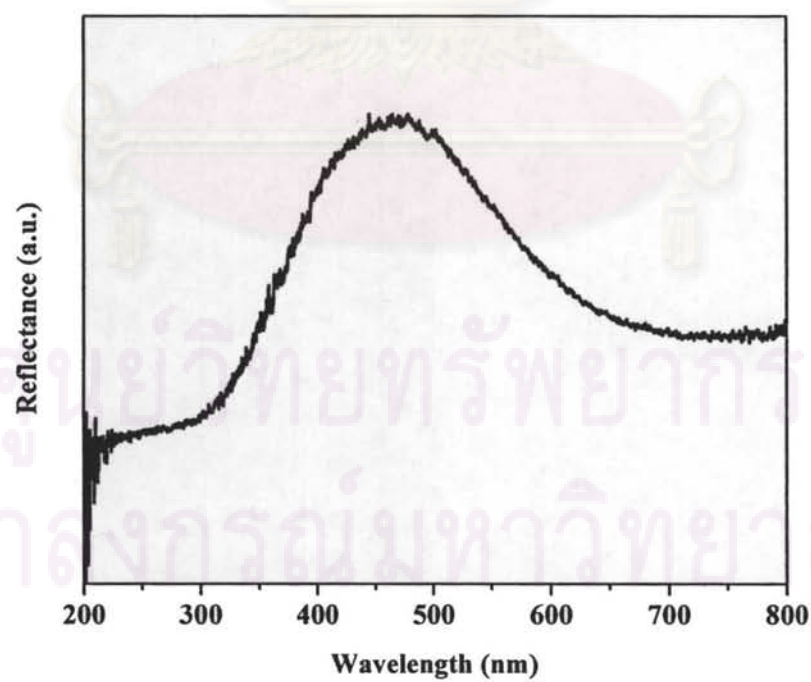


Figure D.8 DRUV spectrum of $\text{Cu}_{1.0}\text{Mg}_{2.9}\text{Al}$ oxide.

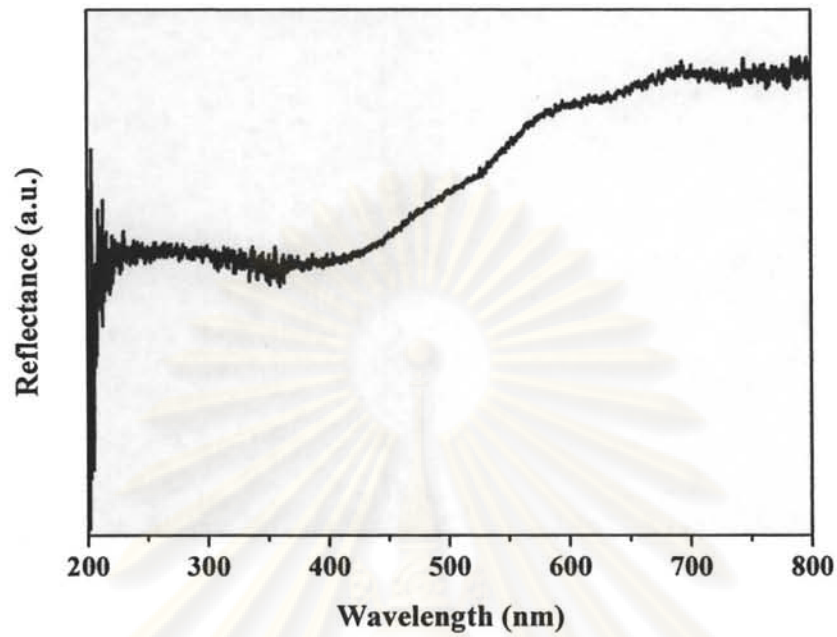


Figure D.9 DRUV spectrum of $\text{Mn}_{0.9}\text{Mg}_{2.2}\text{Al}$ oxide.

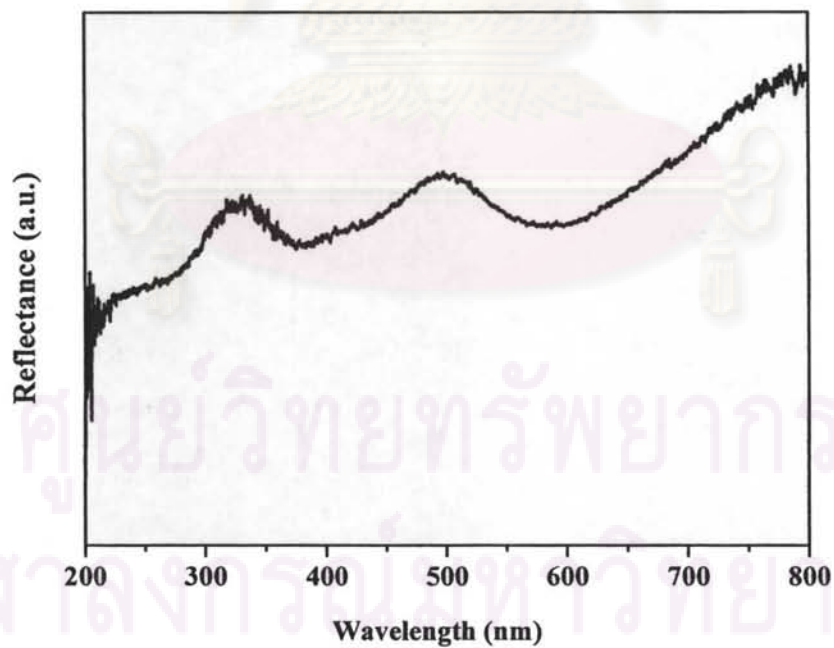


Figure D.10 DRUV spectra of $\text{Cr}_{0.8}\text{Mg}_{2.4}\text{Al}$ oxide.

APPENDIX E

PRODUCT ANALYSIS

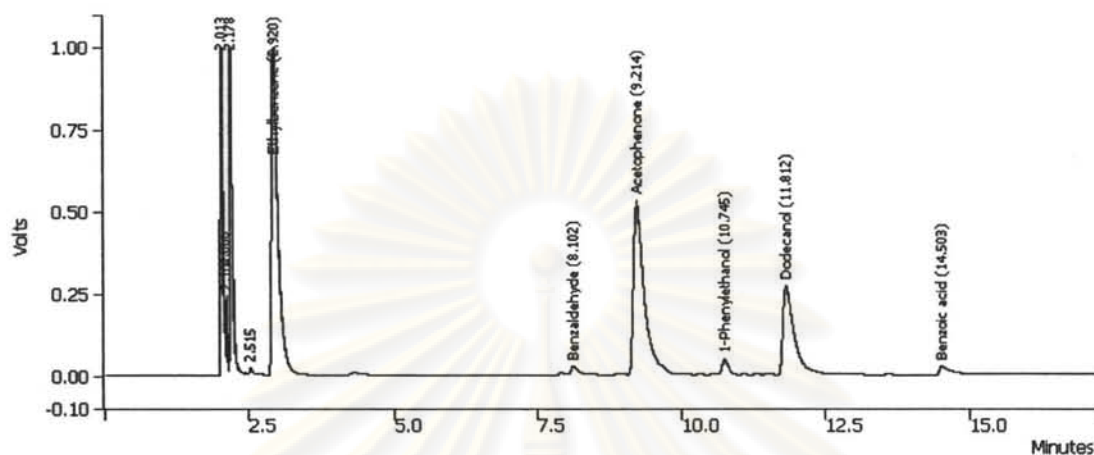


Figure E.1 GC diagram of ethylbenzene oxidation and their oxygenated products using $\text{Ni}_{4.8}\text{Al}$ oxide.

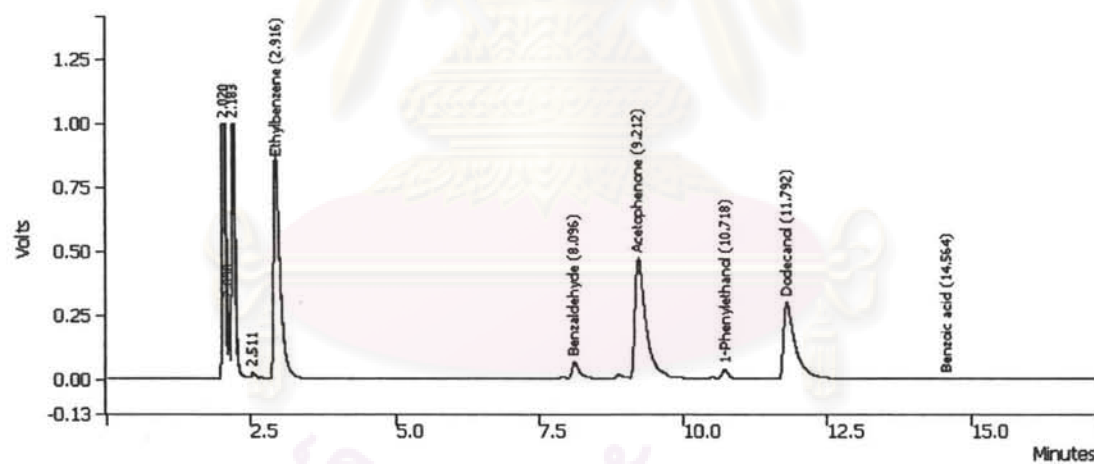


Figure E.2 GC diagram of ethylbenzene oxidation and their oxygenated products using $\text{Cu}_{1.0}\text{Mg}_{2.9}\text{Al}$ oxide.

จุฬาลงกรณ์มหาวิทยาลัย

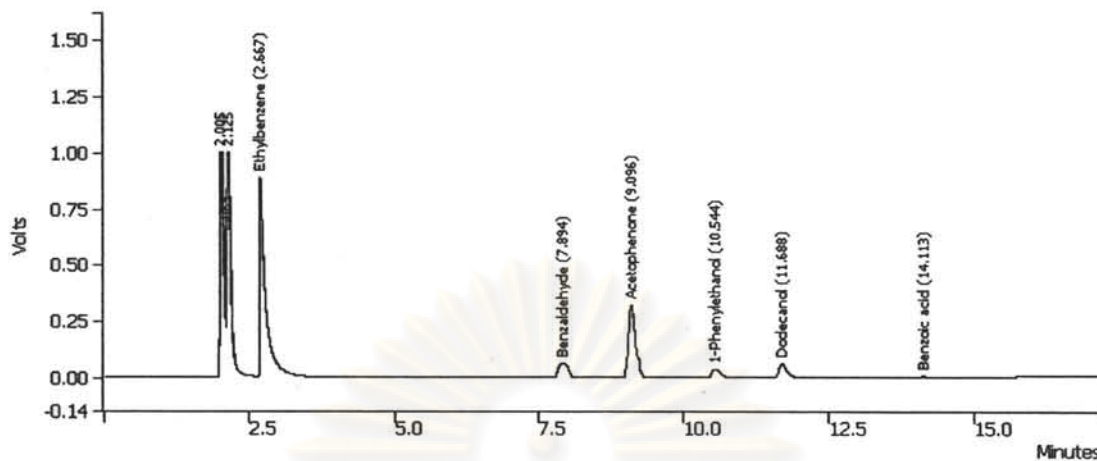


Figure E.3 GC diagram of ethylbenzene oxidation and their oxygenated products using $\text{Cu}_{1.0}\text{Mg}_{2.9}\text{Al}$ oxide in the presence of hydroquinone.

ศูนย์วิทยทรัพยากร
จุฬาลงกรณ์มหาวิทยาลัย

APPENDIX F

Soluble basicity

Table F.1 Soluble basicity of binary LDHs and mixed metal oxide catalysts

Catalyst	Basicity ($\mu\text{mol/g}$)
Ni _{5.0} Al LDH	42
Co _{5.0} Al LDH	39
Ni _{3.1} Al oxide	20
Ni _{4.8} Al oxide	48
Co _{4.5} Al oxide	43
Cu _{4.9} Al oxide	88
Mg _{4.9} Al oxide	125
Ni _{5.1} Cr oxide	55
Co _{4.8} Cr oxide	44
Mg _{4.9} Cr oxide	121

ศูนย์วิทยทรัพยากร
จุฬาลงกรณ์มหาวิทยาลัย

APPENDIX G

Fourier transform infrared spectroscopy (FTIR)

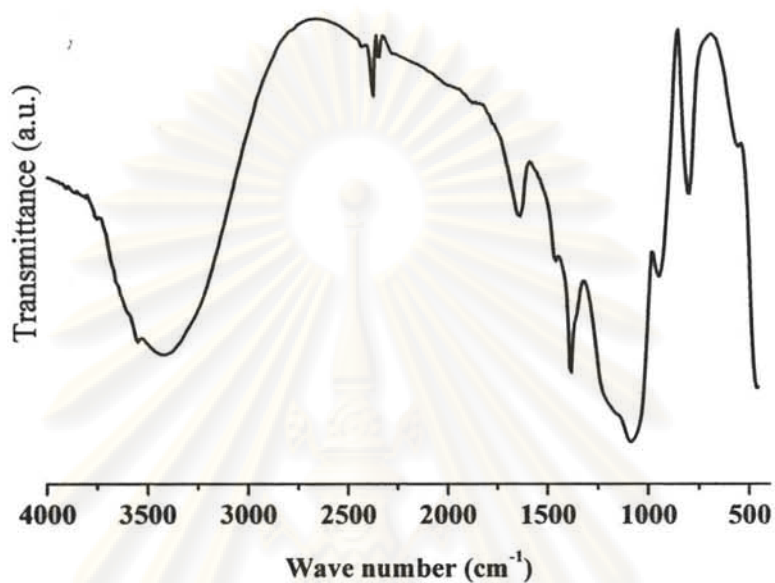


Figure G.1 FTIR spectrum of Ni(NO₃)₂-xerogel.

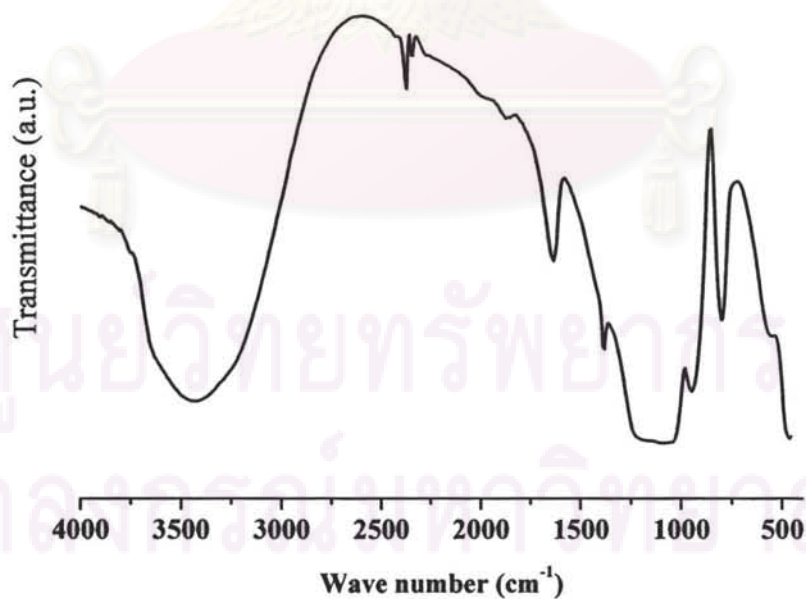


Figure G.2 FTIR spectrum of Cr(NO₃)₃-xerogel.

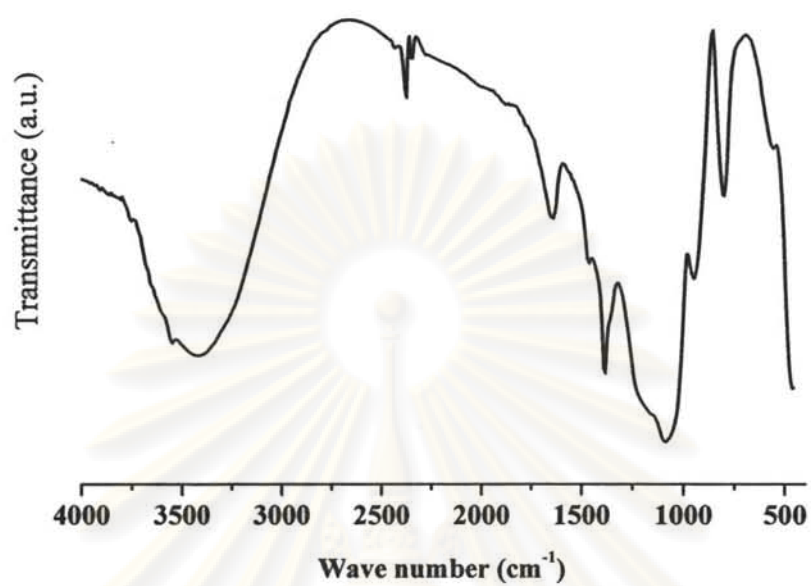


Figure G.3 FTIR spectrum of Mn(NO₃)₂-xerogel.

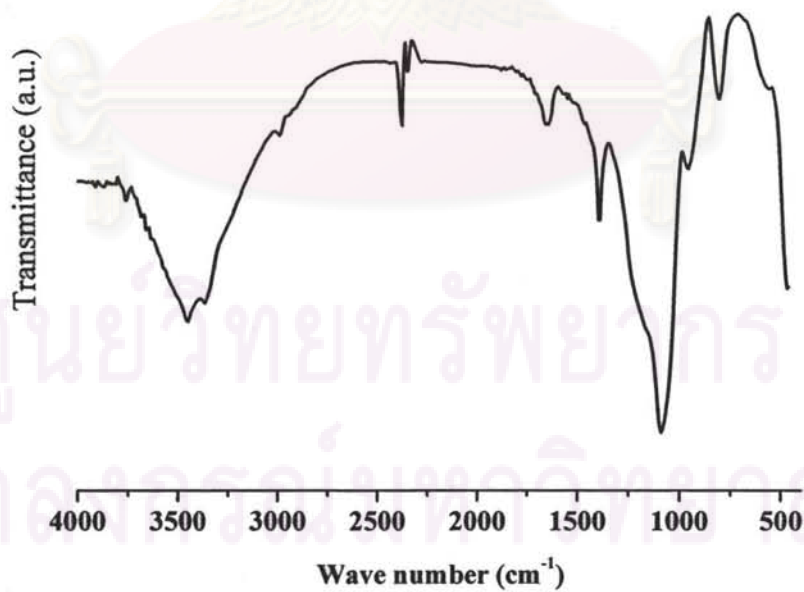


Figure G.4 FTIR spectrum of Cu(NO₃)₂-xerogel.

APPENDIX H

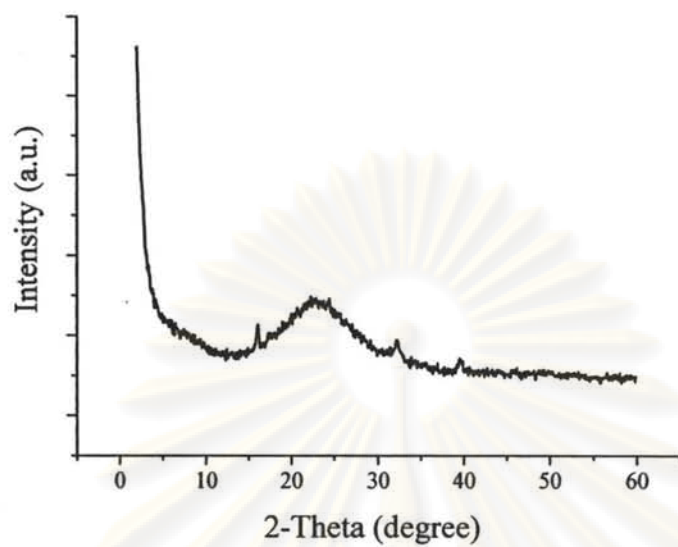


Figure H.1 XRD pattern of Cu(NO₃)₂-xerogel.

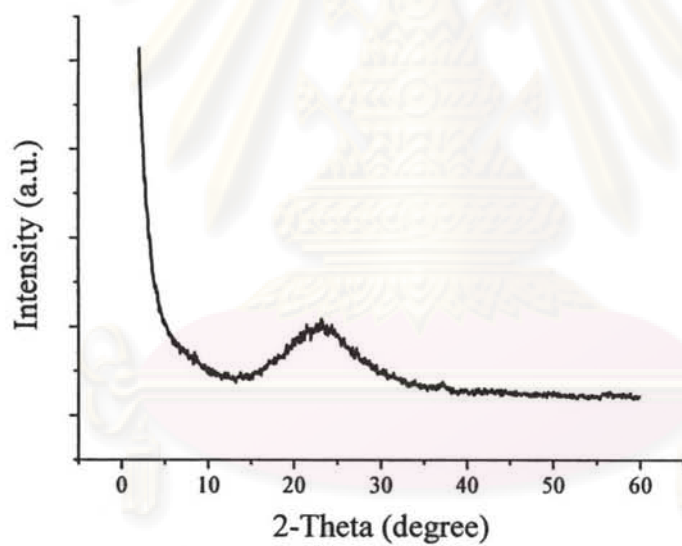


Figure H.2 XRD pattern of Ni(NO₃)₂-xerogel.

ศูนย์วิจัยทรัพยากร
จุฬาลงกรณ์มหาวิทยาลัย

APPENDIX I

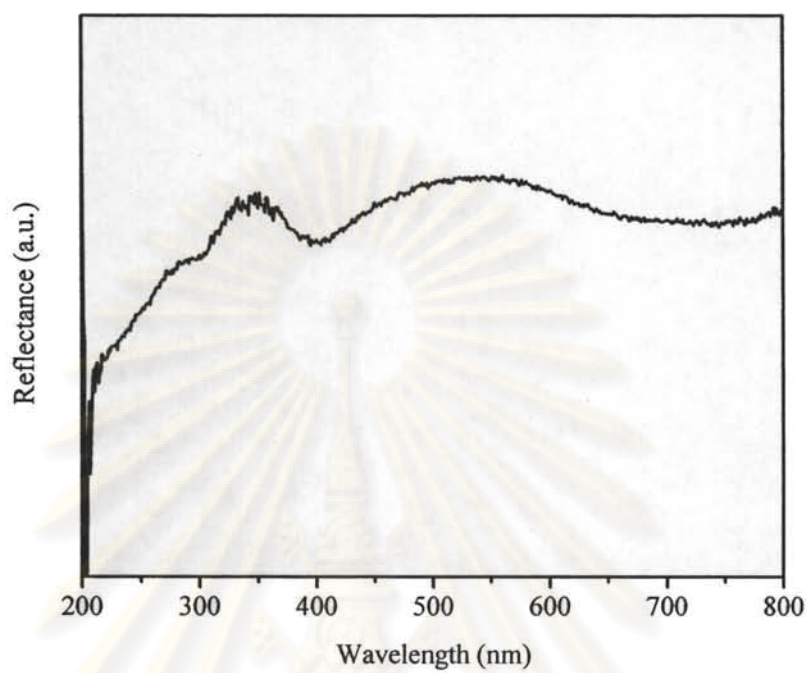


Figure I.1 DRUV spectrum of Ni(NO₃)₂-xerogel.

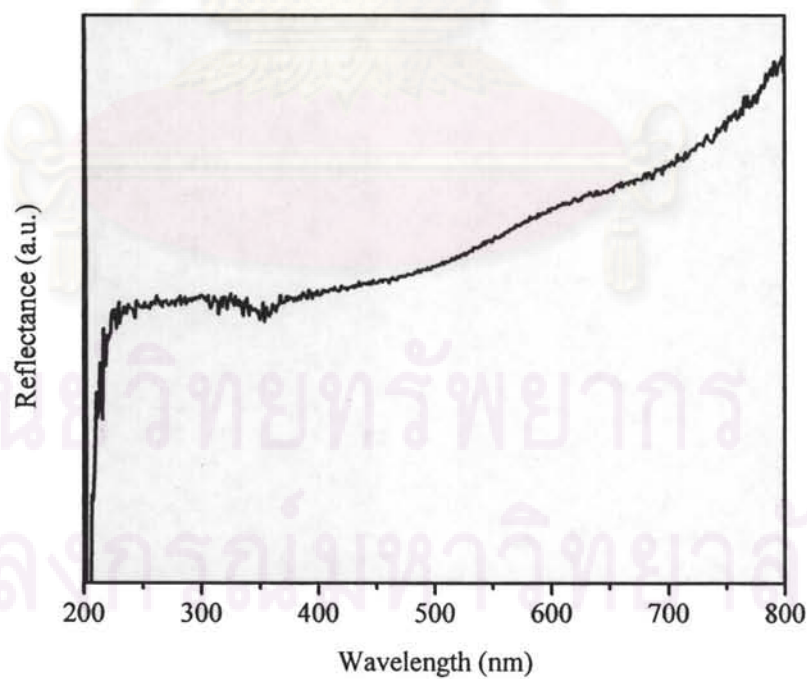


Figure I.2 DRUV spectrum of Cr(NO₃)₃-xerogel.

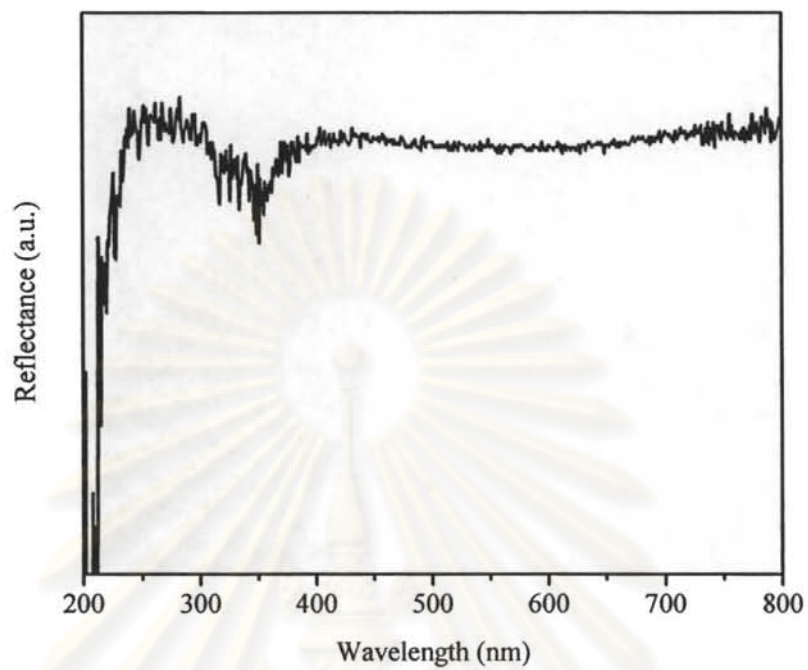


Figure I.3 DRUV spectrum of Mn(NO₃)₂-xerogel.

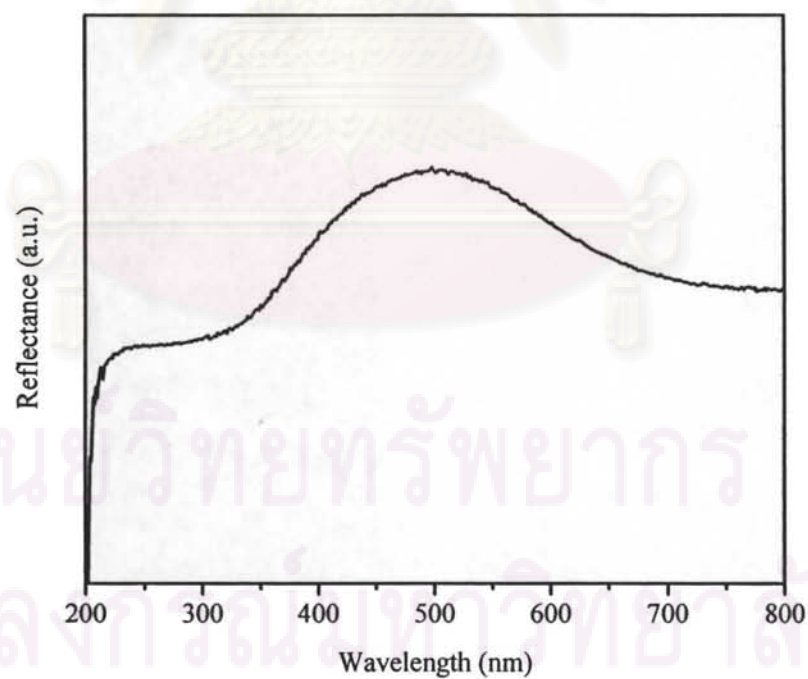


Figure I.4 DRUV spectrum of Cu(NO₃)₂-xerogel.

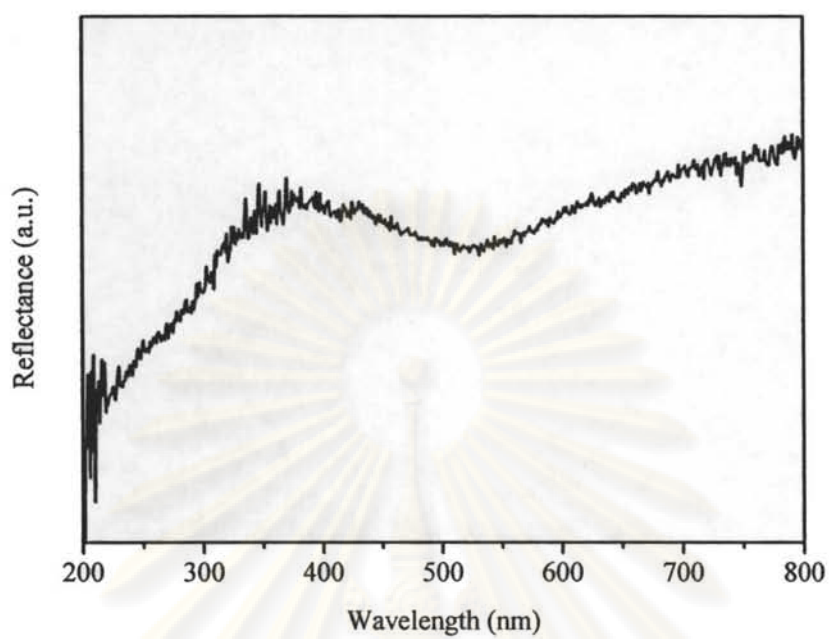


Figure I.5 DRUV spectrum of Co(NO₃)₂-xerogel.

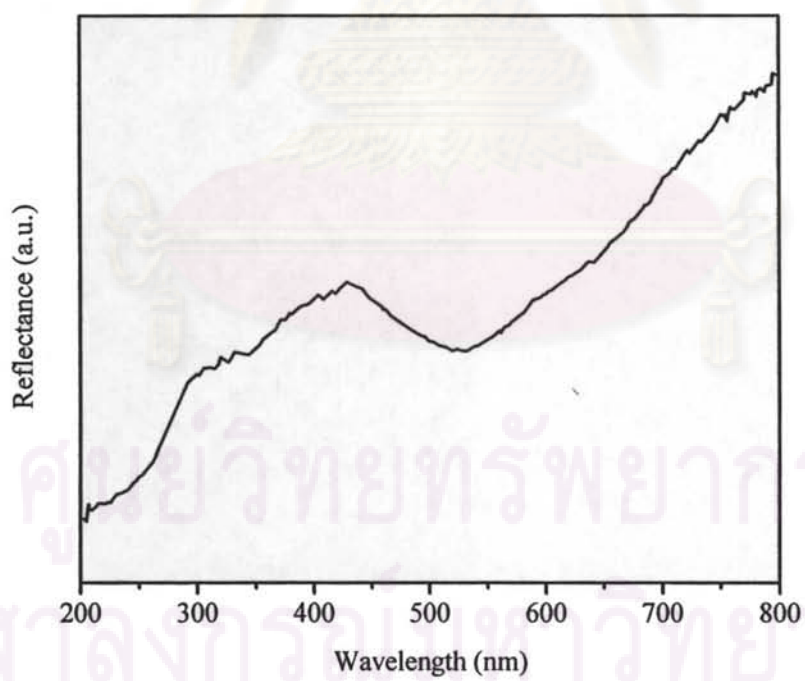


Figure I.6 DRUV spectrum of Co(OAc)₂-xerogel.

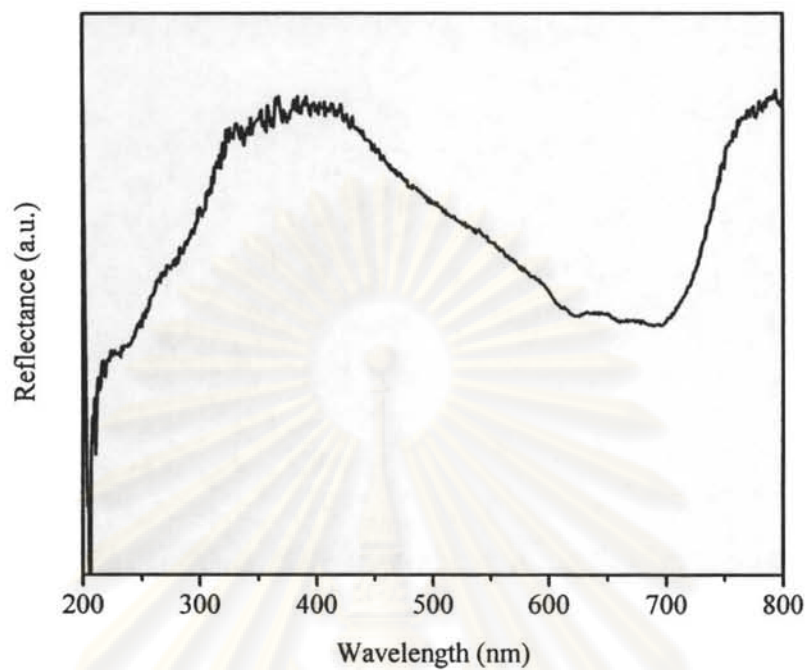


Figure I.7 DRUV spectrum of CoCl₂-xerogel.

ศูนย์วิทยทรัพยากร
จุฬาลงกรณ์มหาวิทยาลัย

VITAE

Miss Warangkana Kanjina was born on September 22, 1976 in Chiangmai, Thailand. She graduated a Bachelor Degree of Science, Major of Chemistry from Chiangmai University in 1999. She received a Master Degree in Petrochemistry and Polymer Science Program, Faculty of Science, Chulalongkorn University in 2004. She continued her study in Program of Petrochemistry, Faculty of Science, Chulalongkorn University in 2009.

PRESENTATIONS:

October 9-13, 2007.

Poster Presentation: "Oxidation of Alcohols and Hydrocarbons Catalyzed by Polyoxometalates in Solvent-free System" The 41st Western Regional Meeting American Chemical Society, San Diego, California, USA.

January 30-February 1, 2008.

Oral Presentation: "Oxidation of Hydrocarbons Catalyzed by Mono-substituted Silicotungsten in Biphasic System" Pure and Applied Chemistry International Conference, Bangkok, Thailand.

June 18-19, 2008.

Poster Presentation: "Catalytic Oxidation of Ethylbenzene using Layered Double Hydroxides" The 2nd Joint Symposium between Yonsei University, Korea and Chulalongkorn University, Yonsei University, Korea.

December 17-19, 2008.

Oral Presentation: "Ethylbenzene Oxidation using Layered Double Hydroxide and Mixed Metal Oxide Catalyst" The 4rd Mathematics and Physical Science Graduate Congress (3rd MPSGC), Singapore.